ABSTRACT

BATTYE, WILLIAM HOWARD. Satellite, Aircraft, and Ground Level Measurements to Characterize Ammonia Emissions from Agricultural Sources. (Under the direction of Dr. Viney P. Aneja).

As carbon fueled the industrial revolution, nitrogen fertilizer has fueled the agricultural revolution. Humankind's production of reactive nitrogen compounds, by the production of fertilizer and other processes, is five times higher than it was 60 years ago. Current worldwide anthropogenic production of reactive nitrogen is estimated at 190 Tg yr^{-1}. The central estimate for natural production of reactive nitrogen in terrestrial ecosystems is 84 Tg yr^{-1}, and the combined natural production from terrestrial and marine ecosystems is estimated at 240 Tg yr^{-1}. Thus, the global human production of reactive nitrogen is more than double the best estimate for natural production in terrestrial ecosystems, and is approaching the combined worldwide production from land and oceans.

A significant portion of the reactive nitrogen used in agriculture is lost to the environment through runoff, leaching, and volatilization of nitrogen compounds, including a large volume in the form of ammonia gas (NH_3). NH_3 emissions react with other pollutants in the atmosphere, and can contribute to elevated levels of fine particulate matter ($PM_{2.5}$), which is associated with adverse human health effects. NH_3 and its reaction products are also deposited from the atmosphere to terrestrial and marine ecosystems, fertilizing the landscape. This can affect species diversity and lead to eutrophication of aquatic ecosystems. Atmospheric chemistry models such as the Community Multiscale Air Quality (CMAQ) model are used to analyze the impact of NH_3 emissions on air pollution, and the deposition of NH_3 and its reaction products to terrestrial and aquatic ecosystems.

In the current research, CMAQ predictions for NH_3 are evaluated using ground based measurements, *in situ* aircraft measurements, and satellite based measurements. Two detailed case study analyses were performed, drawing on measurements in Northeast Colorado, and in North Carolina. Both of these areas include regions of high NH_3 emissions in proximity to sensitive ecosystems.

The Colorado case study used measurements gathered in the DISCOVER-AQ Colorado field campaign in July and August 2014. *In situ* aircraft measurements of atmospheric NH_3 suggest that the CMAQ model underestimated the NH_3 concentration in Northeastern Colorado by 63%. Ground-level monitors and satellite measurements gave similar results. The underestimation of NH_3 was not accompanied by an underestimation of particulate NH_4^+, which is affected by other factors including acid availability, removal rate, and gas-particle partition.

In the North Carolina case study, based on initial model testing, a lower-end estimate was developed for NH_3 emissions from emissions from swine operations, resulting in the lowering of statewide NH_3 emissions by an average of 42%. Even with the downward adjustment of NH_3 emissions, the model overpredicted atmospheric NH_3 by an average of 60% when compared with hourly measurements in Clinton, NC, in the vicinity of the densest NH_3 emissions. The average concentration measured by the monitor was 6.6 ppbv for July 2011, while the average predicted by the model was 10.5 ppbv. However, the model underpredicted wet deposition of NH_4^+ by 17-22%. The combination of an overestimation of NH_3 and underestimation of wet and dry deposition suggests that the overstatement in NH_3 may be partially attributable to an underestimation of wet and dry deposition in North Carolina.

Results for both Colorado and North Carolina indicate that further improvement of the emission inventories and modeling approaches are required to reduce the bias in NH_3 modeling

predictions. This process must take into account the diversity of the inventory in different regions of the country. Satellite measurements provide a valuable tool for evaluating the broad spatial patterns of NH_3 emissions and transport.

Satellite, Aircraft, and Ground Level Measurements to Characterize Ammonia Emissions from Agricultural Sources

by
William Howard Battye

A dissertation submitted to the Graduate Faculty of
North Carolina State University
in partial fulfillment of the
requirements for the degree of
Doctor of Philosophy

Marine, Earth and Atmospheric Sciences

Raleigh, North Carolina

2018

APPROVED BY:

_____	_____
Dr. Viney P. Aneja Committee Chair	Dr. Stacy A. Nelson
_____	_____
Dr. William H. Schlesinger	Dr. Daniel Q. Tong

_____
Dr. John T. Walker

DEDICATION

To my parents, who sacrificed to put me through college the first time, 45 years ago, and who provided great encouragement in this return to academia. To my wife and daughter, who have supported me in this late-career excursion, initially with enthusiasm and later with tolerant forbearance as the demands of a Ph.D. candidate schedule encroached on my time for other activities.

BIOGRAPHY

I'm a returning student, having completed my first round of education 41 years ago in Chemical Engineering, with Bachelor's and Master's Degrees from the Massachusetts Institute of Technology. After my first graduation, I went to work as an environmental consultant, and 29 years ago cofounded an environmental consulting company with my wife. I stepped out of the management of that company to return to NCSU as a Ph.D. student. It has been an adventure, as I have been able to pursue coursework and research in fields which did not even exist when I was in school the first time.

ACKNOWLEDGMENTS

Support for this research was provided by the NASA Earth and Space Science Fellowship (NESSF) program, grant No. NNX15AN15H and by the Kenan Fund. I acknowledge the support of my research committee. Dr. Viney Aneja, the committee chair, provided essential advice and counsel for this research. Dr. Daniel Tong, along with Drs. Pius Lee, and Youhua Tang performed critical air quality modeling for this research under the NOAA National Air Quality Forecast Program. Dr. John T. Walker provided advice in interpreting and screening continuous monitoring data for ammonia. Dr. William Schlesinger provided support in the evaluation of reactive nitrogen fluxes in the environment. Dr. Stacy Nelson provided advice in evaluating remote sensing data. I acknowledge the large team of researchers who carried out the DISCOVER-AQ and FRAPPE measurement campaigns, results of which were used in this study. In addition, the North Carolina Department of Environmental Quality (NCDEQ) collected and provided the hourly ground-level measurements used in this study. Dr. Joette Steger of the NCDEQ provided advice on the interpretation and screening of the NCDEQ measurements. The Atmospheric Spectroscopy group of the Université Libre de Bruxelles, Belgium (ULB-LATMOS) provided access to IASI retrievals, and advice on using the data; and the French AERIS database (http://iasi.aeris-data.fr) platform provided for the retrieval of the IASI data. I also acknowledge the important support of the North Carolina State University Air Quality Research Group.

TABLE OF CONTENTS

LIST OF TABLES

LIST OF FIGURES

Chapter 1

Introduction

Just as carbon fueled the Industrial Revolution, nitrogen has fueled an Agricultural Revolution. The use of synthetic nitrogen fertilizers and the cultivation of nitrogen-fixing crops both expanded exponentially during the last century, with most of the increase occurring after 1960 (Battye *et al*, 2017; Erisman *et al*, 2008). As a result, the current flux of reactive, or fixed, nitrogen compounds to the biosphere due to human activities is roughly equivalent to the total flux of reactive nitrogen from all natural sources, both on land masses and in the world's oceans. Reactive nitrogen compounds are distinguished from non-reactive nitrogen (N_2) gas in the atmosphere. These include all nitrogen compounds which are biologically active, chemically reactive, and radiatively active in the Earth's atmosphere and biosphere.[*] Microbes which convert atmospheric N_2 into reactive nitrogen compounds are termed nitrogen-fixing, and plants which live in symbiosis with these microbes are termed nitrogen-fixing plants.

Natural fluxes of reactive nitrogen are subject to very large uncertainties, but anthropogenic production of reactive nitrogen has increased almost five-fold in the last half-century, and this rapid increase in anthropogenic reactive nitrogen has removed any uncertainty on the relative importance of anthropogenic fluxes to the natural budget. The increased use of nitrogen has been critical for increased crop yields and protein production needed to keep pace

[*] Reactive nitrogen includes inorganic chemically reduced nitrogen compounds such as ammonia (NH_3) and ionic ammonium (NH_4^+); inorganic chemically oxidized nitrogen compounds such as nitrogen oxides (NO_X), nitric acid (HNO_3), nitrate ion (NO_3^-), and nitrous oxide (N_2O); and organic nitrogen compounds such as urea, amino acids, and proteins.

with the growing world population. However, similar to carbon, the release of reactive nitrogen into the natural environment is linked to adverse consequences at local, regional, and global scales. Anthropogenic contributions of reactive nitrogen continue to grow relative to the natural budget, with uncertain consequences.

In the U.S., emissions of ammonia (NH_3) constitute a large anthropogenic source of reactive nitrogen which is essentially unregulated. These emissions emanate primarily from agricultural sources (Aneja *et al.*, 2009). Because of the diffuse nature of NH_3 emissions, there is no smokestack plume that can be seen. Atmospheric chemistry models are needed to assess the impacts of NH_3 emissions on the atmosphere, and the deposition of emissions to terrestrial and aquatic ecosystems. Such modeling studies are also critical to demonstrating the potential benefits of measures taken to control NH_3 emissions. However, the NH_3 emissions estimates used in these modeling efforts are subject to considerable uncertainties (Battye *et al*, 2003).

Extensive data on NH_3 concentrations in the atmosphere have become available in the last decade, including ground-based measurements, satellite-based measurements, and *in situ* aircraft measurements. This current study aims to use these measurements to validate predictions of NH_3 in ambient models and to improve the ability to track emissions of NH_3. A particular aim is to identify methods for making use of satellite measurements of atmospheric NH_3 in air quality modeling efforts.

Figure 1-1. Is nitrogen the next carbon?

1.1. Is Nitrogen the Next Carbon?

Almost 50 years ago, C. C. Delwiche (1970) wrote in *Scientific American* "Of all man's recent interventions in the cycles of nature the industrial fixation of nitrogen far exceeds all the others in magnitude." Since then, the climate change impacts of human contributions to the carbon cycle have come under intense scrutiny and debate (IPCC, 2014). Meanwhile anthropogenic production of reactive nitrogen has continued to increase. The increased production of reactive nitrogen is associated with adverse environmental consequences. As in the case carbon dioxide (CO_2), some impacts of reactive nitrogen are difficult to measure on a short timescale. Reactive nitrogen also has a place in the agricultural revolution which is analogous to the role of carbon in the industrial revolution. This leads us to ask the question: is the anthropogenic augmentation of the nitrogen cycle growing to a point where it may have adverse environmental consequences on a global scale, and where the critical role of reactive nitrogen in the agricultural system will make it very difficult to mitigate these consequences? Or "Is nitrogen the next carbon?" (Battye *et al*, 2017)

1.1.1. Trends in Human Nitrogen Use

Nitrogen-rich manure has been used to fertilize crops for millennia – long before the discovery of nitrogen as a distinct chemical element (Columella, 70). The role of nitrogen as a crop nutrient was explored scientifically in the 1800s (Boussingault, 1856), and a market developed for nitrogen-rich deposits of mineralized guano from South America and the South

Pacific islands, reaching about 1 Tg N y^{-1} by 1900 (Cushman, 2013). Though small by today's standards, the trade in nitrogen fertilizer was a main object of contention in the 1879 War of the Pacific, between nascent South American nations (Ortega, 1984). Industrial processes for fixing nitrogen, especially the Haber-Bosch process, greatly expanded the availability of nitrogen-based fertilizers in the early 1900s (Smil, 2001). Nevertheless, use of synthetic fertilizers did not become routine until the mid-twentieth century. In the U.S., less than 40% of farms reported the use of any synthetic fertilizer in 1939, but more than 60% reported the use of chemical fertilizer in 1954 (Hurley *et al*, 1954).

As shown in Figure 1-2, synthetic nitrogen fertilizer usage grew to about 12 Tg N y^{-1} in 1960, more than a 10-fold increase over mineral nitrogen fertilizer usage prior to the commercialization of the Haber-Bosch process (1911). Since 1960, synthetic nitrogen fertilizer use has grown almost another 10-fold to 110 Tg N y^{-1} in 2013. Initially, this growth occurred in the U.S. and Europe. Consumption in these regions levelled off in about 1990, and the growth since then has occurred primarily in Asia (IFA, 2016).

The last half of the 20th century also saw large increases in the cultivation of nitrogen-fixing crops, especially soybeans. Figure 1-3 shows the increase in reactive nitrogen as a result of this trend. The trend lines in Figure 1-3 were computed by combining nitrogen fixation rates from Herridge *et al* (2008) with statistics on historical crop cultivation and production (FAO, 2015a). Soybeans have been cultivated in Asia for at least 1000 years, but after the nitrogen-fixing capabilities of the crop were recognized, cultivation in other parts of the world grew rapidly. World soybean production increased by more than a factor of 3 between 1910 and 1960 (Shurtleff and Aoyagi, 2004); with production in the U.S. exceeding Asian production by 1955 (FAO, 2015a). Since 1960, world production of soybeans has increased by a factor of 10, with

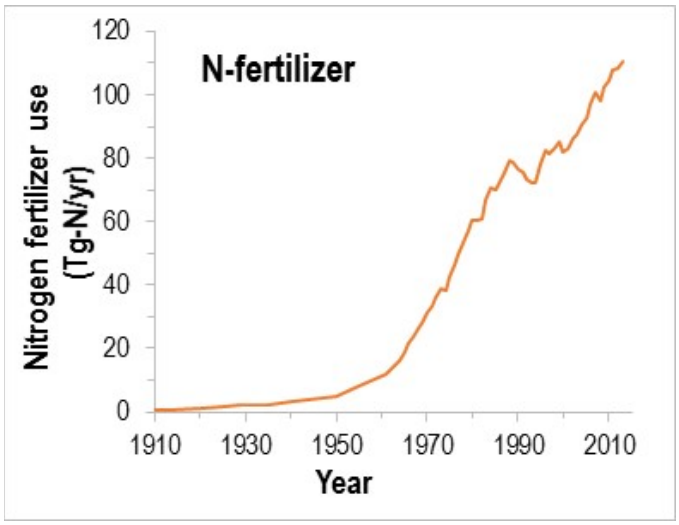

Figure 1-2. Global increase in the use of synthetic and mined nitrogen fertilizer since 1910.

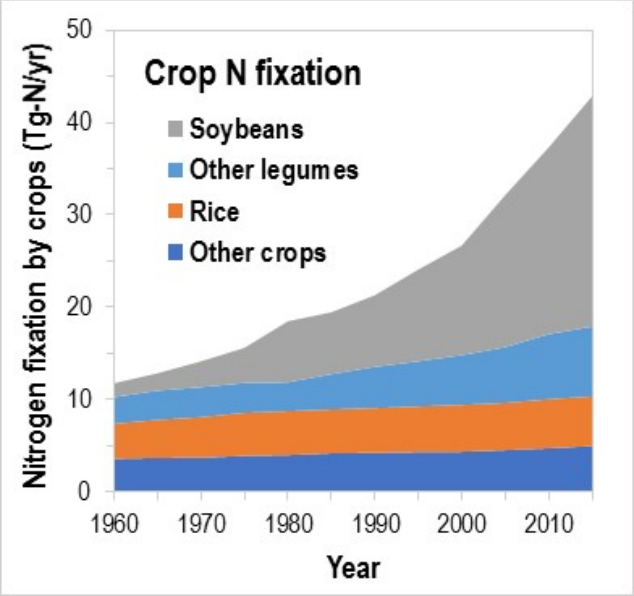

Figure 1-3. Global increase in reactive nitrogen produced by nitrogen-fixing crops since 1960.

the largest share of new production occurring in South America. Soybeans are often grown in rotation with other crops, such as corn. This crop rotation serves to increase the amount of nitrogen available and to break the cycles of crop pests.

Cultivation of other legumes (e.g. peas, beans, lentils and peanuts) has increased by a factor of about 2.6 since 1960. Total global nitrogen fixation in croplands is estimated at about 43 Tg N y^{-1}, with a range from 30 to 51 Tg N y^{-1} based on the ranges of nitrogen fixation yields (Herridge *et al*, 2008). This estimate includes soybeans, other beans and legumes, and inadvertent nitrogen fixation by cyanobacteria associated with the cultivation of rice, sugar, and other crops. The estimate for croplands does not include legumes in pasturelands or savannas used for grazing. However, nitrogen fixation in these ecosystems may also be increased by anthropogenic activities.

Populations of animals raised for food have also increased in recent decades. Figure 1-4 shows the estimated increase in the amount of reactive nitrogen in animal wastes as a result of increased animal populations since 1960. The trend lines were computed by combining animal population statistics (FAO, 2015b) with standard estimates of waste nitrogen content (IPCC, 2006). Animals convert only a fraction of the nitrogen in their feed to meat protein or milk protein for human consumption (U.S. EPA, 2011). Much of the balance is excreted in the form of urea and other nitrogen compounds in the animal waste, which is generally applied to crops to provide nitrogen fertilizer.

A substantial portion of the nitrogen from animal waste and synthetic fertilizer is lost to the surrounding environment, through runoff, leaching to groundwater, and emissions of NH_3, nitrogen oxides (NO_X), and other nitrogen compounds (Galloway and Cowling, 2002; Conant *et al*, 2013). NO_X emissions from combustion sources also constitute a source of reactive nitrogen.

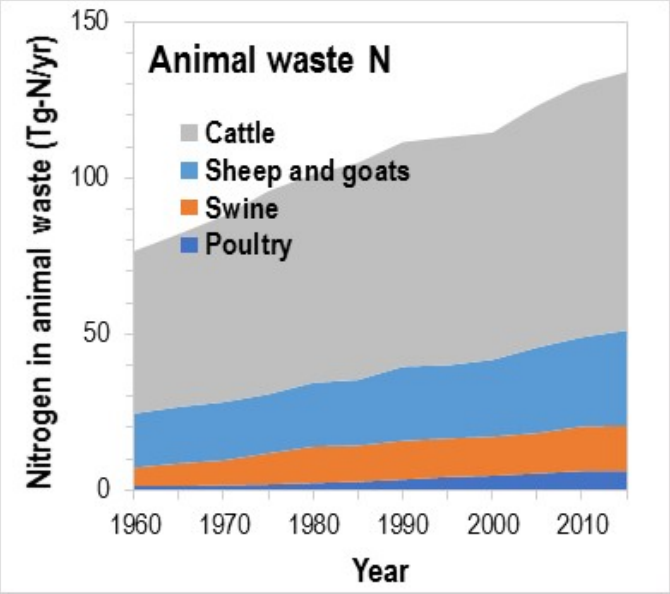

Figure 1-4. Global increase in reactive nitrogen present in animal wastes since 1960.

These emissions increased from ~5.8 Tg N y^{-1} in 1910 to ~38 Tg N y^{-1} in 2010. Figure 1-5 shows trends in estimated annual global NO_X emissions since 1900. The figure also shows trends in global NH_3 emissions from agricultural activities, and projected future emissions of NO_X and NH_3 under the potential range of representative concentration pathways used in climate change projections (UN, 2010). Since the 1990s, NO_X emission sources have been subject to pollution controls in the U.S. and Europe, resulting in substantial emission reductions. Emissions continue to increase in the developing world, especially China, but these are projected to decline in the coming decades (UN, 2010). NH_3 emissions are projected to continue increasing.

Figure 1-6 summarizes the combined trajectory of anthropogenic production of reactive nitrogen since 1900, with contributions from synthetic fertilizer, increased cultivation of nitrogen-fixing crops, and increased emissions of NO_X. The total of these three sources for 2014 is 190 Tg N y^{-1}, with a plausible range from 160 to 210 Tg N y^{-1}. Nitrogen compounds in animal waste are not included in this total, since they do not represent a new addition of biologically available nitrogen to the environment. Rather, the nitrogen in animal waste is derived from plant proteins consumed by the animals. However, losses of N gases and runoff of animal waste components are important pathways for the release of nitrogen compounds from farms to the surrounding environment. Therefore, the increased animal populations also affect the nitrogen cycle.

Figure 1-6 compares the trend in anthropogenic reactive nitrogen with the trajectory of CO_2 (Boden *et al*, 2013; IEA, 2017). The CO_2 curve shows a sharp upward inflection in the mid-1940s. The nitrogen curve lags the CO_2 curve by 10 to 15 years, showing an upward inflection about 1960. The trends for anthropogenic nitrogen and CO_2 in the last half of the 20^{th} century are similar. While reported global CO_2 emissions have not shown an increase since about 2013, the

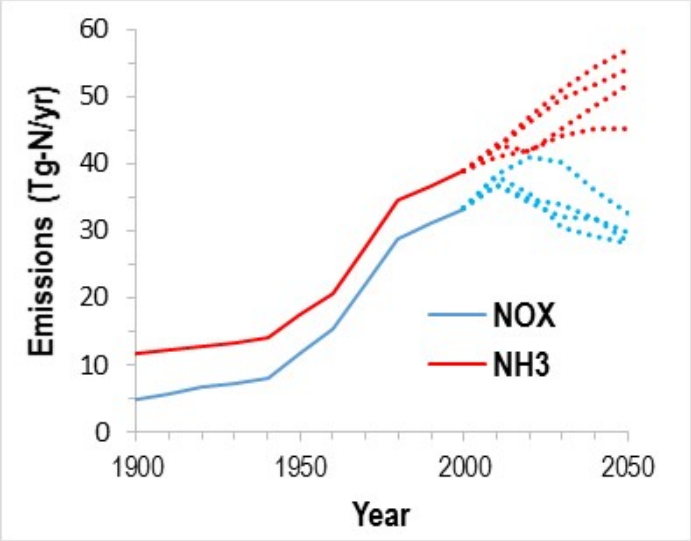

Figure 1-5. Historic trends and projected future global emissions of NH_3 and NO_X from 1900 to 2050.

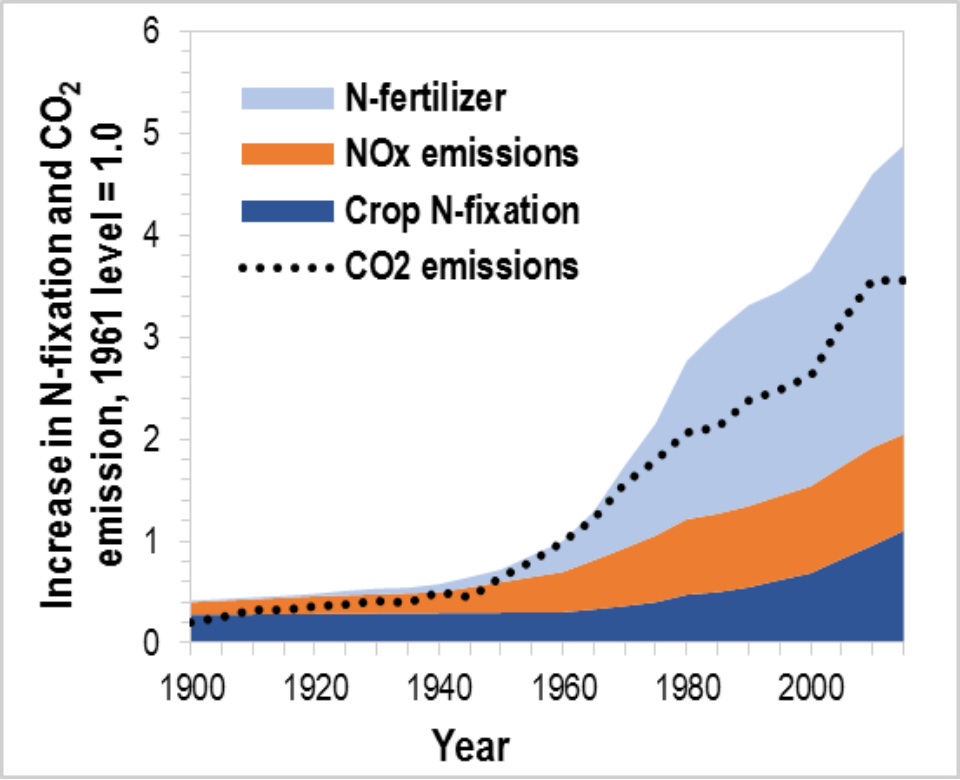

Figure 1-6. Trend in anthropogenic nitrogen compounds since 1900 compared with the trend in anthropogenic CO_2 emissions.

use of nitrogen fertilizers and the cultivation of nitrogen-fixing crops are expected to continue to increase in most future scenarios (Bouwman *et al*, 2013a; Winiwarter *et al*, 2013, IEA, 2017).

1.1.2. Human Impacts on the Nitrogen Cycle

Figure 1-7 illustrates the natural nitrogen cycle, showing how anthropogenic inputs of nitrogen compounds contribute to this cycle. Nitrogen-fixing bacteria convert nitrogen gas (N_2) to biologically available nitrogen compounds, which are in turn taken up by plants and incorporated into proteins and other essential molecules. Nitrogen compounds in decomposing plant matter and animal waste are released as ammonium (NH_4^+), which is oxidized by bacteria, producing nitrate ion (NO_3^-), which is consumed by other bacteria that perform denitrification. The denitrification reaction completes the cycle by producing N_2 gas, but also produces some gaseous nitrous oxide (N_2O) and nitric oxide (NO).

Both the use of synthetic nitrogen fertilizer and the anthropogenic cultivation of nitrogen-fixing crops increase the overall mass of biologically available nitrogen compounds. This nitrogen is intended to remain within the farm system, ultimately for the production of food for humans or for animals raised to feed humans. However, a substantial portion of the reactive nitrogen (~70%) escapes to the surrounding environment (Galloway and Cowling, 2002). Fertilizers and residues from nitrogen-fixing crops, and deposited nitrates all ultimately increase the amount of nitrate processed by denitrifying bacteria, both on farmlands and in surrounding ecosystems.

The magnitudes of fluxes in the natural nitrogen cycle are subject to considerable uncertainty, as stated colorfully in the title of a 1980 paper by Burris: “The global nitrogen budget – science or séance?” (Burris, 1980). Galloway *et al* (2004) gave a global estimate of 120 Tg N y^{-1} for biological nitrogen fixation in terrestrial ecosystems under pre-industrial

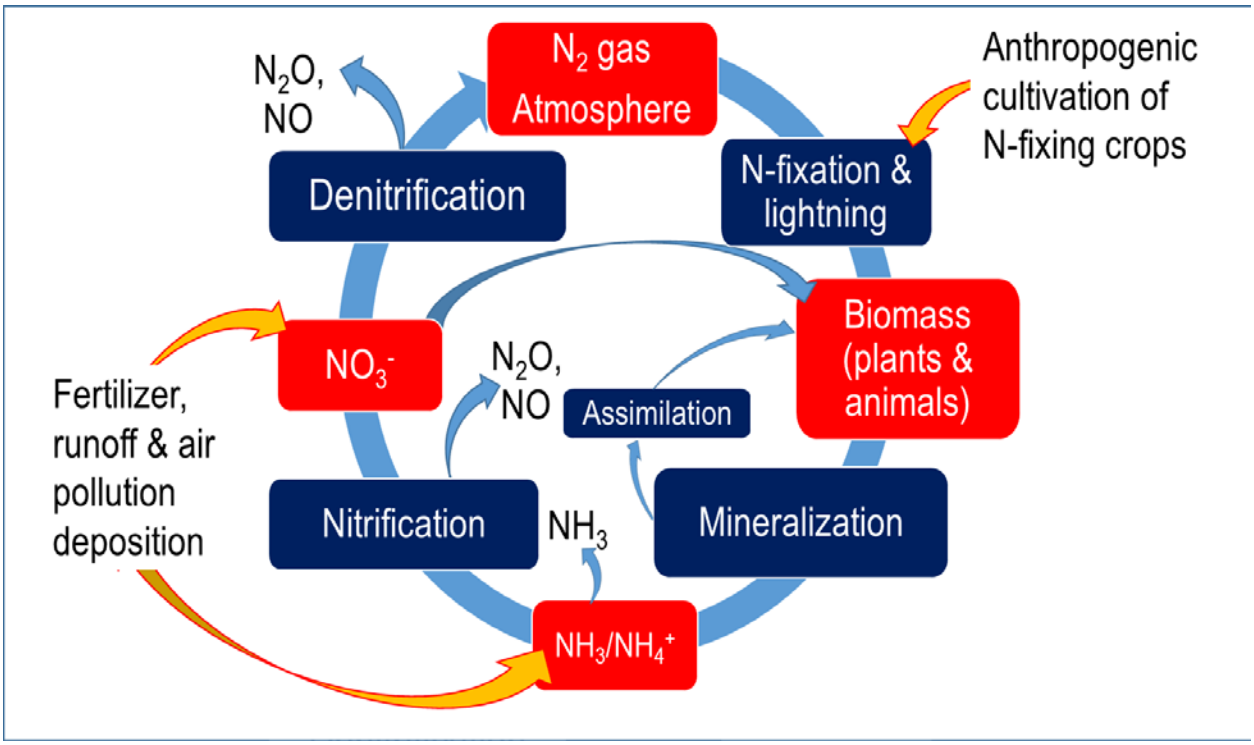

Figure 1-7. The nitrogen cycle.

Note: Anthropogenic inputs are denoted by orange arrows.

conditions based on a compilation of nitrogen fixation fluxes from various ecosystems. Using nitrogen-isotope abundances, Vitousek *et al* (2013) obtained a considerably lower pre-industrial estimate of 58 Tg N y^{-1} for terrestrial nitrogen fixation, with a possible range from 40 to 100 Tg N y^{-1}. This lower estimate is adopted by Fowler *et al* (2013). Cleveland *et al* (2013) estimate natural nitrogen fixation in terrestrial ecosystems at 127 Tg N y^{-1}, based on biogeochemical modeling of the contributions of different terrestrial ecosystems.

Estimates of nitrogen fixation in marine ecosystems range from 121 Tg N y^{-1} to 177 Tg N y^{-1} (Groβkopf *et al*, 2012; Jickells *et al*, 2017). Lightning strikes are estimated to account for an additional 5.4 Tg N y^{-1} on a global basis (Galloway *et al*, 2004). Combining these estimates with the range of values for terrestrial ecosystems, we estimate the global rate for production of reactive nitrogen at 166 to 302 Tg N y^{-1} under pre-industrial conditions. Using central estimates for terrestrial nitrogen fixation and marine ecosystems, the overall global pre-industrial nitrogen fixation rate would be about 240 Tg N y^{-1}. Table 1-1 summarizes estimates of anthropogenic and natural fluxes of reactive nitrogen.

Even considering the uncertainty in the magnitude of fluxes in the nitrogen cycle, anthropogenic sources of reactive nitrogen represent a significant perturbation to the terrestrial nitrogen cycle and to the global nitrogen cycle as a whole. Figure 1-8 shows that the anthropogenic nitrogen contribution would have surpassed the lower end estimate of pre-industrial nitrogen fixation in terrestrial ecosystems by 1960; and would have surpassed the upper end estimate for terrestrial ecosystems by about 1980. (The trend for the anthropogenic nitrogen contribution includes synthetic fertilizer, cultivation of nitrogen-fixing crops, and NO_X emissions from fossil fuel combustion.) Based on the central estimates given in Table 1-1, the current anthropogenic contribution accounts for about 70% of total production of reactive

Table 1-1. Fluxes of reactive nitrogen

-	Sources (Tg N y^{-1})			Range (for present values)	-
	1910	1960	Present		References
Sources					
Anthropogenic					
Synthetic or mined fertilizers	1	12	110		a,b,c
N-fixing crops					
Soybeans	0.4	1.5	25		d,e,f
Other beans and legumes		2.9	7.5		e,f
Other		7.4	10		e,f
Total N-fixation		12	43	30 - 51	
NO_X from combustion	2.5	15	38		g
Total anthropogenic	~4	39	190	160 - 210	
Natural					
Terrestrial N-fixation			84	40 - 127	h,i,j
Rock weathering			14	11 - 18	k
Lightning			5.4		h
Marine N-fixation			150	121 - 177	h,l
Total natural sources			250	166 - 310	
Total sources			440		
Sinks					
Denitrification					
Agricultural soils				22 - 87	m
Total terrestrial			130	58 - 175	n,o
Fresh water and groundwater			120	39 - 216	o
Marine			150	107 - 331	n,o,p
Total denitrification			400	210 - 720	
Other sinks					
Terrestrial & soil biomass change			9	9	q
Marine sediments			13	10 - 16	h,q
Total sinks			420	220 - 745	

[a]Cushman, 2013.
[b]IFA, 2016.
[c]Smil, 2001.
[d]Shurtleff & Aoyagi, 2004.
[e]FAO, 2015.
[f]Herridge *et al*, 2008.
[g]UN, 2010.
[h]Galloway *et al*, 2004.
[i]Vitousek *et al*, 2013.
[j]Cleveland *et al*, 2013.
[k]Houlton *et al*, 2018.
[l]Groβkopf *et al*, 2012.
[m]Hofstra *et al*, 2005.
[n]Seitzinger *et al*, 2006.
[o]Eugster, 2012
[p]DeVries *et al*, 2013a.
[q]Schlesinger & Bernhardt (2013)

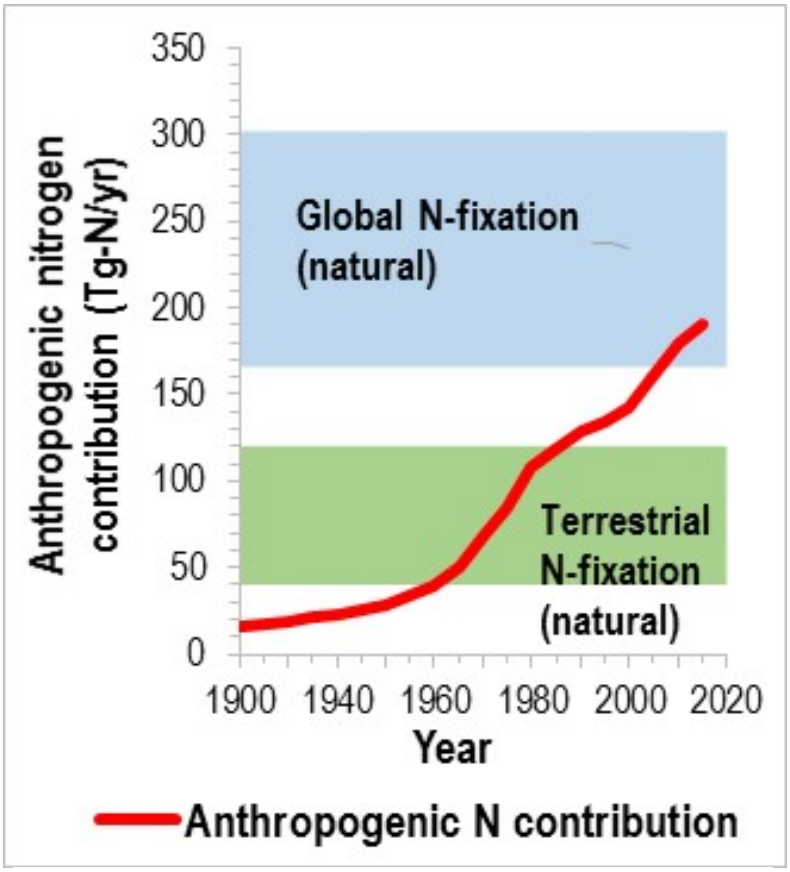

Figure 1-8. Trend in the anthropogenic contribution of new fixed nitrogen relative to the estimated ranges of global nitrogen fixation under pre-industrial conditions.

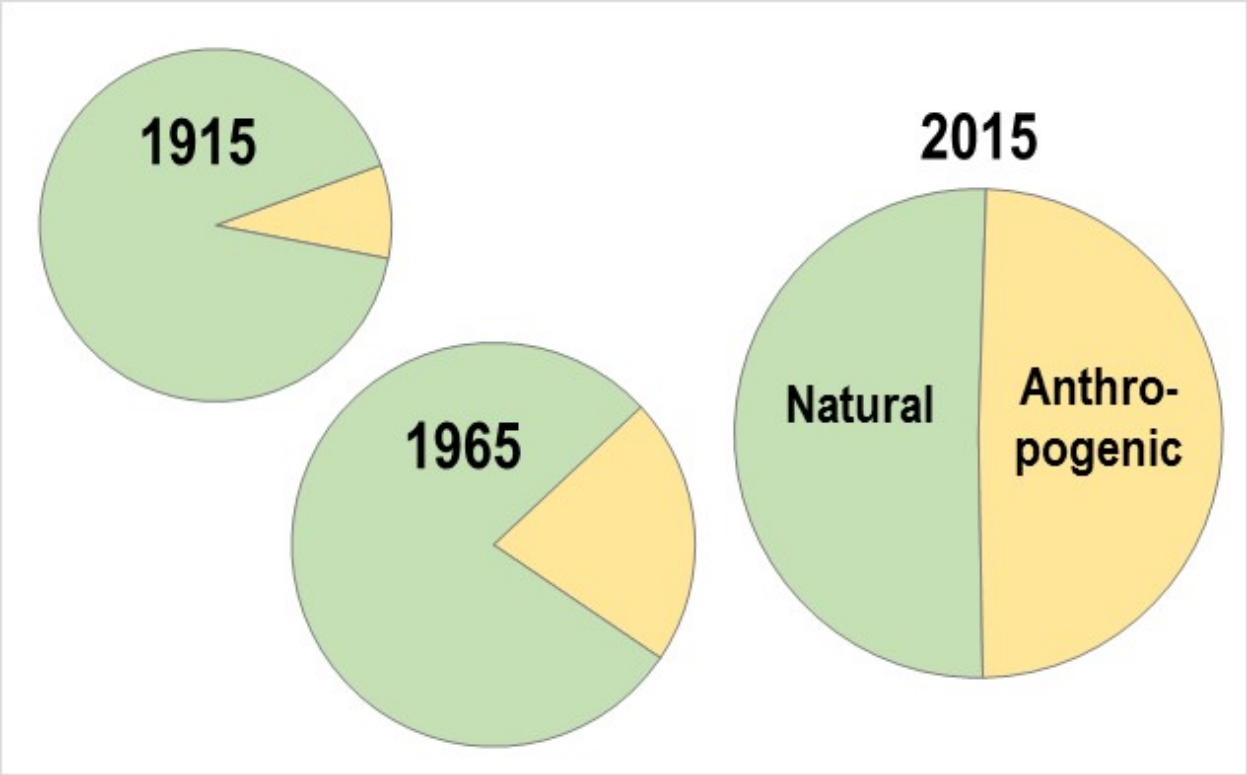

Figure 1-9. Growth in anthropogenic nitrogen fixation over the last 100 years. Natural nitrogen fixation includes both terrestrial environments and the oceans.

nitrogen in terrestrial ecosystems. The anthropogenic contribution is close to our best estimate of overall global nitrogen fixation under pre-industrial conditions (240 Tg N y^{-1}), and is increasing across the uncertainty bar for the global estimate. This suggests that the anthropogenic inputs may now account for about half of the total reactive nitrogen flux on Earth. Figure 1-9 illuatrates the growth of the anthropogenic reactive nitrogen in relation to the natural budget over the past century.

Anthropogenic reactive nitrogen produces multiple impacts at local, regional, and global scales. Emissions of NH_3 and NO_X contribute to the formation of fine particulate matter ($PM_{2.5}$), which is associated with various adverse human health impacts, including premature death (Kwok *et al*, 2013; Pope *et al*, 2009; Lelieveld *et al*, 2017). $PM_{2.5}$ can also contribute to visibility impairment and regional haze (Wang *et al*, 2012).

Reactive nitrogen fertilizes terrestrial and aquatic ecosystems, which can affect species diversity and can lead to eutrophication of aquatic ecosystems (Jones *et al*, 2013; Paerl *et al*, 1988; U.S. EPA, 2007). Deposition of reactive nitrogen can also contribute to soil acidification (Lu *et al*, 2014). The use of synthetic nitrogen in agricultural operations has been associated with the depletion of other soil nutrients in agricultural systems. In India, crop yields have leveled off despite increases in the use of synthetic nitrogen fertilizer (IPC, 2008).

Reactive nitrogen compounds can leach into ground water, contaminating drinking water supplies (UNEP, 2007, Tomich *et al*, 2016). Increased levels of nitrate have been detected in the Pacific Ocean (Kim *et al*, 2014). A portion of reactive nitrogen processed by soil and aquatic microbes is also converted to N_2O, which reenters the atmosphere. N_2O is a long-lived absorber of infrared radiation, with a climate change potential approximately 300 times that of CO_2

(IPCC, 2014). Nitrous oxide is also associated with the depletion of stratospheric ozone (Ravishankara et al. 2009).

The impacts of reactive nitrogen on the environment have different time scales. Elevated levels of $PM_{2.5}$ may persist for only a few days, but may also be chronic. Impacts on groundwater, the oceans, and climate have much longer time scales. The lifetime of N_2O in the atmosphere is estimated at 121 years (IPCC, 2014).

1.1.3. Fate of Anthropogenic Nitrogen

Most of anthropogenic augmentation of reactive nitrogen is believed to be removed ultimately by denitrification, producing nitrogen gas (N_2) and N_2O. Some of this denitrification occurs in agricultural soils, with estimates of global flux ranging from 22 to 87 Tg N y^{-1} (Hofstra and Bouwman, 2005). Denitrification in agricultural soils has the effect of reducing the release of reactive nitrogen to surrounding ecosystems. However, this is indicative of an inefficiency of nitrogen use, and also results in the production of N_2O.

Estimates of the sinks for reactive nitrogen are also subject to considerable uncertainty. Recent estimates of global denitrification flux range from 58 to 175 Tg N y^{-1} for terrestrial ecosystems (Bouwman *et al*, 2013b; Seitzinger *et al*, 2006), 39 to 216 Tg N y^{-1} for freshwater and groundwater, and 107 to 331 Tg N y^{-1} for marine ecosystems (Jickells *et al*, 2017; Eugster *et al*, 2012; DeVries *et al*, 2013a). Combining these estimates gives a total global flux of 210 to 720 Tg N y^{-1}. If we combine the estimates for natural and anthropogenic nitrogen fixation, the range of estimates for total nitrogen fixation extends from 326 Tg N y^{-1} (160 anthropogenic + 166 natural) to 520 Tg N y^{-1} (210 anthropogenic + 310 natural). The range of estimates for the denitrification flux extends from below the lower-end estimate for total global nitrogen fixation

to above the upper-end estimate. Thus, the global denitrification flux may or may not be large enough to balance global nitrogen fixation (Table 1-1).

Seitzinger *et al* (2006) estimate that about 40% of land-based reactive nitrogen is denitrified in soils, while 35% is denitrified in freshwater or groundwater, and 25% is denitrified in estuaries and oceans. The total global denitrification flux is estimated at 600 Tg N y^{-1}, 58% from the oceans, 20% from freshwater and groundwater, and 22% from soils. This global denitrification flux would be sufficient to balance the rate of nitrogen fixation, including the anthropogenic increment. However, both nitrogen fixation and denitrification fluxes are subject to large uncertainties. Even if the sources and sinks of reactive nitrogen are in balance on a global basis, there are imbalances on local and regional scales which lead to adverse environmental impacts.

Sgouridis and Ullah (2015) found that natural and semi-natural terrestrial ecosystems denitrified about half of the reactive nitrogen deposited to them. Similarly, Houlton and Bai (2009) estimate that denitrification accounts for about one third of the flux of reactive nitrogen from natural terrestrial ecosystems. This finding is compatible with the estimates of Seitzinger *et al* (2006), which indicate a residual flux of reactive nitrogen from terrestrial to marine ecosystems. Jickells et al (2017) estimate the flux of reactive nitrogen from terrestrial systems to the oceans at 73 Tg N y^{-1}. Some of the anthropogenic increment of reactive nitrogen may be accumulating in terrestrial biomass and soils. This increment has been estimated at 9 Tg N y^{-1} (Schlesinger, 2009). Sgourdis and Ullah (2015) further suggest that this should alert us to the threat of chronic nitrogen saturation within terrestrial systems receiving nitrogen deposition.

Eugster and Gruber (2012) carried out inverse modeling of both nitrogen fixation and denitrification rates in the oceans, and estimated that the overall nitrogen cycle in the ocean is

balanced to within 3 Tg N y^{-1}, with a possible range from -38 to +40 Tg N y^{-1}. In addition to nitrogen fixation and denitrification, this balance calculation includes loss to sediments.

An additional 10-16 Tg N y^{-1} may be sequestered in ocean sediments (Galloway *et al*, 2004; Schlesinger and Bernhardt, 2013). Based on the ranges of reactive nitrogen inputs to the oceans (Table 1-1 and Seitzinger *et al*, 2006), between 18 and 45% of this sequestered nitrogen would derive from anthropogenic sources. The rates of accumulation of nitrogen in ocean sediments and in soils are subject to large uncertainties. Nor can these be corroborated by mass balance, because of the large uncertainties in global flux terms. It is not known whether these sinks might represent a significant build-up of reactive nitrogen over time, which could result in increased emissions of N_2O in the future.

Duce et al (2008) highlight the importance of atmospheric deposition of reactive nitrogen in the oceans. Although isotopic studies in the Atlantic have found that the importance of the anthropogenic contribution may be less than that of ocean sources (Altieri *et al*, 2016), studies in the Pacific have suggested that atmospheric deposition has caused an increase in nitrogen concentration there (Kim *et al*, 2014; Kim *et al*, 2011).

Many terrestrial, freshwater, and marine ecosystems are historically nitrogen limited (Elser *et al*, 2007) Thus, export of reactive nitrogen from farmlands to these ecosystems can adversely affect biodiversity (DeVries *et al*, 2013b; Zaehle *et al*, 2011). It is possible that the deposition of reactive nitrogen to forested ecosystems may increase the sequestration of carbon in soils and biomass (Pinder *et al*, 2013). However, the deposition of reactive nitrogen in natural ecosystems also enhances production of N_2O as a byproduct of microbial denitrification reactions. The climate change impacts of the increased N_2O may offset the impacts of carbon sequestration (Zaehle *et al*, 2011; Butterbach-Bahl *et al*, 2011).

Ice core analyses provide a record of the increase in the atmospheric concentration of N_2O (Bullister, 2015), and in the long range transport of reactive nitrogen in the form of NO_3^- (Hastings *et al*, 2009). Figure 1-10 compares trends for N_2O and NO_3^- with trends measured for CO_2 (Etheridge *et al*, 1996; WMO, 2016). (Trend lines are smoothed by averaging over 5-years.) The increases in ice-core concentrations of CO_2 and N_2O are believed to reflect trends in the global concentrations of these gases, since they are well-mixed in the atmosphere. The ice core measurements of NO_3^- (in Greenland) are believed to be related to an increase in regional transport of NO_3^-. This increase corresponds with a change in the isotopic composition of nitrate-N in the ice cores, reflected by a reduction in the abundance of nitrogen-15 relative to nitrogen-14 [$\delta^{15}N$].The change in isotopic composition may be indicative of an increased contribution of agricultural sources (Felix and Eliot, 2013). However, the fractionation of nitrogen isotopes is complex, and the samples from Greenland ice cores may be open to different interpretations (Hastings *et al*, 2009).

There is growing recognition of the impact of anthropogenically produced nitrogen compounds on the nitrogen cycle (Gruber and Galloway, 2008; Fowler *et al*, 2015; Sutton *et al*, 2011; U.S. EPA, 2011). Researchers have used the concept of planetary boundaries to evaluate the magnitudes of human impacts which allow the sustainable maintenance and development of human society (DeVries *et al*, 2013b; Rockstrom *et al*, 2009). Within this construct, the planetary boundary for the anthropogenic contribution to total reactive nitrogen is estimated at 62-82 Tg N y^{-1}, based on the risk of eutrophication of terrestrial and aquatic ecosystems (Steffen *et al*, 2015). This threshold was exceeded in the 1970s, and the current anthropogenic contribution is approximately 153 Tg N y^{-1}.

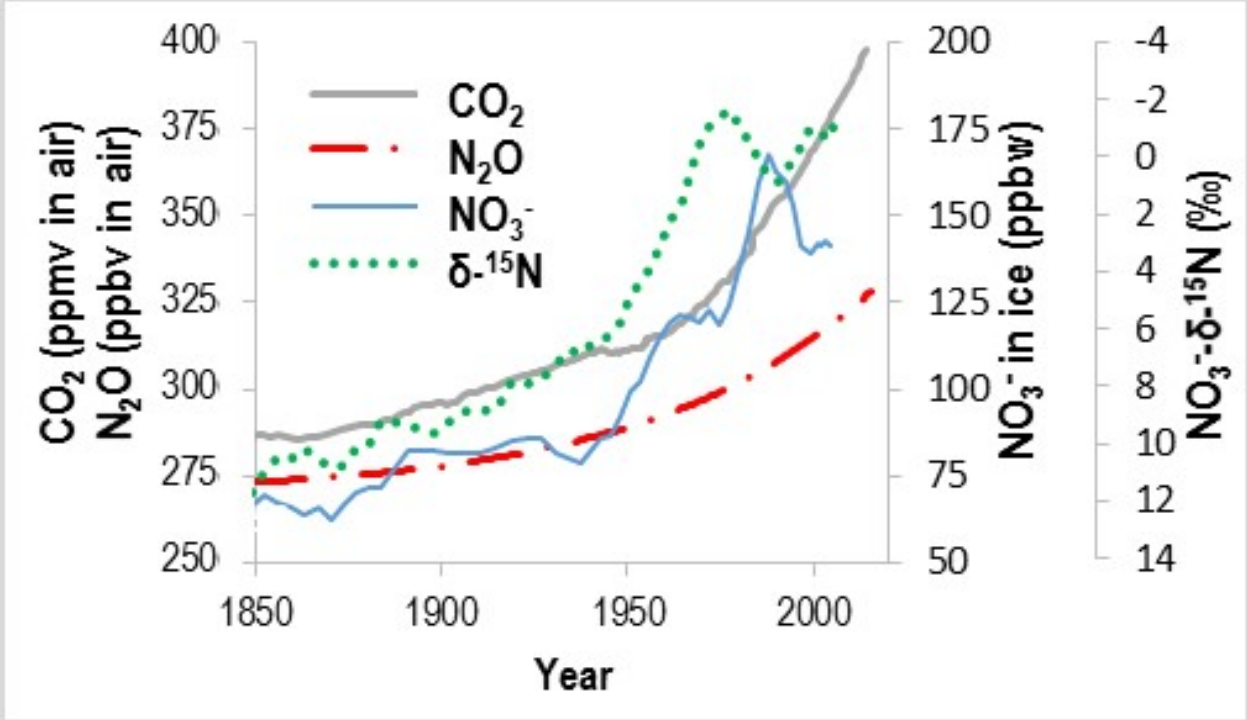

Figure 1-10. Trends in CO_2, N_2O, NO_3^-, and isotopic composition of NO_3^- as reflected in ice cores.

1.1.4. Future Prospects

Regulatory and voluntary measures have been adopted to address some components of the nitrogen stream. In the United States, livestock production facilities are required to obtain permits under the Clean Water Act in order to ensure that the surface waters surrounding the operations are not negatively impacted by animal waste. In implementing this permit system, states have identified Best Management Practices (BMPs) for the management of animal waste and for the use of synthetic nitrogen fertilizers.

Nitrogen-use efficiency has increased in the U.S. and Europe in recent years. Although the trend in nitrogen fertilizer usage in developed nations has been flat since the 1990s, agricultural production continues to increase. This suggests that increases in nitrogen-use efficiency can abate or perhaps reverse the worldwide increase in nitrogen fertilizer use (Zhang, 2015). Changes in dietary habits and food wastage can also help reduce the need for synthetic nitrogen fertilizers.

NO_X emissions from combustion sources have been the target of pollution controls in order to mitigate acid rain and smog in the U.S. These controls have produced a 50% reduction in nationwide NO_X emissions since 1996 (U.S. EPA, 2017). Total deposition of inorganic nitrogen has declined by 19 to 32% since the 1980s (Burns *et al*, 2011). This demonstrates that NO_X emissions can be reduced without preventing economic growth.

Unfortunately, there is no integrated regulatory approach for control of reactive nitrogen compounds (Aneja *et al*, 2008, 2009). In particular, agricultural emissions of reactive nitrogen compounds to the atmosphere are not regulated in the U.S. Because of its contribution to the formation of $PM_{2.5}$, individual states can regulate NH_3 as part of their approaches to meeting $PM_{2.5}$ standards. However, the U.S. has not adopted a national program for NH_3 emissions. NH_3

is the largest volume air pollutant for which no national or regional control program has been developed. Some European nations have adopted control measures for NH_3, which have produced significant reductions in emissions from agriculture (Erisman *et al*, 2008). A combination of best management practices and engineered solutions for the management of animal waste and for the use of synthetic nitrogen fertilizers can reduce releases of NH_3 and other reactive nitrogen compounds to the natural environment (Galloway *et al*, 2008; Erisman *et al*, 2015).

Human-induced changes to the global nitrogen cycle bear a number of similarities to our changes in the global carbon cycle. Fixed N and fossil C have provided great benefits to the human standard of living. The increased use of nitrogen has been critical for increased crop yields and protein production to keep pace with the growing world population. Like the burning of fossil carbon, increased fixation of nitrogen can have adverse environmental consequences at local, regional, and global scales. In addition, our use of fossil carbon and synthetically reactive nitrogen have both grown exponentially in the past 150 years. Anthropogenic production of reactive nitrogen has grown in relation to natural sources, so that the anthropogenic increment is nearly as great as the best estimate of the total natural nitrogen fixation in terrestrial and marine environments.

Some measures for reducing CO_2 emissions will reduce releases of reactive nitrogen, and vice versa. For instance, renewable energy sources generally will reduce fuel consumption, thereby reducing NO_X emissions. Switching from coal to natural gas also reduces both CO_2 and NO_X emissions. Thus improvements in nitrogen-use efficiency would reduce CO_2 emissions as well as releases of reactive nitrogen.

There are also important differences pertaining to human impacts on the carbon and nitrogen cycles. A significant fraction of anthropogenic CO_2 emissions has been taken up by the oceans. In contrast, nitrogen fixation and denitrification are roughly in balance. Although some reactive nitrogen may be accumulating in soils and in ocean sediments, the fraction is much smaller than the fraction of carbon taken up by the oceans. This could mean that the nitrogen cycle could possibly recover more quickly from anthropogenic perturbation than the carbon cycle if releases of reactive nitrogen are mitigated. However, demands for increased nitrogen usage will continue as world population and agricultural production continue to rise. Thus, reducing the demands for reactive nitrogen may prove to be more difficult than reducing emissions of CO_2.

The impacts of anthropogenic perturbations on the reactive nitrogen cycle are still mainly local and regional. Current estimates indicate that global nitrification fixation is balanced by denitrification, although these budget calculations are subject to large uncertainties. Thus, the large increase in anthropogenic production may be balanced by increased denitrification. Nevertheless, if anthropogenic production continues to increase, denitrification processes may not continue to offset the increased production. Continued increases in reactive nitrogen production could may accelerate species diversity impacts and N_2O production.

Similar to CO_2 from fossil fuels, anthropogenic releases of reactive nitrogen to the environment have increased dramatically in the last century, with adverse impacts at local, regional, and global scales. As with carbon, public awareness of the impact of reactive nitrogen is also increasing. We anticipate that reactive nitrogen may be similar to the situation with carbon in another respect. The environmental impacts of anthropogenic reactive nitrogen may become more difficult to rectify as time passes. In the case of carbon, we are accumulating a

burden of CO_2 that will impact the atmosphere far into the future (IPCC, 2014). In the case of reactive nitrogen, anthropogenic contributions continue to grow in relation to the natural budget, with uncertain consequences. “Is nitrogen the next carbon?” is a thought provoking question. Mitigating both carbon and nitrogen is a grand challenge.

1.2. Need for Improved Means of Tracking NH_3 Emissions

Emissions of NH_3 represent a large source of reactive nitrogen which is essentially unregulated in the U.S. There is currently no broad air pollution control program for NH_3 emissions in the U.S. comparable to the program for NO_X. States can adopt control measures for NH_3 as part of their State Implementation Plans (SIPs) to attain the NAAQS for $PM_{2.5}$. However, current SIPs for $PM_{2.5}$ focus on direct emissions of $PM_{2.5}$, and emissions of other precursors – SO_2, NO_X, and organic compounds. In the U.S., NH_3 is the largest volume air pollutant for which no national or regional control program has been developed. In addition, wet deposition of NH_4^+ has increased in much of the U.S. by ~22% in the last 20 years (Li *et al*, 2016).

The lack of regulatory attention for NH_3 emissions is understandable. Although the adverse impacts of NH_3 emissions are significant, they are also subtle, so that the effect of any given source can be difficult to ascertain. For instance, NH_3 alone cannot produce elevated concentrations of $PM_{2.5}$; it must react with sulfates and nitrates in the atmosphere. The concentration of NH_3 necessary to contribute to an exceedance of the NAAQS for $PM_{2.5}$ is less than 10 ppbv, while the odor threshold for NH_3 is 2.6 ppmv, or 2,600 ppbv (Smeets *et al*, 2006, tested using guidelines by the European Committee for Standardization). Thus, an amount of NH_3 which is imperceptible to human senses can contribute to an exceedance of the $PM_{2.5}$ standard. Similarly, the impacts of NH_3 deposition on eutrophication or species diversity are also difficult to separate from the impacts of other factors.

Atmospheric chemistry models such as the Community Multiscale Air Quality (CMAQ) model (Byun and Schere, 2006) are used to simulate the reactions of NH_3 and other precursors to form $PM_{2.5}$. CMAQ can also simulate the deposition of NH_3 and NH_4^+ to terrestrial and aquatic ecosystems. This type of modeling analysis is essential in evaluating the impacts of NH_3 emissions and the potential benefits of NH_3 controls. However, CMAQ modeling of NH_3 and NH_4^+ in $PM_{2.5}$ is subject to considerable uncertainty. Validation studies of NH_3 emissions estimates in CMAQ have focused on secondary indicators such as wet deposition of NH_4^+ ions, and the concentration of NH_4^+ in $PM_{2.5}$ (Gilliland *et al*., 2006, Kelly *et al.,* 2014).

An important source of uncertainty for NH_3 modeling is the inventory of emissions used in CMAQ (Battye *et al*, 2003). Agricultural sources account for approximately 90% of atmospheric NH_3 emissions in the U.S. (Aneja *et al.,* 2009). These emissions emanate primarily from animal waste management and synthetic nitrogen fertilizer application (Battye *et al.,* 2002). NH_3 emissions estimates are calculated by applying emission factors and emission models to the agricultural census (U.S. EPA, 2009). These emissions are allocated to different times of the year and to geographic modeling grids using temporal and spatial allocation factors, which add to the uncertainty of model emissions estimates.

1.3. Data and Methods

The availability of data on atmospheric NH_3 has increased substantially in recent years. These data include *in situ* aircraft measurements, ground level concentration measurements, and satellite-based estimates of atmospheric NH_3 based on infrared absorption. Aircraft measurement programs provide rich datasets for the analysis of air pollution through the vertical profile of the atmosphere. However, any given measurement campaign must necessarily be restricted in its duration and geographical scope. The network of ground level monitors for NH_3 is also sparse.

Satellite retrievals of NH_3 are of particular interest, because they provide spatial coverage and resolution superior to the ground-based measurement network. This current study aims to make use of all of these types of measurements to evaluate the handling of NH_3 in the NAQFC air quality model, and to identify potential improvements to emissions estimates for NH_3 in the U.S.

1.3.1. Air Quality Model

This work is being carried out in collaboration with the U.S. National Oceanic and Atmospheric Administration (NOAA) Air Resources Laboratory, which is responsible for forecasting elevated levels of air pollution within the National Air Quality Forecast Capability (NAQFC) (Tang *et al*., 2015). NOAA uses the Community Multiscale Air Quality (CMAQ) model version 5.0.2 to predict air pollutant concentrations for the continental U.S. (Byun and Schere, 2006, CMAS 2016). Meteorological predictions to drive the air quality model are generated using the Weather Research and Forecasting Advance Research WRF (WRF-ARW) regional meteorological model. The horizontal resolution of both models is 12 km, with 42 vertical layers with a domain top at 50 hectopascals (hPa). The height of the lowest vertical layer was 8 meters above the ground. Aerosol chemistry is based on the AERO5 module of CMAQ version 4.7.1 (Binkowski and Shankar, 1995), and dry deposition computed for NH_3 is based on the M3Dry module (Mathur *et al*., 2005). The configuration of the CMAQ and WRF-ARW models within the NAQFC is described in more detail in Tang *et al*. (2015). Air pollutant emissions for the NAQFC are derived from the National Emissions Inventory (NEI), prepared every three years by the U.S. Environmental Protection Agency (U.S. EPA).

CMAQ includes an optional bidirectional surface exchange model for NH_3 (Cooter *et al*. 2012; Bash *et al*. 2013; Pleim *et al*. 2013). This model allows for the potential evaporation of NH_3 to the air from vegetated landscapes, offsetting the NH_3 deposition flux and resulting in

higher atmospheric concentrations of NH_3. In testing of the bidirectional flux model, predicted atmospheric NH_3 concentrations were 10% higher, on average, than previous predictions with the unidirectional deposition flux approach (Cooter *et al*. 2012; Bash *et al*. 2013). This difference was larger in areas with denser NH_3 emissions. The current research includes a mixture of analyses with and without the bidirectional NH_3 exchange option.

1.3.2. Ground Level Measurement Networks for NH_3 Vapor and NH_4^+ in Airborne Particulate Matter

The Ammonia Monitoring Network (AMoN) has recently become a source of data on long-term NH_3 gas concentrations across the U.S. (NADP 2014) which can be used to evaluate CMAQ NH_3 predictions. The density of AMoN sites has been somewhat limited, but is improving – from 55 sites nationwide in 2011 to about 100 sites in 2015. AMoN monitors use passive diffusion collectors which are changed every two weeks. The detection limit of the AMoN passive sampler is approximately 0.16 ppbv for samples collected over a two-week period, with an accuracy of $\pm$41% (Puchalski *et al*, 2011) and an average bias of −9% compared with an annular denuder system (Puchalski *et al*, 2015). Many AMoN sites are collocated with Clean Air Status and Trends Network (CASTNET) sites which analyze the concentration of NH_4^+ and other ionic species in airborne particulate matter. CASTNET measurements for NH_4^+ have a precision of ±20% (AMEC, 2013; U.S. EPA, 2018a).

NAQFC CMAQ NH_3 predictions are compared with these passive sampler measurements. NH_3 concentration results were extracted for the grid cells surrounding each monitor location, in the lowermost model layer. The model grid cell results were interpolated to the monitor location sites and averaged for the passive sampler measurement periods. The rate of conversion of gaseous NH_3 to particulate NH_4^+ is a potential source of discrepancy between the

modeled and measured NH_3 concentrations. Therefore, we also compare modeled and measured values for particulate NH_4^+, and for NH_X, the sum of gaseous NH_3 and particulate NH_4^+.

1.3.3. Local and Regional Measurements with Ground-Based and Aircraft-Based Continuous Monitors

Continuous measurements of NH_3 vapor have been made as part of locally- and regionally-targeted studies. In addition, some intensive field measurement campaigns have included continuous aircraft-based measurements of gaseous NH_3, particulate NH_4^+, and other pollutants as the aircraft flies over the target region. In the current research, we used these aircraft-based continuous monitoring results for a study of model performance in Northeastern Colorado, and ground-based continuous monitoring results for a study of North Carolina. These measurements are described in detail in the Data and Methods sections of Chapters 2 and 3.

1.3.4. Satellite Measurements

This research also draws on estimates of atmospheric NH_3 from three satellite measurement systems. These three systems are the Tropospheric Emission Sounder (TES) on the Aura satellite, the Atmospheric Infrared Sounder (AIRS) on the Aqua satellite, and the Infrared Atmospheric Sounding Interferometer (IASI) on the MetOp satellite. Table 1-2 summarizes the differences between these satellite measurements. In each case, NH_3 concentrations are retrieved from the spectrum of infrared radiation measured above the atmosphere (at an altitude of 702 to 817 km). The retrieval algorithms rely on the change in infrared intensity across a number of specific wavelength bands covering absorption bands for NH_3 (Shephard *et al*, 2012; Warner *et al*, 2016; Van Damme *et al*, 2017; and Whitburn *et al*, 2015).

Retrievals are available for historic NH_3 concentrations starting in 2003 for AIRS, 2004 for TES, and 2008 for IASI. Another system, the Cross-track Infrared Sounder (CrIS), was

Table 1-2. Comparison of satellite measurements for NH_3

	TES	IASI	AIRS
Dates of NH_3 retrievals	2004 – present	2008 – 2016	2002 – 2015
Time of satellite passage	~1:30 pm	~10 am	~1:30 pm
Retrieval frequency for a given location	16 days	~1 day	~2 days
Footprint or spatial resolution	5 km x 8 km	~$(12\ km)^2$	$(45\ km)^2$
Spectral frequencies used (cm^{-1})	960–970	800–1200	860–875, 928–932, 965–967
Spectral resolution	~0.5 cm^{-1}	~0.5 cm^{-1}	~0.1 cm^{-1}
Parameters retrieved	Ground level concentration Vertical profile Total column	Total column loading	Concentration at 918 hPa
Method	Optimal estimation *a priori* from GEOS-CHEM	Neural network No *a priori* assumption	Optimal estimation *a priori* from GEOS-CHEM

launched in 2011 on the Suomi NPP satellite. NH_3 retrievals for this system have not yet been made publicly available, but may become available in the near future (Shephard and Cady-Pereira, 2015). CrIS will provide temporal and spatial resolution similar to AIRS and IASI, with an improved spectral resolution and the potential for improved accuracy.

In each case, a forward radiative transfer model (RTM) is used to compute the expected intensity of radiation in the selected bands at the top of the atmosphere. The RTM requires input information on the atmospheric density, relative humidity and concentrations of other trace gases. For the TES and AIRS retrievals, an *a priori* assumption is made for the concentration of NH_3. The retrieval for NH_3 is carried out after retrievals for temperature and other trace gases. The concentration profile of NH_3 is computed to minimize the error between the spectrum predicted by the RTM and the spectrum actually measured by the satellite. This results in an estimate of the concentration of NH_3 for the region sensed by the satellite. In the current study, only those measurements which pass quality assurance checks were used.

The estimated concentration of NH_3 is affected by and may tend to be biased toward the *a priori* assumption made for NH_3. In addition, the satellite is seeing an absorption by the entire atmospheric column. Although the retrieval algorithm is used to estimate the vertical distribution of NH_3, this vertical distribution is also subject to uncertainties and is affected by the *a priori* assumption. The IASI retrieval is the only case where no *a priori* assumption is made for NH_3.

1.3.5 Model-to-Measurement Comparisons

Prediction accuracy for the NAQFC CMAQ model is quantified by computing the normalized mean bias (NMB), and the ratio of the average measured concentration to the average model prediction ($R_{o/m}$):

$$NMB = \frac{\sum_{i=1}^{N}[C_{mod}(i) - C_{obs}(i)]}{\sum_{i=1}^{N} C_{obs}(i)}$$

and:

$$R_{o/m} = \frac{\sum_{i=1}^{N} C_{obs}(i)}{\sum_{i=1}^{N} C_{mod}(i)}$$

where $C_{mod}(i)$ and $C_{obs}(i)$ are, respectively, the model prediction and the observed concentration at a given location and time, and N is the number of observations. $R_{o/m}$ and NMB are related to one another as follows:

$$NMB = \frac{1}{R_{o/m}} - 1$$

The Pearson correlation coefficient (r) and the concordance correlation coefficient (ρ_c) are used to evaluate correlation of the measured concentrations with predicted concentrations. The concordance correlation coefficient is also known as the reproducibility index, and gives a more rigorous test of whether modeled values predict observed values (Lin, 1989, 1992).

1.4. Objectives

The objectives of this research are:

1) To evaluate the performance of the NAQFC CMAQ model for predicting atmospheric concentrations of NH_3 using available measurement data from aircraft and ground based monitors.

2) To evaluate the potential for using satellite retrievals of NH_3 to test model simulations.

3) To use the CMAQ, coupled with satellite retrievals and other measurement data, to identify potential improvements in the emission inventory for NH_3, including the spatial and temporal allocation of emissions.

4) To assess trends in atmospheric NH_3 concentrations over the past decade.

Chapter 2

Evaluation of Model Predictions in Northeastern Colorado

A detailed local analysis was carried out using measurements gathered in the DISCOVER-AQ Colorado field campaign and the concurrent Front Range Air Pollution and Photochemistry Experiment (FRAPPE) to test performance of the NAQFC CMAQ modeling framework for predicting NH_3. The DISCOVER-AQ Colorado field campaign and the FRAPPE campaign were was carried out from July 17 through August 10, 2014 in the Front Range of the Rocky Mountains in Northeast Colorado (Battye *et al*, 2016). These included in-situ aircraft measurements, ground-based measurements, and satellite measurements. Figure 2-1 shows the locations of the aircraft flights, ground level monitors, and the swath of satellite measurements.

2.1. Data and methods

2.1.1. Air Quality Model

This work is being carried out in collaboration with the U.S. National Oceanic and Atmospheric Administration (NOAA) Air Resources Laboratory, which is responsible for forecasting elevated levels of air pollution within the National Air Quality Forecast Capability (NAQFC) (Tang *et al*., 2015). NOAA uses the Community Multiscale Air Quality (CMAQ) model version 5.0.2 was used to predict air pollutant concentrations for the continental U.S. (Byun and Schere, 2006, CMAS 2016).

Meteorological predictions to drive the NAQFC CMAQ model are generated using the Weather Research and Forecasting Advance Research WRF (WRF-ARW) regional meteorological model.

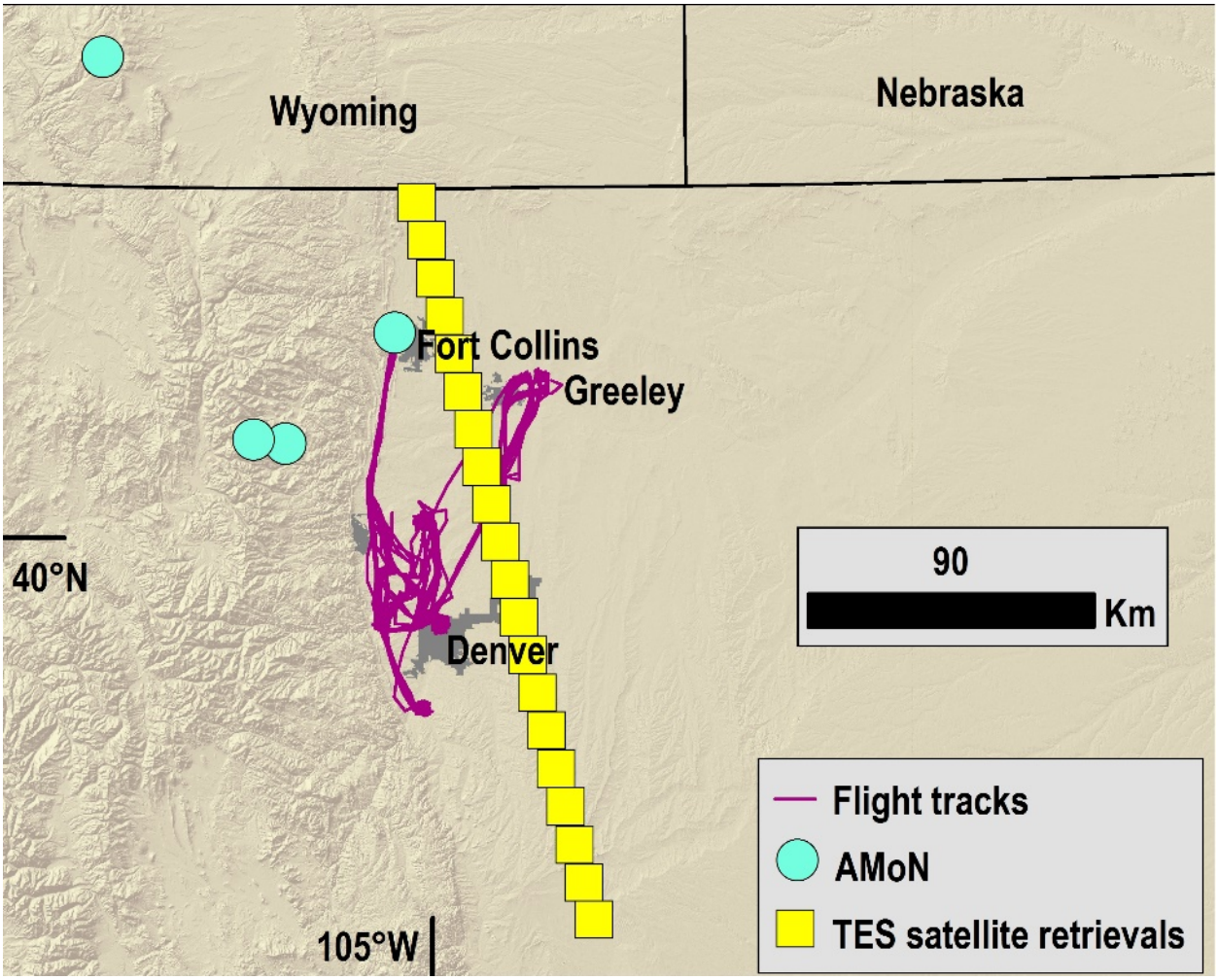

Figure 2-1. Domain of the DISCOVER-AQ Colorado measurement campaign, showing flight paths for low level in situ aircraft measurements, locations of ground level monitors, and the path for TES satellite measurements.

The horizontal resolution of both models is 12 km, with 42 vertical layers with a domain top at 50 hPa. More vertical layers are used below 1 km. The height of the lowest vertical layer is 8 meters above the ground within the DISCOVER-AQ domain. The configuration of the CMAQ and WRF-ARW models within the NAQFC is described in more detail in Tang *et al*. (2015).

Air pollutant emissions for the NAQFC are derived from the U.S. National Emissions Inventory (NEI). At the time of the Colorado field study, the 2005 NEI was being used, with several major updates as described in Tong *et al* (2015). For NH_3, the NEI provides county-level estimates of annual emissions. These annual emissions estimates are allocated the 12-km model grid and to hourly values using the Sparse Matrix Operator Kernel Emissions (SMOKE) system (Vukovich and Pierce, 2002). Aerosol chemistry is based on the AERO5 module of CMAQ version 4.7.1 (Binkowski and Shankar, 1995), and dry deposition computed for NH_3 is based on the M3Dry module (Mathur *et al*., 2005).

2.1.2. Aircraft Measurements

We compared NAQFC CMAQ model predictions of gaseous NH_3 with measurements made in flight by a Lockheed P3B Orion aircraft operated by the National Aeronautics and Space Administration (NASA). The rate of conversion of gaseous NH_3 particulate NH_4^+ is a potential source of discrepancy between the modeled and measured NH_3 concentrations. Therefore, we also compared modeled and measured values for the sum of gaseous NH_3 and particulate NH_4^+, NH_X. The aircraft measurements were made at elevations ranging from ground level to 5 km above ground level, and included upward spirals, downward spirals, and transect flights in the Front Range of the Rocky Mountains, around Denver, Boulder, Fort Collins, and Greeley, Colorado.

The measured values of NH_3 and NH_4^+ were obtained from the DISCOVER-AQ Colorado field campaign archive. P3B aircraft measurements of NH_3 and NH_4^+ are described in detail in Müller *et al*. (2014) and Sun *et al*. (2015). Ambient air was directed to an array of instruments located on-board the aircraft. NH_3 was measured using a proton transfer reaction time-of-flight mass spectrometer (PTR-MS). NH_3 concentrations were measured every 10 s; and 1-minute averages were also computed. The 1-minute averages were used for model-to-measurement comparisons.

The PTR-MS measurement system for NH_3 was evaluated in a previous DISCOVER-AQ campaign in the San Joaquin Valley of California (Sun *et al.,* 2015). The PTR-MS system was found to have a measurement accuracy of ±35% and a 1σ measurement precision of 5.5–6.5 ppbv at 1 s time resolution, or 0.75 ppbv for a 1-minute average. This variability results in a low signal-to-noise ratio, especially for NH_3 in the free troposphere, where concentrations are below 1 ppbv. In order to reduce the impact of this low measurement precision, our comparisons of aircraft data with model predictions focus on measurements made at altitudes below 1,000 m above ground level, as measured by radar.

Concentrations of NH_4^+ aerosol, and other soluble aerosols were measured by a Particle-into-Liquid-Sampler followed by ion chromatography (PILS-IC). The NH_4^+ concentration was recorded every minute. In side-by-side comparisons, the NASA PILS-IC system showed good correlation with filter measurements, giving a slope of ~0.93, intercept of ~0.24 μg m^{-3}, and r-value of 0.94. Precision for calculated at ~0.4 μg m^{-3}. (Orsini *et al*, 2003).

As air pollutant concentrations were recorded, the location, altitude, speed, bearing, and angle of ascent or descent were recorded using data from the aircraft navigation system and global positioning system (GPS). The height above ground level was also measured using radar.

NAQFC model predictions of NH_3 and NH_4^+ were extracted for comparison with for each 1-minute average aircraft measurement. The NAQFC model prediction at a given measurement location and time is computed by 4-dimensional interpolation across space and time, using the model grid cells surrounding the measurement point at the appropriate model layer height.

2.1.3 Satellite Measurements

NAQFC model predictions were also compared with NH_3 concentrations retrieved from infrared spectra gathered by the TES instrument on the Aura satellite. TES performed 5 transect measurements over the DISCOVER-AQ study domain between July 29 and August 14, 2014. These were all daytime passes, between 1:00 and 1:30 PM local standard time.

The NH_3 retrievals rely on the change in intensity of infrared radiation across a number of specific wavelength bands which are chosen to cover a sharp feature in the NH_3 infrared absorption spectrum (940–970 cm^{-1}). A forward radiative transfer model (RTM) is used to compute the expected intensity of radiation in the selected bands at the top of the atmosphere. The RTM requires input information on the atmospheric density, relative humidity and concentrations of other trace gases, as well as an a priori assumption on the concentration of NH_3. The retrieval for NH_3 is carried out after retrievals for temperature and other trace gases. The assumed concentration profile of NH_3 is varied to minimize the error between the spectrum predicted by the RTM and the spectrum actually measured by the satellite. This results in an estimate of the concentration of NH_3 for the region sensed by the satellite. (Shephard *et al*, 2012). In the current study, only those measurements which passed TES quality assurance checks were used (Species Retrieval Quality = 1).

The estimated concentration of NH_3 is affected by and may tend to be biased toward the a priori assumption made for NH_3. In addition, the satellite is seeing an absorption by the entire

atmospheric column. Although the retrieval algorithm is used to estimate the vertical distribution of NH_3, this vertical distribution is also subject to uncertainties and is affected by the *a priori* assumption.

2.2. Results and Discussion

2.2.2. Comparison of Model Predictions with in Situ Aircraft Measurements

Table 2-1 summarizes the results of the comparison of *in situ* aircraft measurements with model predictions for of NH_3, NH_4^+ in $PM_{2.5}$ and NH_X. For each measurement location, the corresponding NAQFC model prediction was interpolated based on the surrounding grid cells at the appropriate model layer heights. The concentration pairs were then compared directly, without any adjustment for altitude. The aircraft measurements were carried out during the day, and our comparisons were restricted to measurements taken below 1000 m in altitude. Therefore, these measurements are generally within the well-mixed planetary boundary layer (Arya, 1999). The average measured NH_3 concentration was 6.1 ppbv (3.9 μg/m^3), with a standard deviation of 6.9 ppbv (4.2 μg/m^3) and a maximum measured value of 90.0 ppbv (53.1 μg/m^3). In comparison, the average model prediction at the locations and times corresponding to these measurements was 2.2 ppbv (1.4 μg/m^3). The standard deviation of the model prediction was 1.6 ppbv (1.4 μg/m^3) and the maximum model prediction was 15.3 ppbv NH_3 (9.1 μg/m^3). The average measured concentration of NH_3 was a factor of 2.7 higher than the average of model predictions at the sample locations. This corresponds to a normalized mean bias for NH_3 of –63%.

The average measured concentration of particulate NH_4^+ was 0.29 μg/m^3, which reflects an average conversion of 7% of NH_3 to NH_4^+. The average model prediction was 0.34 μg/m^3, corresponding to an average conversion of 23%. The ratio of the average measured concentration on particulate NH_4^+ to the average model prediction was 0.85, corresponding to a normalized

Table 2-1. Comparison of ground-based measurements with model predictions for NH_3.

	NH_3 (ppbv)	NH_3 ($\mu g/m^3$)	NH_4 ($\mu g/m^3$)	NH_X ($\mu g/m^3$)
Measured concentrations				
Average	6.1	3.9	0.29	4.2
Standard deviation	6.9	4.2	0.38	4.6
Maximum	90.0	53.1	2.05	53.3
Model predictions				
Average	2.2	1.4	0.34	1.7
Standard deviation	1.6	1.0	0.20	1.1
Maximum	15.3	9.1	1.46	9.2
Comparison statistics				
Normalized mean bias		-63%	18%	-60%
Ratio of average measured value to average modeled value		2.7	0.85	2.5
Correlation coefficient (r)		0.52	0.37	0.54
Concordance correl. coeff. (ρ_c)		0.16	0.29	0.17
Number of observations		2,372	1,700	1,637

mean bias of +18%. Thus, the underestimation of gaseous NH_3 was not accompanied by an underestimation of particulate NH_4^+. However, the relative magnitude of predicted NH_3 gas and particulate NH_4^+ suggests that the formation of NH_4^+ was not limited by availability of NH_3.

The results of a comparison for NH_X (the combination of NH_3 vapor and particulate NH_4^+) are similar to the results for gaseous NH_3 alone. The average measured concentration of NH_X is a factor of 2.5 higher than the average of corresponding model predictions, and the normalized mean bias is an under-prediction of 60%. These values are slightly lower than the values for NH_3 vapor alone.

Figure 2-2a plots the measured concentrations of NH_3, on the y-axis, against model predictions on the x-axis. Figures 2-2b and 2-2c provide similar plots for NH_4^+ and NH_X, respectively. Each measurement is plotted as a point. Two lines are also included in each plot. The dotted lines show a 1:1 slope, where points would have fallen if the measurements and model predictions were in complete agreement (measured = modeled). The dashed lines show the 1:1 slope displaced by the NMB.

The graphs in Figure 2-2 show substantial scatter for all three pollutants. In all three cases, high measured values can occur where model predictions are low, and vice versa. For both NH_3 and NH_X, the majority of measurements fall above the prediction line (measured = modeled). For NH_4^+, the measurements fall evenly on both sides of the line.

Figure 2-3 compares a histogram of the measured NH_3 concentration with a histogram of the modeled NH_3 concentration. The figure illustrates that the distribution of model predictions falls off much more swiftly than the distribution of measured concentrations. However, the structure of the two profiles is similar. Figure 5.1-3 shows that the model does not produce the full range of values found in the measured data set at the high end. The 98^{th} percentile of

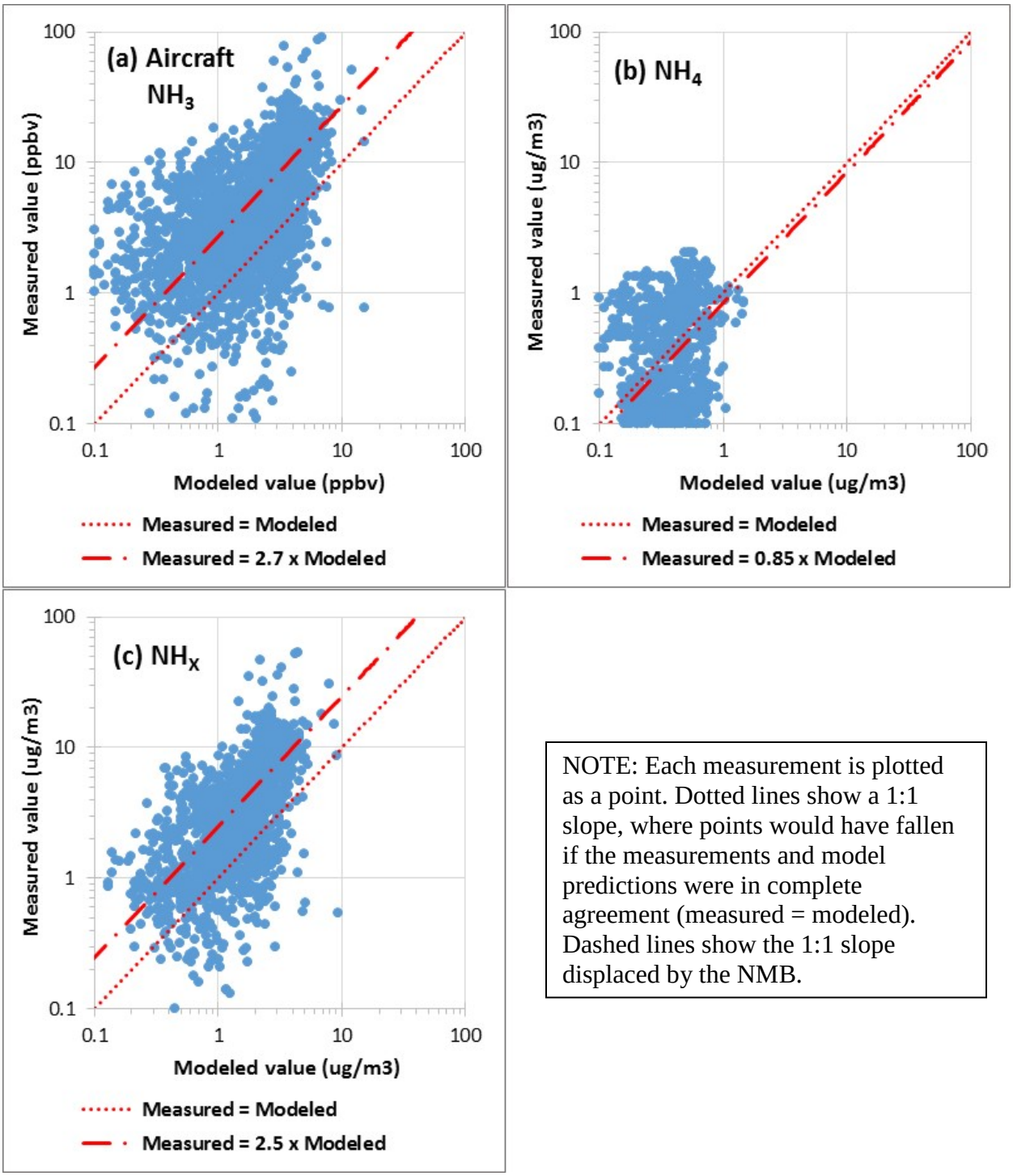

NOTE: Each measurement is plotted as a point. Dotted lines show a 1:1 slope, where points would have fallen if the measurements and model predictions were in complete agreement (measured = modeled). Dashed lines show the 1:1 slope displaced by the NMB.

Figure 2-2. Aircraft in situ measurements of NH_3 (a), NH_4^+ (b), and NH_X (c), plotted against model predictions.

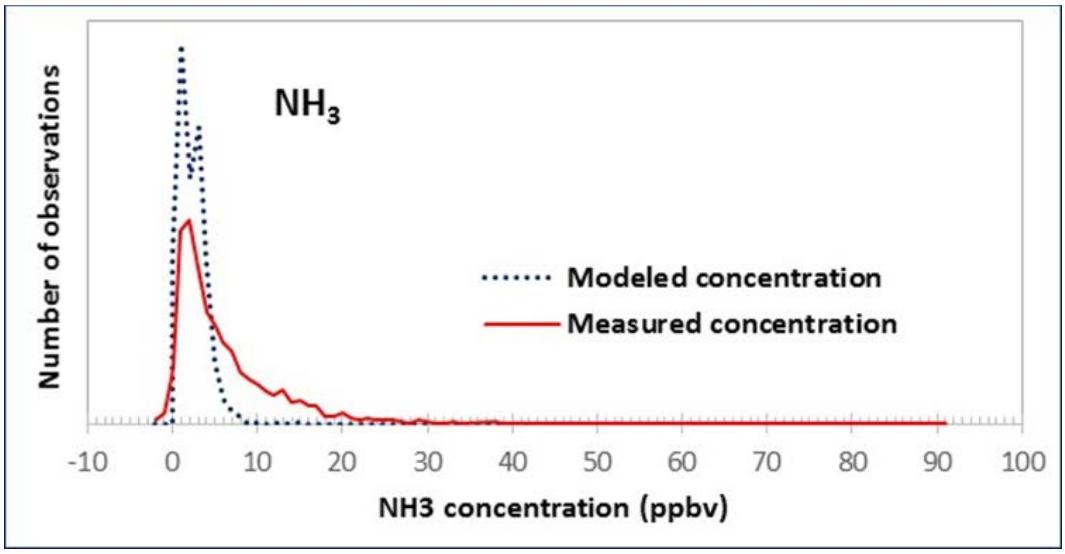

Figure 2-3. Histogram of aircraft measurements compared with histogram of model predictions at the corresponding times and locations.

measured values was 23 ppbv while the 98th percentile level of corresponding modeled values was 6 ppbv. However, Figure 2-2a shows that the underestimation in not restricted to the high end, but affects the full range of NH_3 concentrations.

In order to identify spatial patterns in the model prediction error, NMB and $R_{o/m}$ were computed using the *in situ* aircraft measurements within each 12-km modeling grid. Figure 2-4 presents the results of this analysis. In the figure, a background raster (in blue) shows the average NAQFC CMAQ prediction during the DISCOVER-AQ campaign. Round icons indicate the ratio of the average measured concentration to the average model prediction ($R_{o/m}$). The largest differences between modeled and measured NH_3 were around Greeley, in Weld County.

Over 1,300 cattle operations are located in Weld County (USDA, 2014), including two feedlots which are among the largest in the U.S. (CSU, 2016). The inventory of cattle in Weld County is over 500,000, the 3rd largest cattle population of any U.S. county (USDA, 2014). The concentration of cattle operations in the Greeley area resulted in model predictions of NH_3 which were higher than those in the rest of the modeling region. Measured NH_3 in the Greeley area were a factor of 3 to 4.3 higher than the model predictions. Similar ratios of measured-to-modeled NH_3 were found near Denver; however the magnitude of both modeled and measured NH_3 concentrations were lower than in the area around Greeley.

Each of the icons for $R_{o/m}$ in Figure 2-4 represents multiple measurements (85 on average), with the icon at the Northeastern of the loop near Greeley representing 113 measurements. Nevertheless, these measurements are localized along the path of the aircraft. Thus, it is possible that the measurements are affected by local hotspots of NH_3, so that the large values of $R_{o/m}$ may apply to only a fraction of the modeling grid.

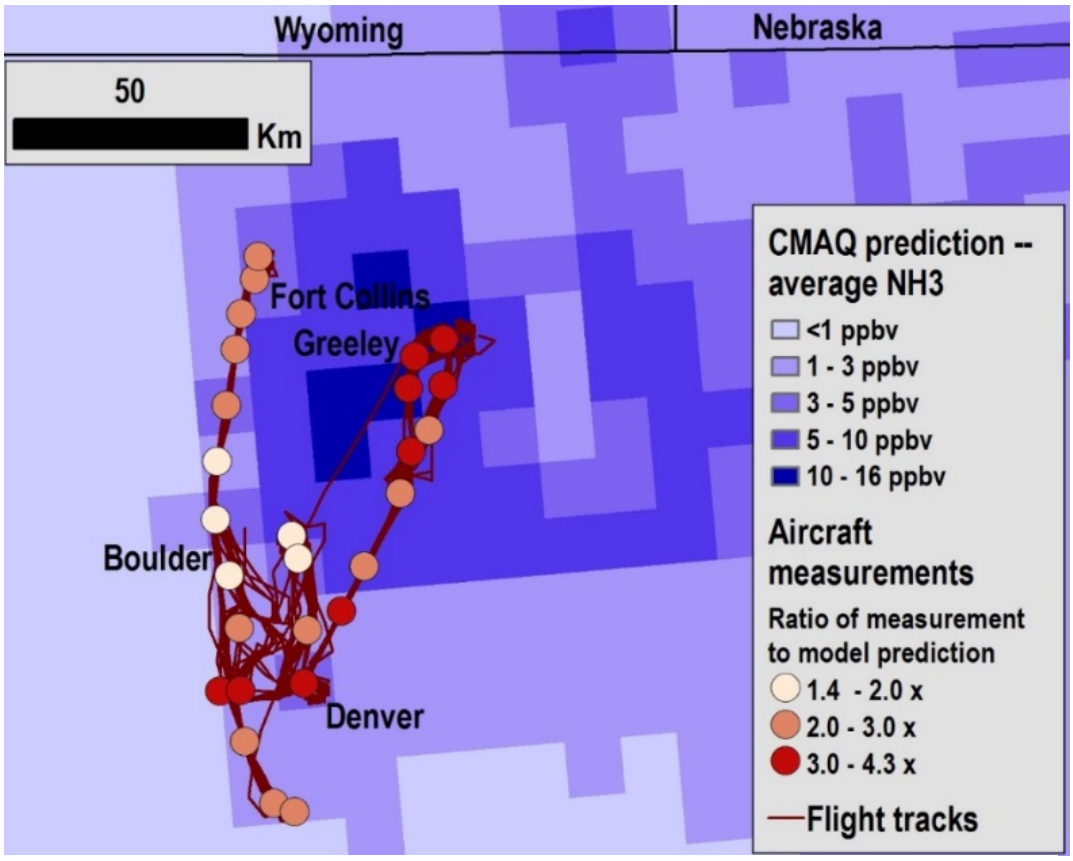

Figure 2-4. Spatial variation of model prediction error from in situ aircraft measurements.

In summary, the average concentration of NH_3 measured by in situ aircraft sampling was a factor of 2.7 higher than the average of model predictions at the sample locations. However, the underestimation of gaseous NH_3 was not accompanied by an underestimation of particulate NH_4^+. The under prediction of NH_3 was more pronounced in an area around Greeley with high NH_3 emissions. In addition, the highest concentrations of NH_3 predicted by the model were considerably lower than the highest measurements.

2.2.2. Model Predictions Compared with Ground Level Passive Measurements

Table 2-2 and Figure 2-5 summarize the results of the comparison of measured concentrations with model predictions for 3 passive NH_3 samplers operated under the AMoN network. One of the AMoN sites is located in Fort Collins, Colorado, with the Rocky Mountains to the west and an agricultural region to the east. The remaining three AMoN sites are in remote areas, including two in the Rocky Mountain National Park. In each comparison between the model and a ground-level measurement, we computed the average model prediction for the entire duration of the ground-level measurement (14 days). Thus, the measurement and the model prediction were compared on the same basis, from the standpoint of averaging time.

The average measured NH_3 concentration for the AMoN all ground-level passive monitors was 3.3 ppbv (2.0 $\mu g/m^3$), with a standard deviation of 3.8 ppbv (2.3 $\mu g/m^3$) and a maximum measured value of 11.6 ppbv (6.8 $\mu g/m^3$). In comparison, the average model prediction at the locations and times corresponding to these measurements was 1.1 ppbv (1.3 $\mu g/m^3$). The standard deviation of the model prediction was 0.7 ppbv (0.8 $\mu g/m^3$) and the maximum model prediction was 3.5 ppbv NH_3 (2.1 $\mu g/m^3$). The average measured concentration of NH_3 was a factor of 3.0 higher than the average of the corresponding model predictions. The

Table 2-2. Comparison of ground-based measurements with model predictions for NH_3.

	NH_3 concentration	
	ppbv	µg/m^3
Measured concentrations		
Average	3.3	2.0
Standard deviation	3.8	2.3
Maximum	11.6	6.8
Model predictions		
Average	1.1	0.7
Standard deviation	1.3	0.8
Maximum	3.5	2.1
Comparison statistics		
Normalized mean bias	-67%	
Ratio of average measured value to average modeled value	3.0	
Correlation coefficient (r)	0.97	
Concordance correl. coeff. (ρ_c)	0.45	
Number of observations	8	

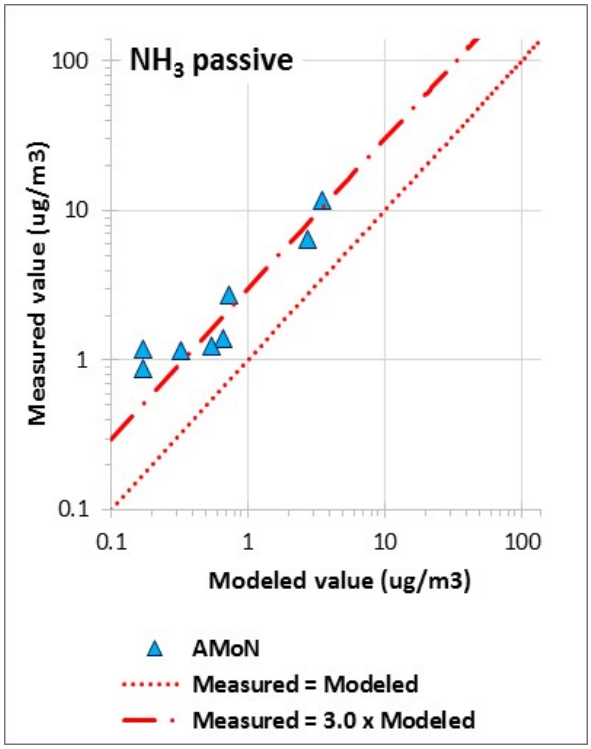

Figure 2-5. Ground-level measurements of NH_3 plotted against model predictions.

normalized mean bias (NMB) for NH_3 was an under-prediction of 67%. This bolsters the result for in situ aircraft measurements, discussed above.

2.2.3. Model Predictions Compared with Satellite Retrievals

Table 2-3 and Figure 2-6 compare NAQFC CMAQ model predictions with NH_3 concentration estimates retrieved from TES satellite spectroscopic measurements. Three separate comparisons were made: one using the estimated total atmospheric column loading, the second using the estimated concentration in the lowest layer of the atmosphere, and the third using the estimated concentration at an altitude of 1740 m above ground level (AGL). This is the altitude where the averaging kernel indicates that the retrieved concentration from the satellite measurement is most sensitive to the actual atmospheric concentration. The NMB for the model prediction of total column loading (−76%, $R_{o/m}$ = 4.2) is somewhat more negative than the NMB for the comparisons with aircraft data and ground level monitoring data. The model prediction for the lowest layer of the atmosphere has a less negative NMB (−33%, $R_{o/m}$ = 1.5) than the prediction for total column loading, or than the comparisons with aircraft and ground level monitor data. The average TES retrieval for the lowest layer of the atmosphere is also lower than concentrations measured in the same region by aircraft (Table 2.1). The NMB of the model prediction at 1740 m AGL (−53%, $R_{o/m}$ = 2.1) is midway between the results for the total column loading and the ground level concentration. Model predictions for this altitude also give a better correlation with the satellite retrieval (r = 0.52) than the ground level concentration (r = 0.09) or the total column loading (r = 0.11).

The NMB from the satellite data analysis is subject to considerable uncertainty, as highlighted by the variability among the different satellite metrics for NH_3 (Table 2-3). However,

Table 2-3. Comparison of TES retrievals with model predictions for NH_3.

	Total atmospheric column loading (mg/m^2)	Concentration in the lowest atmospheric layer		Concentration at the regional averaging kernel peak (ppbv)
		ppbv	$\mu g/m^3$	
Measured concentrations				
Average	2.0	3.0	1.8	0.83
Standard deviation	2.9	4.5	2.7	1.1
Maximum	14.9	21.8	12.9	4.5
Model predictions				
Average	0.5	2.0	1.2	0.39
Standard deviation	0.4	2.1	1.3	0.54
Maximum	1.5	9.2	5.4	2.6
Comparison statistics				
Normalized mean bias	-76%	-33%		-53%
Ratio of average measured value to average modeled value	4.2	1.5		2.1
Correlation coefficient (r)	0.11	0.09		0.52
Concordance correl. coeff. (ρ_c)	0.02	0.07		0.39
Number of observations	65	65		65

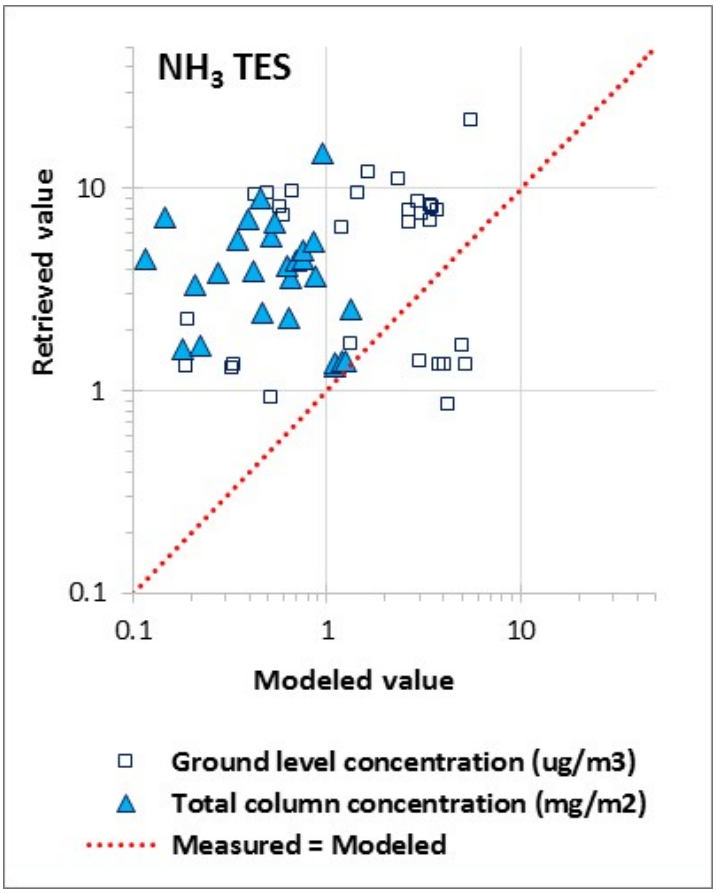

Figure 2-6.TES NH3 retrievals plotted against model predictions.

the satellite results for NH_3 are in agreement with the aircraft and ground-level results discussed above.

2.2.4. Satellite Retrievals Compared with Aircraft Measurements

The TES satellite swath was not aligned with aircraft spiral measurements; however, a number of aircraft flight paths crossed the satellite swath close to the time of satellite passage. We identified 46 *in situ* observations which occurred within an hour of a TES satellite pass, and within 15 km of the center of the satellite swath. These *in situ* measurements were compared with the TES NH_3 retrievals for the atmospheric layer corresponding to the aircraft elevation. Table 2-4 and Figure 2-7 summarize the results of this comparison. The average of aircraft measurements overlapping the TES track was 2.9 ppbv, with a standard deviation of 2.4 ppbv, and a maximum value of 8.1 ppbv. The average of TES retrievals corresponding to these measurement locations was 2.8 ppbv, with a standard deviation of 2.5 ppbv, and a maximum value of 6.6 ppbv. Thus, the normalized mean bias of the TES retrieval with respect to the *in situ* measurement was only –1%. The correlation coefficient (r) and concordance correlation coefficient between the TES retrieval and the aircraft measurement are both 0.78. thus, the TES results exhibit good correlation with the aircraft measurements.

2.2.5. Analysis of Model Bias in Relation to Previous Studies and the NH_3 Emissions Inventory

Gilliland *et al* (2006) performed inverse modeling in order to evaluate the emissions inventory for NH_3 for the U.S. Measurements of NH_4^+ in precipitation were used with a 2001 CMAQ simulation for the continental U.S. Annual emissions estimates were found to be reasonable on average, but inverse modeling results indicated that the NH_3 emissions inventory was too high in winter and too low in summer. On a domain-wide basis, the posterior NH_3

Table 2-4. Comparison of in situ aircraft measurements with TES retrievals for NH_3.

	NH_3 (ppbv)
In situ aircraft measurements	
Average	2.9
Standard deviation	2.4
Maximum	8.1
TES retrievals	
Average	2.8
Standard deviation	2.5
Maximum	6.6
Comparison statistics	
Normalized mean bias of TES retrieval	-1%
Ratio of average measured value to average TES retrieval	1.01
Correlation coefficient (r)	0.78
Concordance correl. coeff. (ρ_c)	0.78
Number of observations	46

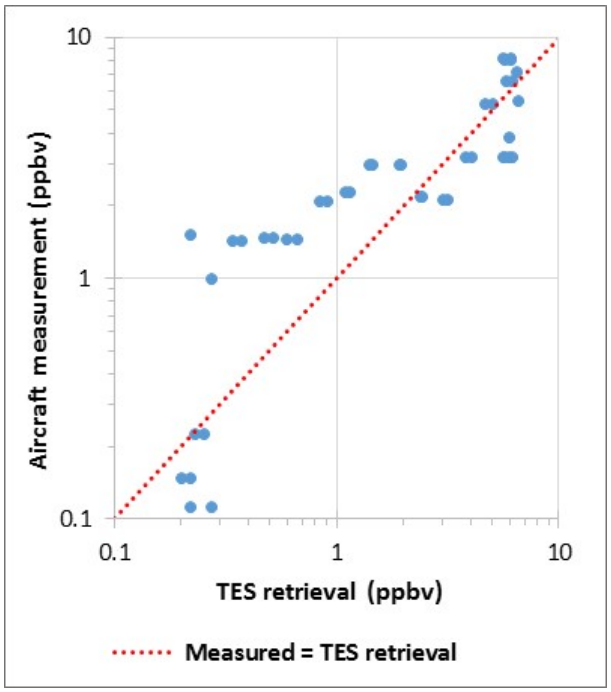

Figure 2-7. Aircraft in situ measurements of NH_3 plotted against TES satellite retrievals.

emissions inventory for the July-August timeframe was 17% higher than the prior inventory. Smaller-scale analyses of the data suggested that the error may have been higher in the western U.S., however these results were unstable due to low precipitation rates.

Butler *et al* (2014) evaluated CMAQ predictions in Susquehanna River Watershed of New York and Pennsylvania using ambient concentration measurements conducted in 2008 and 2009. The model estimates were lower than measured values by 8% to 60%.

Kelly *et al* (2014) evaluated CMAQ predictions in the San Joaquin Valley of California using measurements from the measurement campaign for "California Research at the Nexus of Air Quality and Climate Change" (CalNex) in May and June of 2010. The study analyzed multiple pollutants, including NH_4^+ and NH_3. The model performed well for NH_4^+. NH_3 was over-predicted in some urban areas; however, this was attributed to errors in prediction of the mixing layer behavior. The model under-predicted NH_3 in agricultural regions. In addition, model predictions did not capture the large variations in measured NH_3.

Zhu *et al* (2013) performed inverse modeling of ambient NH_3 in the Continental U.S. using TES satellite data in conjunction with the GEOS-Chem model. TES data were assimilated for April, July, and October of 2006 through 2009. AMoN data were used to evaluate the inverse modeling results. The study found that the initial NH_3 emissions inventory appeared to be an underestimate, especially in the Western U.S.

The current study found that the NAQFC CMAQ model underestimated the NH_3 concentration in Northeastern Colorado in July and August of 2014 by a factor of ~2.7 (NMB = −63%). This difference is larger than the differences found by Gilliland *et al* (2006) and Butler *et al* (2014). However, these studies differed from the current study in important ways. The Gilliland study used deposition measurements to evaluate CMAQ predictions; and the Butler

study focused on a region of low NH_3 concentration. The findings of the current study are comparable to the findings of Kelly *et al* (2014) for an agricultural region in California. Both the current study and the Kelly study included regions with intensive agriculture. A European study using CMAQ as part of the CALIOPE-EU modeling system also found that NH_3 concentrations were underestimated in the summer months (Pay *et al*, 2012).

Measured and modeled concentrations of NH_4^+ were much lower than the measured concentration of NH_3. Therefore, any differences in the conversion of NH_3 to NH_4^+ would be too small to account for the underestimation of NH_3. Rather, the model error for NH_3 is believed to result from either the NH_3 emissions inventory, or to the rate of NH_3 deposition. The NAQFC modeling framework used in the current study did not include a recently-developed bidirectional flux algorithm for NH_3 between the bottom layer of the model and the surface. (Cooter *et al*. 2012; Bash *et al*. 2013; Pleim *et al*. 2013). Testing of the bidirectional flux model has predicted NH_3 concentrations 10% higher, on average, than previous predictions with the unidirectional deposition flux approach (Cooter *et al*. 2012; Bash *et al*. 2013). Thus, we would not expect the incorporation of bidirectional flux, by itself, to correct the underestimation of NH_3 for the DISCOVER-AQ domain.

As illustrated in Figure 2-4, the model bias varies across the DISCOVER-AQ domain, with larger differences in the neighborhood of Greeley and Denver. The Greeley area is a region of intensive agriculture, with high levels of NH_3 emissions in the 2005 NEI. Thus, NAQFC CMAQ model predictions of NH3 in this area are higher than the surrounding region. However, results of the model-to-measurement comparison indicate that emissions in the Greeley region may have been still higher than the levels reflected in the inventory.

The current study also uses NH_3 emissions estimates from the 2005 NEI, which have recently been updated in the 2011 NEI. However, the change in estimated NH_3 emissions from the 2005 NEI to the 2011 NEI was only an increase of 10% within the DISCOVER-AQ Colorado domain (U.S. EPA, 2009 and 2015). Long term NH_3 monitoring trends at the Fort Collins AMoN site also do not show an increase in measured NH_3 concentrations over this period. Figure 2-8 shows that measured concentrations in 2014 at Fort Collins fall within the range of concentrations measured for the preceding 7 years.

On the timescale of the summer measurement campaign, errors in the emissions inventory can arise not only from the overall emission factors, but also from the seasonal allocation of emissions. However, the increase in the measured NH_3 concentration at Fort Collins is less than the increase in NH_3 emissions in the modeling domain, based on the seasonal factors used in the NEI. The measured NH_3 concentration during the monitoring campaign was 1.44 times the annual average concentration at the Fort Collins site in the calendar year 2014. Based on seasonal allocation factors used in the NEI for NH_3, emissions used in July and August are 1.8 times the annual average. Thus, the underestimation in NH_3 for the campaign is not believed to result from errors in seasonal allocation.

2.3. Summary and Conclusions

This chapter describes an evaluation of the NOAA NAQFC predictions of NH_3 and NH_4^+ using a number of different data sources. The primary data source is a large set of aircraft-based *in situ* measurements from the DISCOVER-AQ Colorado campaign. In addition, data were obtained from the ground-based AMoN network, a ground-based study carried out by CSU in concert with the DISCOVER-AQ campaign, and the satellite-based TES instrument. The NAQFC model underestimated Northeastern Colorado NH_3 concentrations during the July and

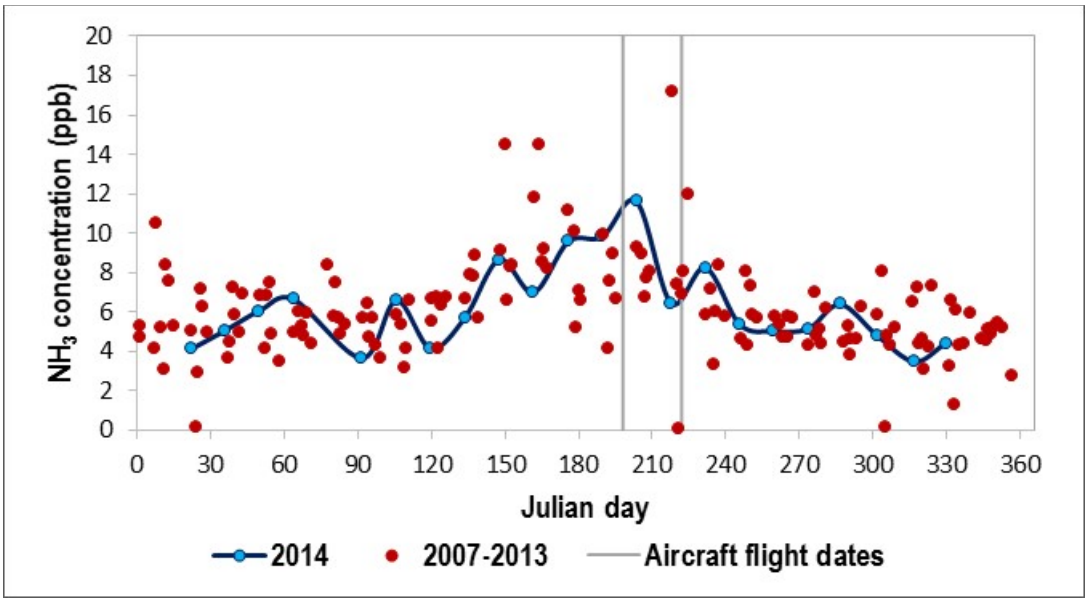

Figure 2-8. Seasonal pattern of NH_3 vapor at the Fort Collins AMoN site in 2014 compared with NH_3 vapor in previous years.

August of 2014 by a factor of ~2.7 when compared to aircraft emissions measurements. Similar results were observed for the AMoN, CSU, and TES datasets, with the model underestimating NH_3 by 1.5 to 4.2 times. However, the underestimation of gaseous NH_3 was not accompanied by an underestimation of particulate NH_4^+.

The model error for NH_3 is believed to result from either the NH_3 emissions inventory, or to the rate of NH_3 deposition. The NAQFC modeling framework did not include a recently-developed bidirectional flux algorithm for NH_3. Although the bidirectional flux algorithm could be expected to raise NH_3 concentrations in the summer months, the magnitude of this increase is not believed to be sufficient to overcome the underestimation of NH_3 which was found in this study.

The underestimation of NH_3 varied across the study domain, with the highest errors occurring in a region of intensive agriculture near Greeley, and in the vicinity of Denver. Seasonal patterns measured at an AMoN site in the region suggest that the underestimation of NH_3 is not due to the seasonal allocation of emissions, but to the overall annual emissions estimate.

Chapter 3

Evaluation of Model Predictions in North Carolina

3.1. Introduction

Ammonia (NH_3) in the atmosphere contributes to the formation of airborne fine particulate matter ($PM_{2.5}$), which is associated with a number of adverse human health effects, including aggravated asthma, irregular heartbeat, and premature death (Pope *et al*., 2009). Ammonium compounds, including ammonium sulfates [NH_4HSO_4 and $(NH_4)_2SO_4$] and ammonium nitrate (NH_4NO_3), make up a large fraction of $PM_{2.5}$ (Kwok *et al.*, 2013). NH_3 can be important in the nucleation of new particles (Holmes, 2007; Herb *et al.*, 2011). NH_3 also contributes to a cascade of other environmental impacts. NH_3 and NH_4^+ in the atmosphere are deposited through both wet and dry processes to terrestrial and aquatic ecosystems, leading to increase levels of biologically available nitrogen, termed reactive nitrogen, in these ecosystems. This can lead to eutrophication of aquatic ecosystems, and losses of species diversity (Jones, 2013; Paerl, 1988; and U.S. EPA SAB, 2007). A portion of the NH_3 and NH_4^+ is also converted to gaseous nitrous oxide (N_2O) by soil and aquatic microorganisms. This N_2O reenters the atmosphere and absorbs infrared radiation, with a climate change potential approximately 250 times that of CO_2 (IPCC, 2014). N_2O also contributes to stratospheric ozone depletion (Revell *et al*, 2015).

The National Oceanic and Atmospheric Administration (NOAA) models the emission, transport, reaction, and deposition of NH_3 and its reaction products within the framework of the U.S. National Air Quality Forecast Capability (NAQFC). The NAQFC uses the Community Multiscale Air Quality (CMAQ) model (Byun and Schere, 2006), with emission inputs from the U.S. Environmental Protection Agency (U.S. EPA), Environment and Climate Change Canada

(ECCC), and Mexico (Pan et al., 2014; Tong et al., 2015). The bulk of NH_3 emissions to the atmosphere in the U.S. emanate from agricultural operations, primarily animal waste management and synthetic nitrogen fertilizer application (Aneja *et al.,* 2009). The magnitude and distribution of agricultural NH_3 emissions are subject to considerable uncertainty (Battye *et al.,* 2003). Emission rates are calculated using emission models coupled with animal population data from the agricultural census (McQuilling and Adams, 2015). Emissions are dependent on waste handling and fertilizer application techniques, and on voluntary measures implemented to prevent losses of surplus reactive nitrogen to the environment. Limited information is available the implementation of such measures. Emission-generating activities are also allotted to different times of the year and to geographic modeling grids using temporal and spatial allocation factors, which add to the uncertainty of model emissions estimates (U.S. EPA, 2015).

The U.S. EPA has recently developed a bidirectional surface exchange model for NH_3 over agricultural land and natural ecosystems (Cooter *et al*. 2012; Bash *et al*. 2013; Pleim *et al*. 2013). This model allows for the potential vaporization of NH_3 to the air from vegetated landscapes, offsetting the NH_3 deposition flux and resulting in higher atmospheric concentrations of NH_3. In testing of the bidirectional flux model, predicted atmospheric NH_3 concentrations were 10% higher, on average, than previous predictions with the unidirectional deposition flux approach (Cooter *et al*. 2012; Bash *et al*. 2013). This difference is larger in areas with denser NH_3 emissions. NOAA is in the process of incorporating the bidirectional NH_3 flux model into the NAQFC.

Methods are needed to evaluate the capability of NAQFC model to predict NH_3 and to identify potential improvements to NH_3 emissions estimates and prediction methods. Such improvements would also help to improve predictions of reactive nitrogen deposition and $PM_{2.5}$

concentrations in the atmosphere. Some previous validation studies of NH_3 predictions in CMAQ have used secondary indicators such as wet deposition of NH_4^+ ions, and the concentration of NH_4^+ in $PM_{2.5}$ (Gilliland *et al*., 2006, Kelly *et al.*, 2014). The Ammonia Monitoring Network (AMoN) has recently become a source of data on long-term NH_3 gas concentrations across the U.S. (NADP, 2018) which can be used to evaluate NAQFC model NH_3 predictions. However, the density of AMoN sites is limited, with only 55 sites nationwide in 2011, being expanded to about 100 sites in 2015. In addition, the network measures two-week average NH_3 concentrations and, therefore, does not provide information on short term variations. Recent satellite infrared spectrometry measurements offer the opportunity to provide an additional source of atmospheric NH_3 concentration data. Satellites can provide spatial coverage and resolution superior to the ground-based measurement network.

This current study evaluates NAQFC model predictions of atmospheric NH_3 in North Carolina (NC), with a particular focus on Eastern North Carolina. This is a region of high NH_3 emissions due to a concentration of Confined Animal Feeding Operations (CAFO) for swine and poultry production. In fact, Sampson and Duplin counties in eastern North Carolina were estimated to have the highest rates of atmospheric NH_3 emissions (per land area) of all U.S. counties in the 2011 and 2014 NEI (U.S. EPA, 2015, 2018b). The North Carolina Department of Environmental Quality (NCDEQ) made hourly measurements of atmospheric NH_3 at three sites in North Carolina (Shendrikar *et al*, 2006). The longest operating site, at the Clinton Crop Research Center in Sampson County, operated from 2004 to 2015. The NCDEQ also maintains a permit database showing the locations of animal waste treatment lagoons. This information provides a unique opportunity to evaluate model performance towards potential improvement of spatial allocation used in the NEI for NH_3 emissions.

In the current study, the NAQFC model is implemented in two separate runs for the month of July 2011. The first run was a test run using the standard 2011 NEI modeling platform and including the bidirectional flux option of CMAQ. In the second run, the spatial allocation of NH_3 emissions within counties was upgraded based on actual CAFO locations from the NCDEQ permit database. Additional modifications were made for the second run based on the findings of the test run, which showed a significant overprediction of atmospheric NH_3 and a spike in NH_3 in the early evening. Because of the overprediction in the initial test run, the bidirectional flux option was not used in the second run. In addition, a revised emissions inventory was developed for North Carolina using a lower end estimate of NH_3 from swine operations. Finally, a small revision was made to the hourly allocation of NH_3 emissions.

Predictions from both the test run and the final model evaluation run are compared with several sets of atmospheric measurements: hourly concentrations of atmospheric NH_3 from the Clinton monitor, biweekly average atmospheric NH_3 concentrations measured at three AMoN sites in North Carolina, atmospheric concentrations of NH_4^+ in particulate matter at monitors collocated with the AMoN sites, and total atmospheric column loadings of NH_3 retrieved from measurements by the Infrared Atmospheric Sounding Interferometer (IASI) on the MetOp satellite (Whitburn *et al*, 2015). Predictions of NH_4^+ deposition from the second (adjusted) model run are also compared with measured deposition at eight sites. Figure 3-1 shows the locations of the different monitoring sites used in this case study. The figure also highlights the location of Sampson and Duplin counties, which have the densest concentration of NH_3 emissions as in the 2011 NEI.

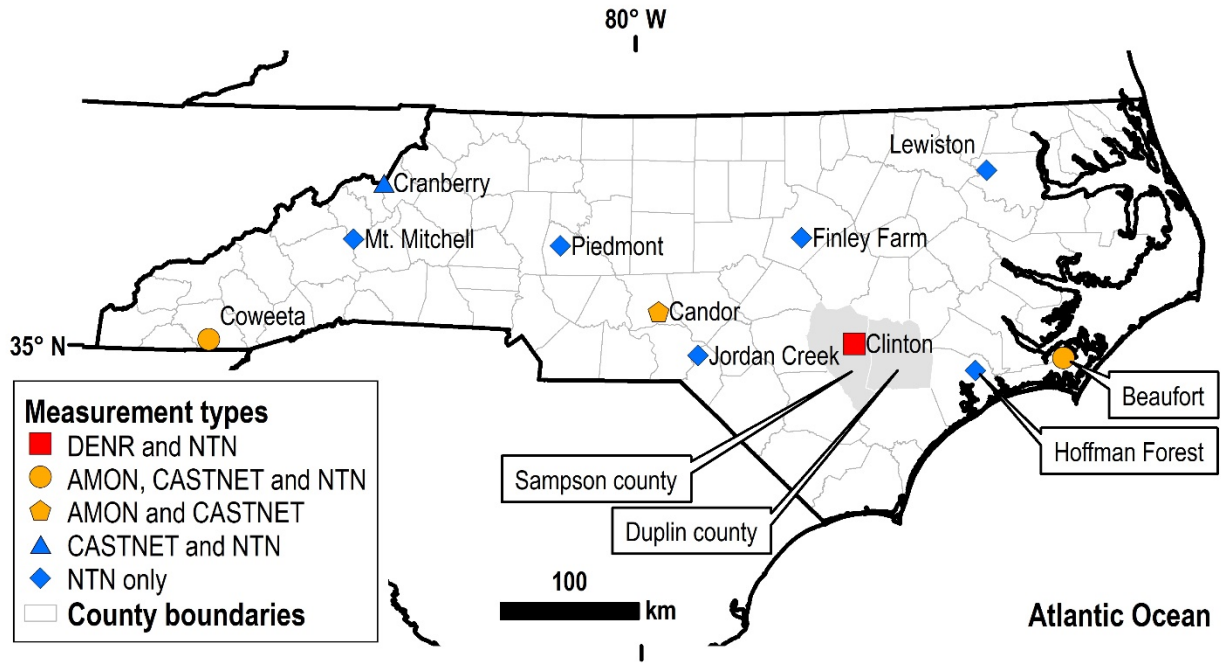

Figure 3-1. North Carolina case study domain, showing locations of measurement sites.

This study is the first use of hourly NH_3 vapor concentrations from the Clinton monitor in Sampson County to evaluate predictions by the NAQFC model. This evaluation provides new information on the performance of the model for reproducing diurnal patterns of NH_3 concentration. In addition, this study shows the impacts of using improved spatial information which is available for NH_3 emission sources in North Carolina and many other states.

3.2. Methods and Data

3.2.1 Air quality model

CMAQ model version 5.1 (Appel et al., 2017) was used to predict air pollutant concentrations and deposition for the continental U.S. in July 2011. The configuration of the CMAQ model within the NAQFC is described in more detail in Tang *et al*. (2017; 2015). Meteorological predictions to drive the air quality model were generated using the Weather Research and Forecasting Advance Research WRF (WRF-ARW) regional meteorological model, version 3.4.1, with the ACM2 planetary boundary layer scheme. The horizontal resolution of both models is 12 km, with 42 vertical layers with a domain top at 50 hPa (about 20.5 km). The height of the lowest vertical layer was 8.3 meters above the ground in the North Carolina domain. The gaseous chemistry is based on Carbon Bond 2005 e51 (CB05e51) chemical mechanism (Appel et al., 2017) and aerosol chemistry is based on the AERO6 module of CMAQ version 5.1.

The initial test model run included the bidirectional surface exchange model for NH_3 (Cooter *et al*. 2012; Bash *et al*. 2013; Pleim *et al*. 2013). The bidirectional flux option was not used in the final evaluation model run. In this run, dry deposition computed for NH_3 is based on the M3Dry module (Mathur *et al*., 2005).

3.2.2. Emissions inventories

Air pollutant emissions for the initial test model run were taken from the 2011 U.S. NEI Emissions Modeling Platform (U.S. EPA, 2016). For NH_3, the NEI modeling platform is based on county-level estimates of annual emissions. Animal waste emissions, which account for the bulk of NH_3 emissions, are derived using county level animal populations compiled in the Census of Agriculture (U.S. EPA, 2015). County level emissions are allocated to 12-km modeling grids based on the distribution of farm land. In the 2011 modeling platform, annual emissions estimates are converted to hourly values using monthly and diurnal temporal allocation factors to prepare hourly model-ready emission input.

In the final model evaluation run, information compiled by the NCDEQ on the location of CAFOs was also used to improve on the spatial allocation of NH_3 emissions. We retained the county level emission values, which are based on animal census data. Within each county, NH_3 emissions from swine were reallocated to 12-km modeling grids using the locations and capacities of swine CAFOs. Information for these calculations was obtained from the NCDEQ CAFO lagoon permit list, which gives the location of each swine CAFO and the number of animals the facility is permitted to house. This location and capacity information was used to determine the number of animals permitted to be housed in each modeling grid. Grid-level emissions for swine were then computed as follows:

$$E_g^N = \sum_C E_C^T \times \frac{P_{gC}}{P_C^T}$$

where E_g^N is the new emissions estimate for grid g, $\sum_c$ refers to the summation over all counties in which any portion of grid g is located, E_C^T is the total emissions estimate for county C, P_g^C is

the permitted population of swine the portion of grid g located within county C, and P_C^T is the total permitted population of swine in county C.

Figure 3-2 shows the location of waste lagoons in the state, and Figure 3-3 shows the impact of the revised spatial allocation on the gridded emissions inventory for NH_3. Figure 3-4 shows the spatial distribution of emissions for the revised emissions inventory. The impact of the change in spatial allocation is particularly significant in the neighborhood of the Clinton measurement site. Based on the distribution of CAFOs in Sampson County, the revised spatial allocation method resulted in a 41% reduction in NH_3 emission density for the model grid containing the Clinton monitor.

The second model also run used a lower end estimate was used for emissions from swine feeding operations in the state. This lower end emissions estimate was developed based on published error ranges for the NH_3 emissions model used in the NEI (McQuilling and Adams, 2015). The normalized mean error of the model is reported at 28% for swine housing and 61% for waste handling. This yields an average normalized mean error of 55% (weighted by the relative emission rates for housing and waste handling). For the current study, NH_3 emissions from swine operations in North Carolina were lowered by 55%, resulting in a 42% reduction in overall statewide NH_3 emissions.

The emissions inventory was also revised to adjust the diurnal NH_3 emission profile, prompted by the diurnal pattern shown by the base case inventory run. The model predicted a dramatic increase in atmospheric NH_3 in the early evening for rural areas with high NH_3 emissions. The high concentration also persisted through the night, resulting in higher average atmospheric NH_3 concentrations at night than during the day. This result disagrees with the hourly measurements from the Clinton monitor, which gives higher atmospheric NH_3

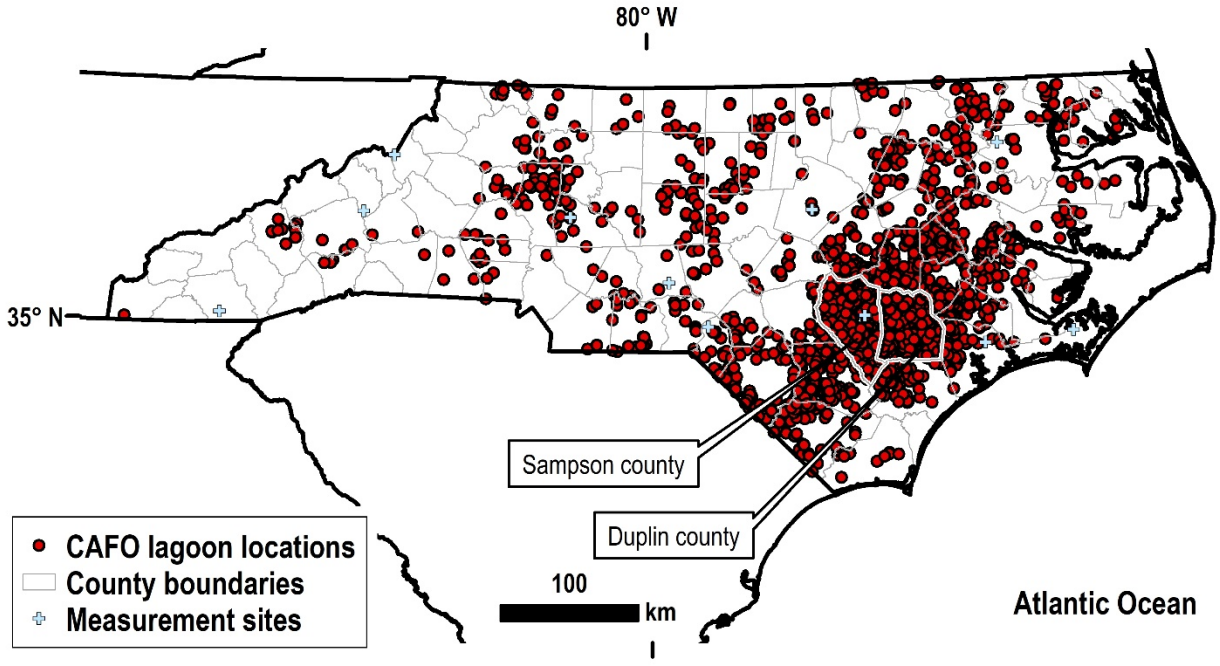

Figure 3-2. Location of CAFO waste handling lagoons based on state permits.

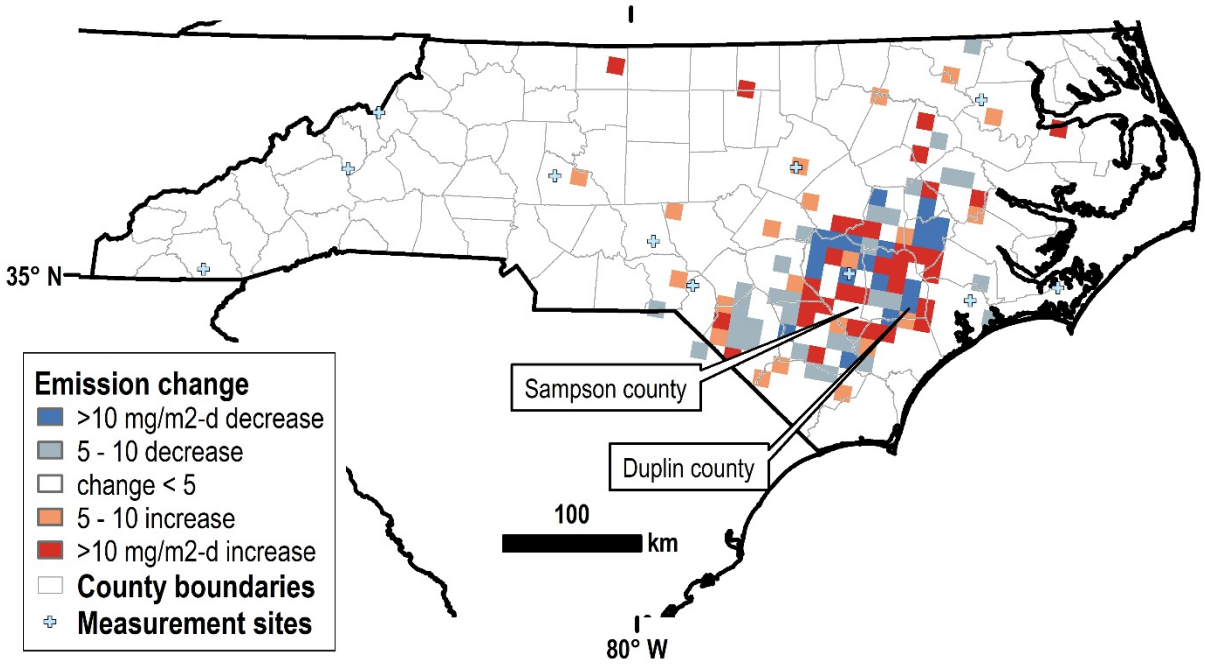

Figure 3-3. Changes in grid level NH3 emissions as a result of the improved spatial allocation process.

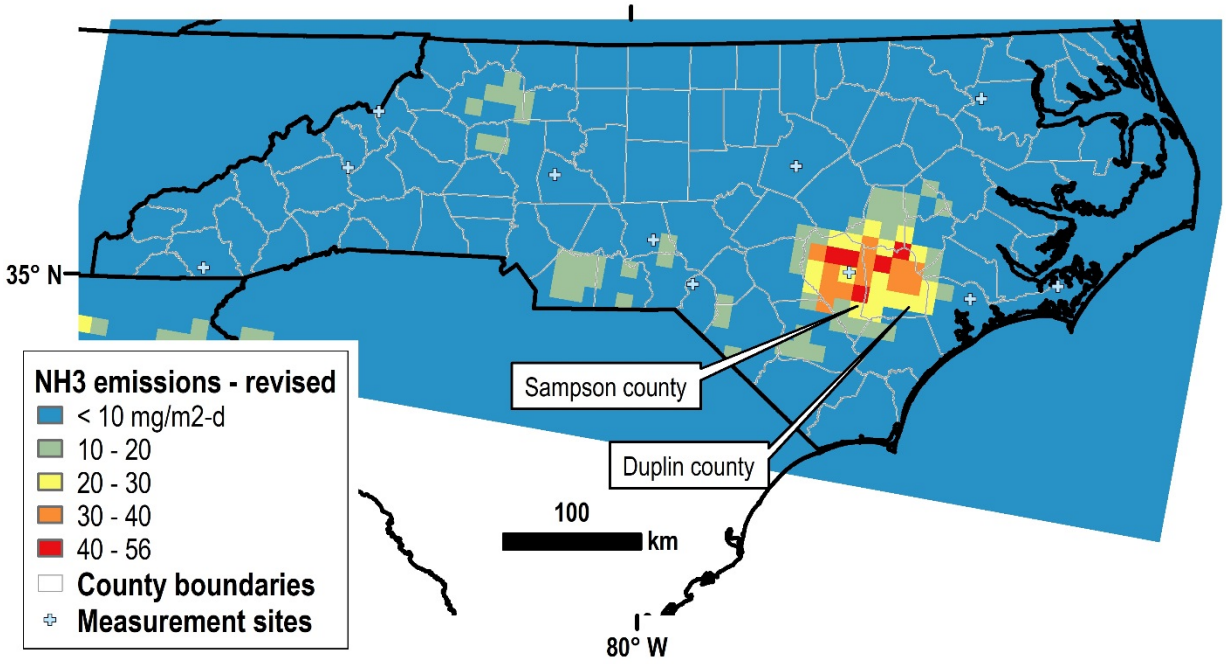

Figure 3-4. Gridded NH3 emissions after revised spatial allocation and CAFO emissions adjustment.

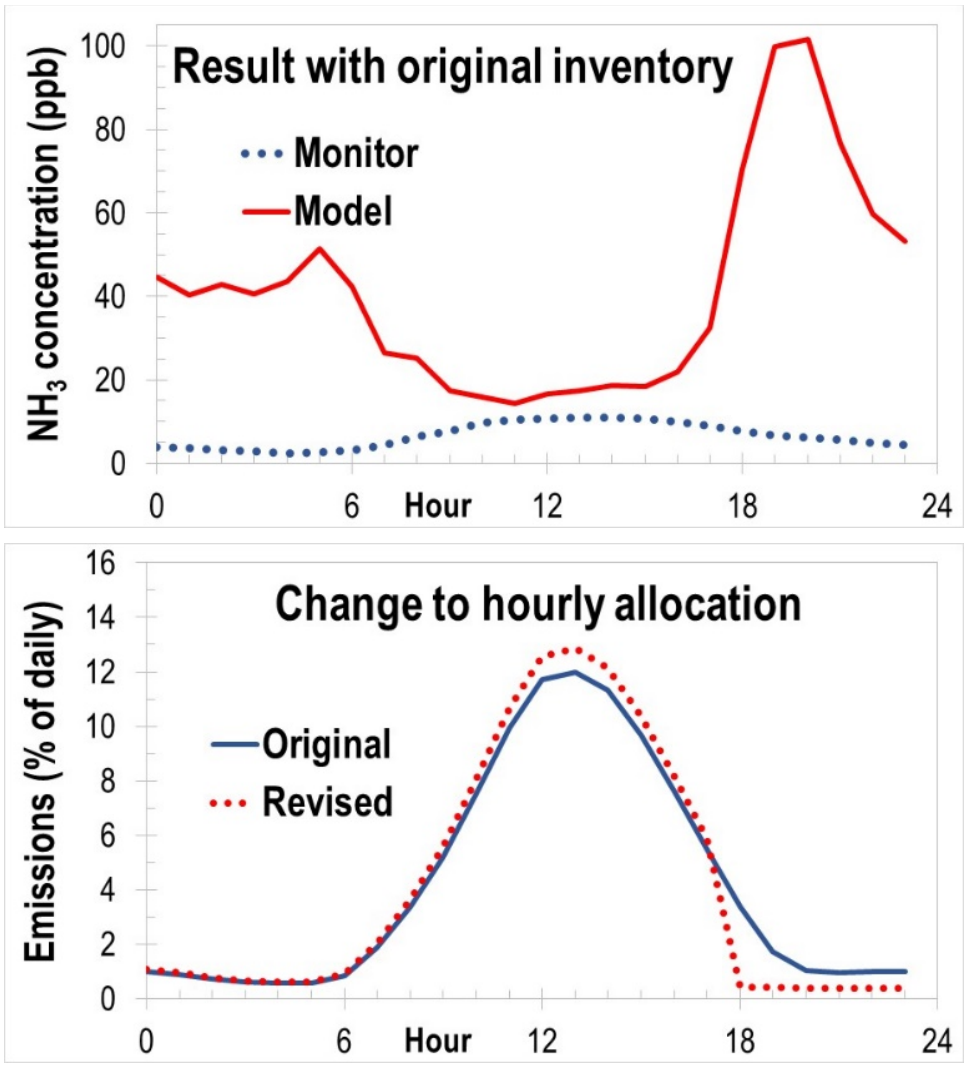

Figure 3-5. Change to hourly allocation of emission, implemented to avoid a concentration spike at the collapse of the mixed boundary layer.

concentrations during daytime (Figure 3-5, top graph). The evening peak appeared to be the result of a mismatch between the diurnal emission pattern and the height of the atmospheric mixed layer. In the NEI temporal allocation, emissions peak at about 1 p.m and then taper off gradually until about 8 p.m. (Figure 3-5, bottom graph). For the revised inventory, we adjusted the hourly temporal allocation factors so that emissions would fall to their evening levels at 6 p.m. (Figure 3-5, bottom graph).

3.2.3. Ground Measurements

Hourly atmospheric NH_3 concentrations were obtained from a continuous monitoring system operated by the NCDEQ at the Clinton Crop Research Station (DCNEQ, 2016; Shendrikar, 2006) between 2004 and 2015. The NCDEQ monitor used a Thermo Scientific Model 17i Ammonia Analyzer. The detection limit of the Thermo Scientific instrument is 1 ppbv, and the precision is 0.4 ppbv (Thermo.2014). The NCDEQ monitors underwent automated calibration on an average frequency of about once every 36 hours. Following the calibration process, concentrations were frequently unstable for about 4 to 5 hours. Therefore, the NCDEQ NH_3 data were filtered so that results were not used for the first 5 hours after calibration. In order to avoid any bias which could be introduced by filtering out more data during any given part of the day, monitored concentrations comparisons were calculated separately for each hour of the day, by averaging hour-1 for all days, etc. The hourly results were then averaged to produce the final concentration result.

Longer term average atmospheric NH_3 concentrations were also obtained from three AMoN sites in North Carolina. AMoN monitors use passive diffusion collectors, changed every two weeks (NADP, 2018). The detection limit of the AMoN passive sampler is approximately 0.16 ppbv with an estimated accuracy of $\pm$41% (Puchalski *et al*, 2011), and an average bias of

−9% in relation to an annual denuder system (Puchalski *et al*, 2015). The AMoN sites are collocated with Clean Air Status and Trends Network (CASTNET) sites which analyze the concentration of NH_4^+ and other ionic species in airborne particulate matter with a precision of ±20% (AMEC, 2013; U.S. EPA, 2018a).

3.2.4. Satellite Measurements

We compare NAQFC predictions with daytime retrievals of total atmospheric column NH_3 which have been published for the IASI instrument on the Metop-A satellite (Whitburn *et al*, 2015). The satellite makes daily passes over the region, and uses a cross-track scanning system to collect infrared spectra for numerous pixels on each pass. The footprint of a measurement ranges from 12 km by 12 km at nadir, up to 20 by 39 km at the edge of the swath. Whitburn *et al* (2015) retrieve NH_3 column loadings from the spectra using a neural network algorithm, which also computes the relative error for each measurement. This IASI retrieval algorithm differs from retrieval algorithms for other satellite systems in that it does not require an *a priori* assumption for the NH_3 loading.

We interpolated the NAQFC prediction of NH_3 column loading at the location of each available IASI measurement and at the time that the measurement was made. The timing of the IASI measurements in North Carolina during the July 2011 study period ranged from 8:40 to 11:00 a.m. local standard time. In accordance with recommendations of the IASI algorithm developers, the analysis was restricted to IASI retrievals with relative errors less than 100 percent.

3.2.5. Deposition Measurements

The National Trends Network (NTN) for precipitation chemistry includes 8 sites that were operating in North Carolina in 2011. These sites measure rainfall amounts and

concentrations of ionic species, including NH_4^+. The detection limit for NH_4^+ is 0.006 mg L^{-1} and the average difference between replicate measurements of NH_4^+ was 2% for the concentration range measured at the North Carolina sites (Dombek, 2012). NAQFC predictions of wet NH_4^+ deposition are compared with NTN measurements for the July 2011 timeframe.

Dry deposition measurements for NH_3 gas are limited. Phillips *et al* (2004) measured the vertical gradient of NH_3 vapor in order to determine dry deposition fluxes in 2002 at the Finley Farm site in central North Carolina, downwind of a research hog CAFO. We compare these with NAQFC model predictions of dry deposition with the summer measurements made at Findley Farm.

3.2.6. Model to Measurement Comparisons

Prediction accuracy for the NAQFC CMAQ model was quantified by computing the normalized mean bias (NMB):

$$NMB = \frac{\sum_{i=1}^{N}[C_{mod}(i) - C_{obs}(i)]}{\sum_{i=1}^{N} C_{obs}(i)}$$

Where: NMB is the normalized mean bias, $C_{mod}(i)$ and $C_{obs}(i)$ are, respectively, the model prediction and the observed concentration at a given location and time, and N is the number of observations.

3.3. Results and Discussion

3.3.1. Impact of the Bidirectional Flux Model on the Diurnal Pattern of NH_3 Vapor

Figure 3-6 shows the diurnal profile of atmospheric NH_3 from the final model run alongside the diurnal profile of measured average concentrations at the Clinton site during July

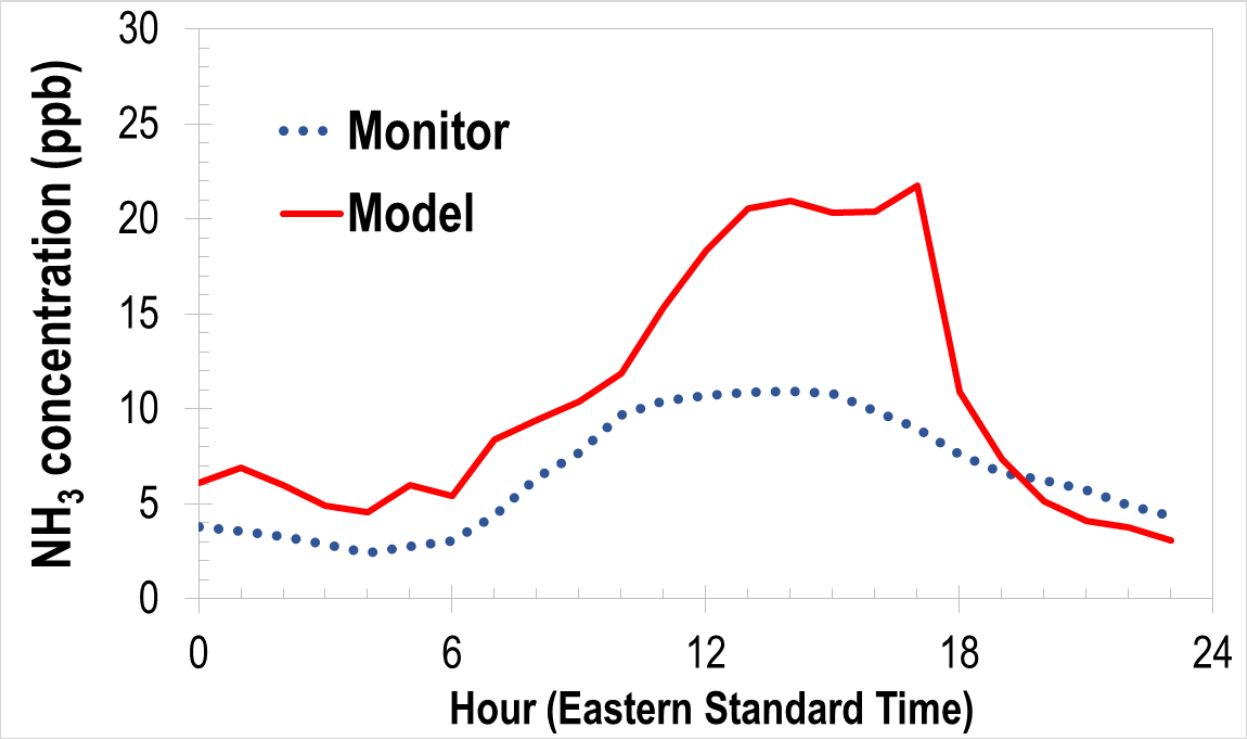

Figure 3-6. Measured diurnal pattern at the Clinton monitor site compared with model predictions using the revised emissions inventory.

2011. The measured diurnal profile at Clinton is similar to measured profiles in other rural areas, which show a relatively flat NH_3 concentration profile, or a moderate increase in the daytime (Walker *et al*, 2006; Saylor *et al*, 2010; Tevlin *et el*, 2017). A comparison of Figure 3-6 with Figure 3-6 illustrates a substantial improvement in the diurnal performance of the NAQFC model in the second run. The second model run, like the measured profile at the Clinton site shows a moderate increase in the mid-afternoon, whereas the first model run showed a pronounced peak in the evening. However, the improvement between the first and second model run was not caused by the adjusted temporal emission profile. Rather, the change resulted from not using the bidirectional flux model in the second model run. This was determined by comparing the results of the first and second model runs in other areas of the continental U.S. where we had made no changes to the NH_3 emissions inventory. Figure 3-7 shows the hourly pattern of atmospheric NH_3 predicted by the NAQFC model with and without the bidirectional flux model for a swine producing region of Iowa. The figure also shows the location of the Iowa site relative to the North Carolina domain.

3.3.2. Model Predictions Compared with Ground Level Air Pollution Measurements

Table 3-1 compares predicted ground level-atmospheric NH_3 concentrations from the two NAQFC model runs with measured concentrations at the continuous monitoring site in Clinton, and at the three North Carolina AMoN sites. The initial test run with the unadjusted NEI overpredicted NH_3 vapor at the Clinton site by more than 500% on average, and by more than a factor of 10 at night. The second run produced a pronounced improvement in the nighttime prediction of NH_3 vapor. The revised inventory also reduced the overprediction at Clinton during the day. This improvement is partially due to the improved spatial allocation and partially due to the reduction in emissions in the revised model run.

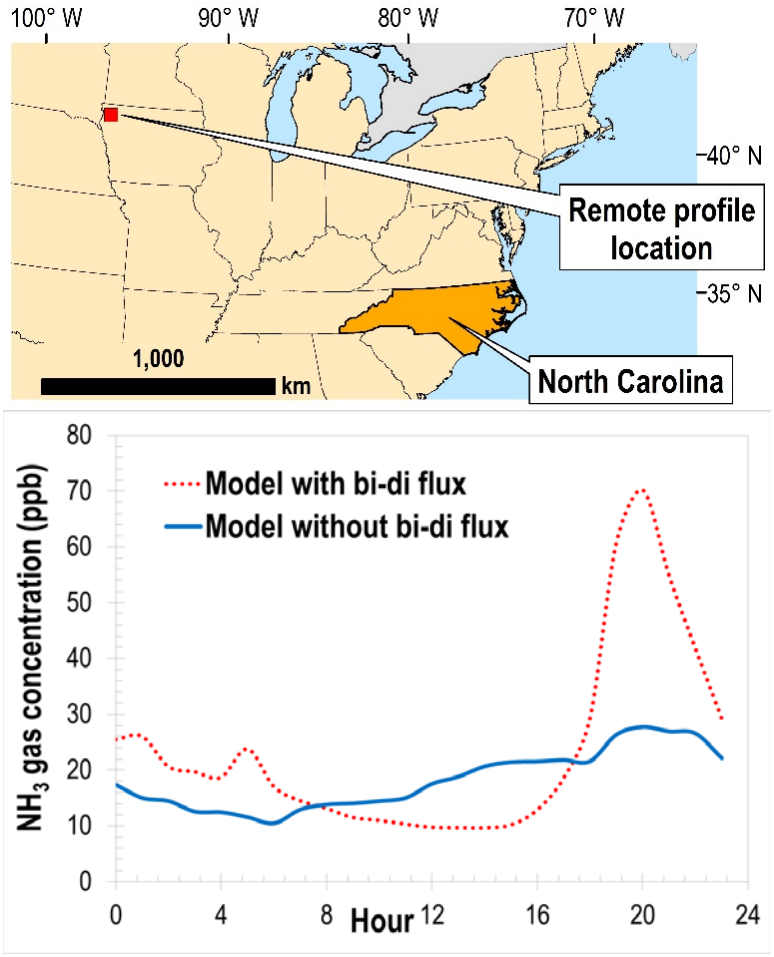

Figure 3-7.Comparison between hourly predictions with and without bi-directional flux, for a location where no changes were made to the emissions inventory.

Table 3-1. NCDEQ and AMoN measurements of NH_3 gas compared with model predictions.

Monitor site and location	Time-frame	Measurement (ppbv)[a]	Model with original emissions inventory and bidirectional flux			Model with revised emissions inventory and without bidirectional flux		
			Prediction (ppbv)[a]	Mean bias (ppbv)	Normalized mean bias (%)	Prediction (ppbv)[a]	Mean bias (ppbv)	Normalized mean bias (%)
Clinton Research Station (NC95), 35.0258N, 78.2783W	Day	9.0 ± 6.6	24.6 ± 22.1	15.6	173	15.7 ± 8.9	6.7	74
	Night	4.1 ± 2.7	58.0 ± 34.8	53.9	1300	5.3 ± 5.5	1.2	27
	Average	6.6 ± 5.8	41.3 ± 32.5	34.8	528	10.5 ± 9.2	3.9	60
Beaufort AMoN site (NC06), 34.8846N, 76.6207W	Note b	1.3 ± 0.2	0.8 ± 0.9	-0.5	-40	0.2 ± 0.3	-1.1	-81
Candor AMoN site (NC26), 35.2632N, 79.8365W	Note b	0.8 ± 0.9	4.0 ± 3.1	3.2	395	1.2 ± 1.0	0.4	54
Coweeta AMoN site (NC25), 35.0605N, 83.4305W	Note b	0.4 ± 0.1	0.8 ± 0.7	0.4	71	0.3 ± 0.6	-0.1	-35

[a] Average with standard deviation.
[b] Two 14-day sampling periods: July 5-19, and July 19-Aug 5.

The final model evaluation run overpredicted atmospheric NH_3 at the Clinton site by an average of 3.9 ppbv, about 60%. Figure 3-6 shows that the diurnal profile of atmospheric NH_3 predicted by the model is similar to the diurnal profile measured at the Clinton site during July 2011. Figure 3-8 shows temporal variations in predicted and measured NH_3 vapor concentrations at the Clinton site on an hourly timescale and on a daily timescale during the July 2011 modeling episode. The figure illustrates that the NH_3 concentration is subject to considerable variability, not only on a diurnal basis, but also day to day. The variability predicted by the model is similar to the measured variability, although daily peaks predicted by the model are not aligned with measured peaks. This is understandable, in that the model incorporates variations caused by meteorological parameters but does not incorporate information on the timing of animal waste handling operations. Animal wastes are periodically distributed to fields using high pressure sprays which can result in emissions of NH_3. However, information on the timing of this operation is not compiled for the inventory.

The three AMoN monitors are more distant from the region of dense CAFO emissions than the Clinton site. Table 3-1 shows that atmospheric NH_3 concentrations at the three North Carolina AMoN sites were 1.3 ppbv or less. Model biases for these monitors were also small, with the exception of the first model run for the Candor site, where the model overpredicted NH_3 by 3.2 ppbv or 395%.

The second model run reduced the bias at the Candor site to 0.4 ppbv or 54%. The second model run underpredicted NH_3 at Beaufort by 1.1 ppbv or 81%. Beaufort is located close to the ocean, and NH_3 emissions from the ocean could be contributing a small increase in NH_3 at the monitor (Paulot *et al*, 2015). Ocean emissions are not included in the emissions inventory. The underestimation of NH_3 in Beaufort could be the result of an underestimation of NH_3 emissions

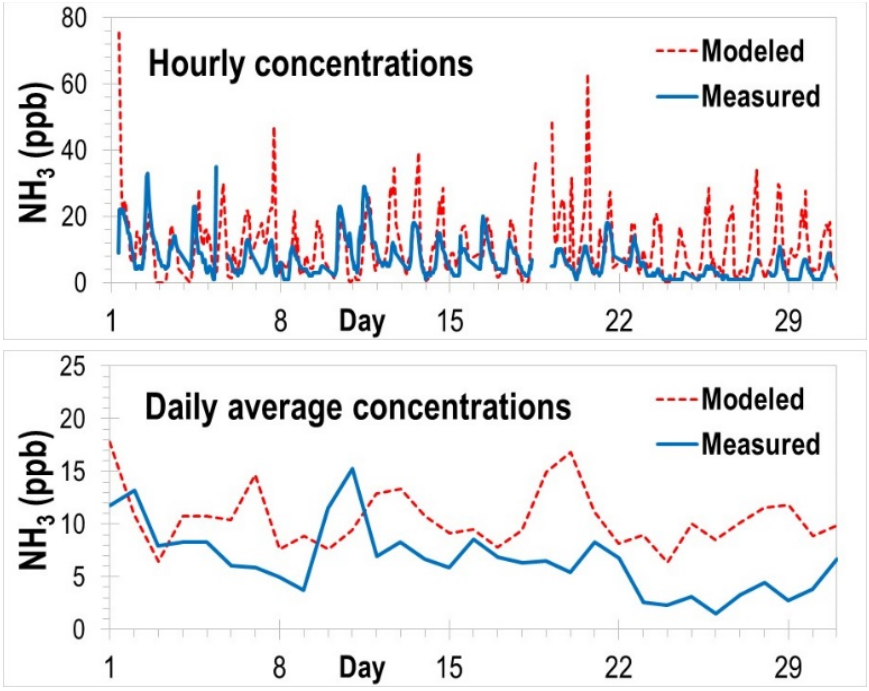

Figure 3-8. Temporal variations in predicted (with revised inventory) and measured NH_3 concentrations at the Clinton monitoring site.

from chemical fertilizer near the site, because the monitor site is adjacent to a large farm which alternates between growing corn and soybeans. Synthetic nitrogen fertilizer is used in the spring months when corn is cultivated (in odd-numbered years), resulting in high measured atmospheric concentrations of NH_3 at the monitor – up to 70 ppbv on a two week average (see Figure 3-9). The spike in NH_3 is attenuated by July, but enhanced levels of nitrogen in the soil could still produce elevated concentrations on the scale of 1 ppbv. The bidirectional model as, implemented by Cooter *et al* (2012), gives an improved treatment of emissions from fertilized crops; however, the model does not currently reflect crop management practices at the model grid scale. Although the model is implemented at the grid scale, inputs on crop management practices are characterized at a larger scale of 10,000 km^2, or about 8 × 8 model grids (Cooter *et al*, 2012).

Table 3-2 compares predicted levels of airborne particulate NH_4^+ with corresponding measurements from CASTNET monitors collocated with the AMoN sites, and at another site in Western North Carolina (Cranberry). The table shows that the first model run overpredicted particulate NH_4^+ at all sites. The second model run improved predictions of NH_4^+ at all sites. All of these errors for the second run were small in absolute terms; the largest difference was an overprediction of 0.4 μg m^{-3} in Beaufort.

3.3.3. Model Predictions Compared with Satellite Retrievals

Satellite retrievals provide an opportunity to evaluate model performance at reproducing regional patterns in NH_3 emissions. Figure 3-10 shows the spatial pattern atmospheric column NH_3 loading based on IASI retrievals for July 2011. In the figure, IASI retrievals are expressed as mg m^{-2}. This refers to the total mass of NH_3 above a given area of land. The grid network is the same as the NAQFC modeling grid. However, each grid value in the figure is actually an

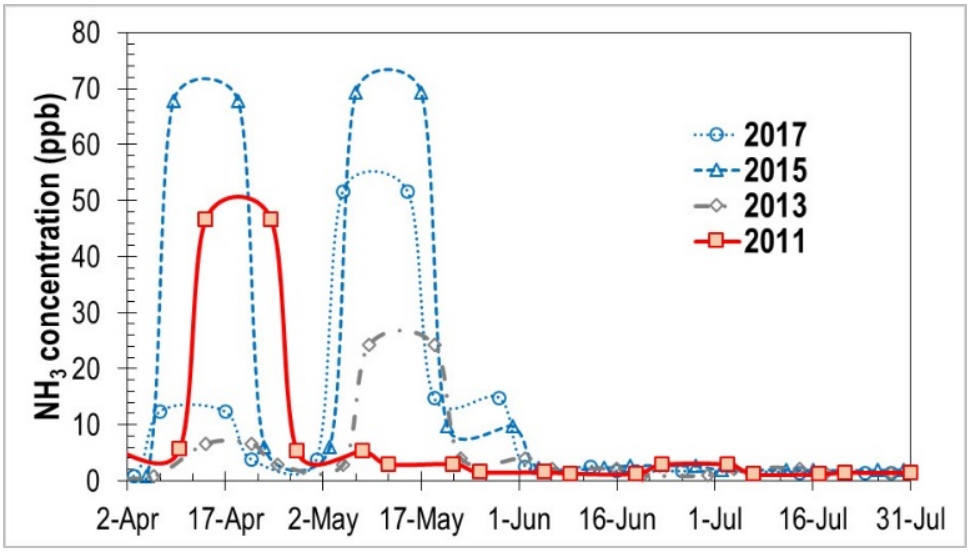

Figure 3-9. NH_3 from associated with fertilizer application for a two-year crop rotation at a large farm adjacent to the Beaufort AMON site.

Table 3-2. CASTNET measurements of NH_4^+ in fine particulate matter compared with model predictions.

Monitor site and location	Measurement (µg m^{-3}) [a,b]	Model with original emissions inventory and bidirectional flux			Model with revised emissions inventory and without bidirectional flux		
		Prediction (µg m^{-3}) [a]	Mean bias (µg m^{-3})	Normalized mean bias (%)	Prediction (µg m^{-3}) [a]	Mean bias (µg m^{-3})	Normalized mean bias (%)
Beaufort (BFT142), 34.8846N, 76.6207W	0.6 ± 0.3	2.6 ± 3.4	2.0	360	1.0 ± 0.7	0.4	80
Candor (CND125), 35.2632N, 79.8365W	1.3 ± 0.4	2.3 ± 1.7	1.0	76	1.5 ± 0.9	0.2	15
Coweeta (COW137), 35.0605N, 83.4305W	1.1 ± 0.2	2.5 ± 1.8	1.4	129	1.0 ± 0.6	-0.1	-9
Cranberry (PNF126), 36.1054N, 82.045W	1.3 ± 0.3	1.8 ± 1.2	0.5	34	1.1 ± 0.7	-0.2	-20

[a] Average and standard deviation.
[b] Five one-week averages from June 28 through August 2.

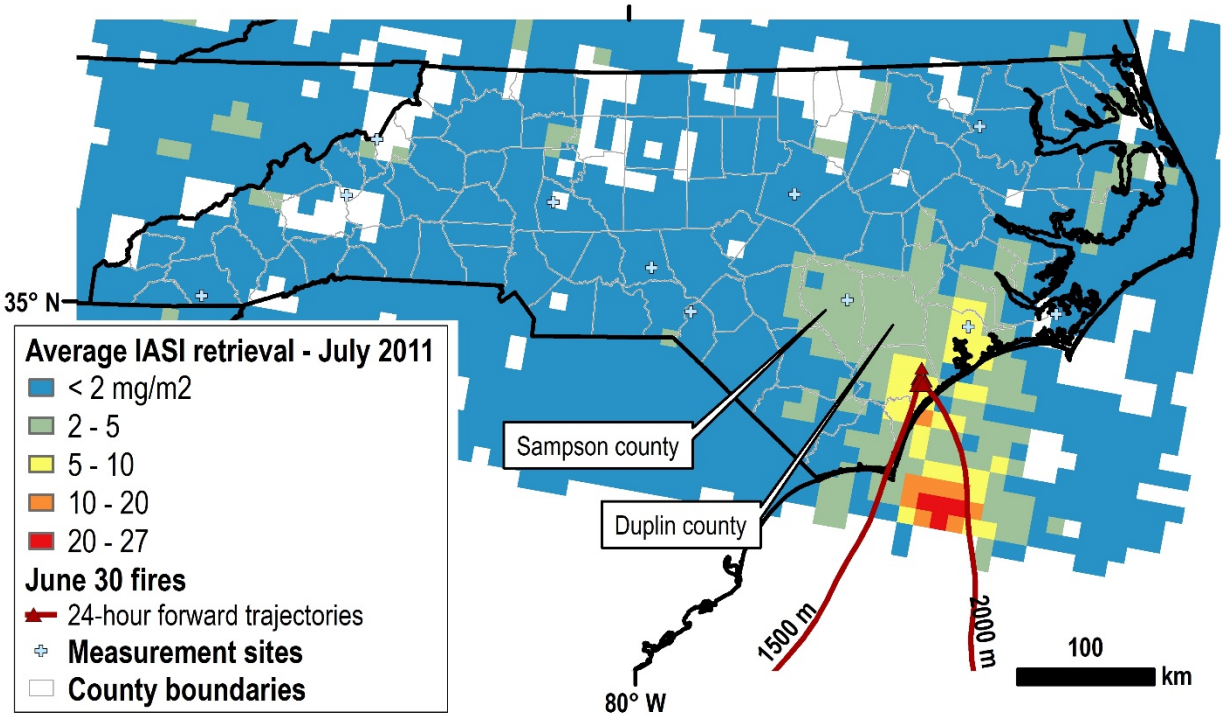

Figure 3-10. Spatial pattern of total atmospheric NH_3 loading based on average IASI retrievals for July 2011.

average of the retrievals for itself and its eight neighbors. This is done in order to increase the number of observations incorporated into each value.

Table 3-3 compares average IASI retrievals of total column NH_3 loading for different geographic regions of the modeling domain with NAQFC predictions using the two emission inventory versions. Model-to-measurement comparisons are made for Sampson and Duplin counties, which have the highest swine population density, as well as for the eastern and western portions of North Carolina and the adjacent coastal waters. In the first model run, the NAQFC model overpredicted NH_3 column loading in all of the land regions. The second model run resulted in improved agreement for all of the land regions.

For both inventories, the NAQFC model underpredicted the NH_3 loading in the offshore waters. This is most likely the result of fires which occurred in the coastal forests in late June and early July. The bulk of these emissions occurred prior to the initiation of the model run (U.S. EPA, 2017), and were not included in the initial conditions of the run. Figure 3-10 includes the locations of these fires, based on the satellite-based burn area measurement database from the Moderate Resolution Imaging Spectroradiometer (MODIS) (Boschetti *et al,* 2009). The figure also shows 24-hour forward wind trajectories at the time of the fires (Stein *et al,* 2015; Rolph *et al*, 2017).

3.3.4. Model Predictions Compared with Deposition Measurements

Table 3-4 compares NAQFC model predictions of wet NH_4^+ deposition using the revised emissions inventory with measured wet deposition at eight NTN sites across North Carolina. The table compares predictions and measurements of rainfall NH_4^+ concentrations, rainfall amounts and deposition rates. Figure 3-11 maps the differences between predicted and measured rainfall concentration and deposition. In general, the model underpredicted rainfall NH_4^+ concentrations

Table 3-3. IASI retrievals of NH_3 in the total atmospheric column compared with model predictions.

Region	IASI daytime retrievals			Model prediction - original emissions inventory				Model prediction - revised emissions inventory			
	Average (mg m^{-2})[a]	Standard deviation (mg m^{-2})	Number of obser-vations	Average (mg m^{-2})	Standard deviation (mg/m^{-2})	Mean bias (mg m^{-2})	Normal-ized mean bias (%)	Average (mg m^{-2})	Standard deviation (mg m^{-2})	Mean bias (mg m^{-2})	Normal-ized mean bias (%)
Sampson and Duplin counties	3.0	1.5	59	6.3	2.5	3.3	112	3.4	1.4	0.4	14
Eastern NC	1.2	2.8	488	2.1	2.4	1.2	72	1.0	1.3	-0.2	-22
Western NC	0.3	2.2	520	0.7	0.8	0.4	102	0.3	0.4	0.06	-21
Coastal waters	0.9	3.0	141	0.4	0.8	-0.5	-52	0.2	0.3	-0.7	-80

[a] In this table, IASI retrievals are expressed as mg m^{-2}. This refers to the total mass of NH_3 above a given area of land.

Table 3-4. NTN measurements of wet deposition compared with model predictions.

Monitor site and location	Rainfall NH_4^+ concentration			Rainfall amount			Total deposition		
	Measured (mg L^{-1})	Modeled (mg L^{-1})	Model bias (%)	Measured (cm)	Model (cm)	Model bias (%)	Measured (kg ha^{-1})	Model (kg ha^{-1})	Model bias (%)
Clinton Research Station (NC35), 35.0258N, 78.2783W	0.70 ± 0.45	0.55 ± 0.13	-22	7.0	7.4	6	0.49	0.41	-17
Beaufort (NC06), 34.8846N, 76.6207W	0.29 ± 0.41	0.19 ± 0.06	-37	5.7	17.0	197	0.17	0.32	89
Lewiston (NC03), 36.1325N, 77.1708W	0.49 ± 0.36	0.32 ± 0.06	-35	13.8	10.0	-27	0.68	0.32	-53
Hofmann Forest (NC29), 34.825N, 77.3228W	0.52 ± 0.48	0.39 ± 0.17	-24	17.2	13.0	-25	0.89	0.51	-43
Finley Farm (NC41), 35.7288N, 78.6802W	0.48 ± 0.13	0.26 ± 0.02	-45	6.8	7.6	13	0.32	0.20	-38
Jordan Creek (NC36), 34.9705N, 79.5281W	0.37 ± 0.13	0.27 ± 0.08	-26	9.8	5.6	-43	0.36	0.15	-58
Piedmont Research Station (NC34), 35.697N, 80.6225W	0.31 ± 0.16	0.23 ± 0.18	-25	19.4	10.2	-48	0.60	0.23	-61
Mt. Mitchell (NC45), 35.7353N, 82.2861W	0.27 ± 0.11	0.27 ± 0.14	0	23.6	15.1	-36	0.64	0.41	-36

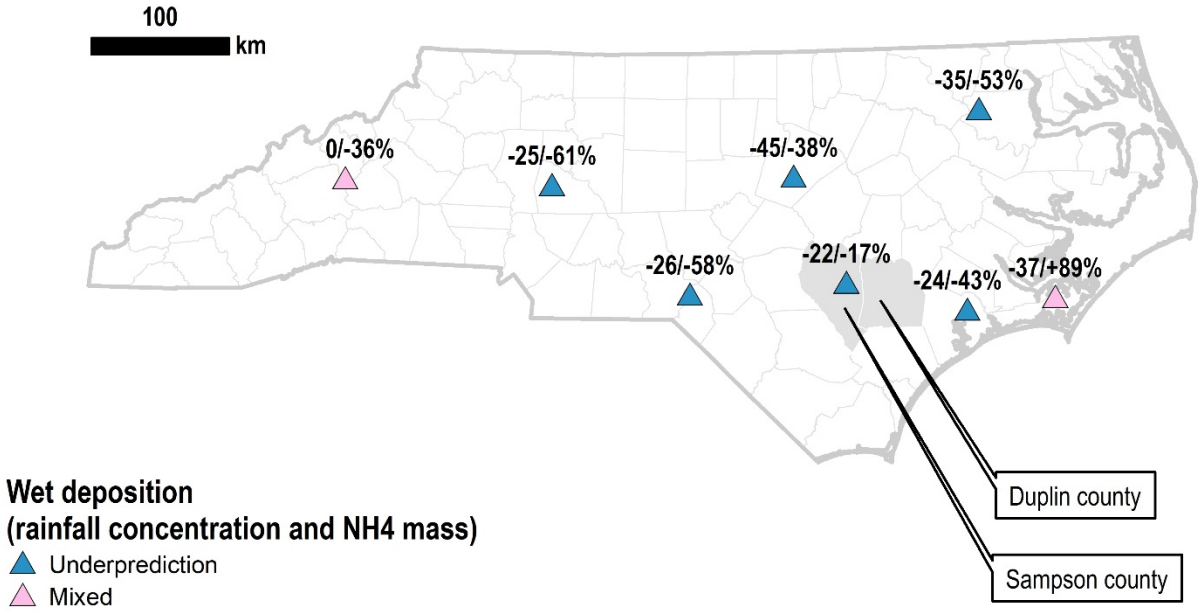

Figure 3-11. Spatial patterns of bias in rainfall NH4+ concentration and mass deposition for the second model run.

by up to 45%, and (with the exception of the Beaufort site) underpredicted the monthly wet NH_4^+ deposition by up to 61%. Model predictions of rainfall were mixed, ranging from a 48% underprediction to almost a 200% overprediction, at the Beaufort site. At the Beaufort site, rainfall NH_4^+ concentration was underpredicted by 37%, but this was offset by an almost 200% overprediction in rainfall volume, resulted in an overprediction of monthly NH_4^+ wet deposition by 89%. Model predictions for the Clinton Crop Research Station, in the region of highest emission density, are closest to the observed results, with a bias of -22% for the NH_4^+ rainfall concentration and -17% for the monthly wet NH_4^+ deposition.

Table 3-5 shows atmospheric NH_3 concentrations, dry NH_3 deposition fluxes, and dry NH_3 velocities measured by Phillips *et al* (2004) at Finley Farm in the summer of 2002. The table compares these values to model predictions for the Finley Farm location in July 2011. Because emissions and meteorological conditions would not be identical in the two years, the model predictions of NH_3 concentration and dry deposition flux would not be expected to directly match measured results for these parameters. The dry NH_3 deposition velocity could be expected to be comparable. (The dry deposition velocity is the ratio of NH_3 deposition flux to the atmospheric concentration.) However, it must also be noted that the model deposition velocity reflects a grid-wide average while the measurement reflects only a point in the grid. The area around Finley Farm includes a mix of forest land and suburban land. As Table 3-5 shows, model predictions of NH_3 concentration and dry deposition flux in July 2011 were both lower than the measurements in 2002. At night, percentage differences between predicted and measured concentration and dry deposition flux were comparable (predictions 74% and 76% lower than measurements for concentration and deposition). Thus, the predicted nighttime dry deposition

Table 3-5. Model predictions of dry deposition compared measurements for the Findley Farm site in 2002.

	Concentration (ppbv)			Deposition flux ($\mu g\ m^{-2}\ s^{-1}$)			Deposition velocity ($cm\ s^{-1}$)		
	Phillips	Model	Bias (%)	Phillips	Model	Bias (%)	Phillips	Model	Bias (%)
Day	6.8 ± 6.8	1.4 ± 1.2	-80	0.185	0.017 ± 0.008	-91	3.9 ± 2.8	1.7 ± 7.2	-57
Night	4.0 ± 3.5	1.0 ± 0.9	-74	0.021	0.005 ± 0.004	-76	0.76 ± 1.7	0.7 ± 1.2	-8
Average	5.4	1.2 ± 1.0	-77	0.110	0.011	-90	3.0	1.3 ± 5.6	-56

velocity was similar to the measurement. However, the predicted daytime dry deposition velocity was much lower than the daytime dry deposition velocity measured in 2002.

3.3.5. Analysis of Model Bias in Relation to Previous Studies

Gilliland *et al* (2006) conducted a CMAQ inverse modeling analysis using wet NH_4^+ deposition measurements to evaluate the 2001 U.S. EPA emission inventory of NH_3 for the continental U.S. This study found that annual emissions estimates were found to be reasonable on average, but that the emissions inventory was about 17% too low in the July-August timeframe. Zhu *et al* (2013) carried out inverse modeling with the GEOS-Chem model using satellite retrievals of ambient NH_3 from the Tropospheric Emission Spectrometer (TES) on the Aura satellite and ground level AMoN measurements between 2006 and 2009 for the Continental U.S. The study found that the emissions inventory for NH_3 appeared to be an underestimate, especially in the Western U.S.

Butler *et al* (2014) found that CMAQ predictions of atmospheric NH_3 were 8% to 60% lower than measured values for the Susquehanna River Watershed of New York and Pennsylvania in 2008 and 2009. Kelly *et al* (2014) evaluated CMAQ predictions of NH_3 vapor and NH_4^+ in airborne particulate matter as part of the California Research at the Nexus of Air Quality and Climate Change (CalNex) campaign in May and June of 2010. Predictions of NH_4^+ were close to measured values, however the model under-predicted NH_3 in agricultural regions and did not capture the large variations in measured NH_3.

Using aircraft-based measurements, ground level measurements, and TES satellite retrievals Battye *et al* (2016) found that the NAQFC model under-predicted atmospheric NH_3 by 33% to 76% in an agricultural region of Northeast Colorado in the summer of 2014, although predictions of particulate NH_4^+ were close to measured values. Bray *et al* (2017) found that the

NAQFC model under-predicted atmospheric NH_3 by 58% for the San Juaquin Valley of California in the summer of 2010.

In general, the previous studies cited above have shown underprediction of NH_3 in for agricultural regions in the summer. This current study differs, showing an overprediction of both NH_3 vapor and NH_4^+ in particulate matter at most monitors. This is perhaps owing to the underprediction of wet and dry deposition in the current modeling effort. NH_4^+ wet deposition was underpredicted at most monitors, and dry deposition of NH_3 is lower than previous measurements (although not concurrent with model predictions).

3.3. Summary and conclusions

An initial test model run using the standard 2011 NEI and the bidirectional flux model overpredicted atmospheric NH_3 vapor in July 2011 by more than 500% at the Clinton continuous monitoring site. This site is located in Sampson County, in a region of dense NH_3 emissions from swine operations. The test run also overpredicted NH_3 vapor as well as the concentration of NH_4^+ in airborne particulate matter at two AMoN sites in Central and Western North Carolina. At a third site in Eastern North Carolina (Beaufort), the model made a small underprediction of NH_3 (less than 1 ppbv in absolute terms), while still overpredicting NH_4^+ in particulate matter. The Clinton monitor provided hourly measurements of NH_3 vapor, which indicated that the diurnal profile predicted by the first model run was essentially inverted from the profile observed by the monitor.

A revised model run was implemented for July 2011 without the bidirectional flux model. In addition, because the initial model run using the standard 2011 NEI significantly overpredicted NH_3, the second run used a lower end estimate of NH_3 emissions from swine operations. Even with a 42% downward adjustment of NH3 emissions from CAFOs in the study

region, the NAQFC CMAQ model overpredicted atmospheric NH_3 in July 2011 by 60% at the Clinton continuous monitoring site. The average concentration measured by the monitor was 6.6 ppbv, while the average predicted by the model was 10.5 ppbv. The second model run also made use of state permit information to improve the spatial allocation of NH_3 emissions from CAFOs. This change resulted in a demonstrable reduction of model bias at the Clinton site. This spatial allocation modification reduced emissions by 41% in the model grid containing the Clinton monitor. Therefore, model bias without the spatial adjustment could be expected to be up to 41% higher than the current overprediction.

This current study is the first to use hourly NH_3 concentrations from the Clinton monitor to evaluate ground level predictions by the NAQFC model, providing new information on the performance of the model for reproducing the diurnal pattern of NH_3 concentration. Previous studies have used passive monitors with a temporal resolution of at least one week. For the second model run without bidirectional flux, the diurnal pattern predicted by the model was similar to the diurnal pattern measured by the continuous monitor, with both showing elevated concentrations in the mid-afternoon and lower concentrations at night.

Three AMoN sites are located in regions of North Carolina which are somewhat removed from zone of dense CAFO emissions. Atmospheric NH_3 concentrations at these sites were 1.3 ppbv or less; and concentrations of particulate NH_4^+ were 1.3 $\mu g\ m^{-3}$ or less. Model errors with respect to these measurements were small in absolute magnitude. The largest differences were at Beaufort, near the seacoast, where the model underpredicted atmospheric NH_3 by 1.1 ppbv and overpredicted particulate NH_4^+ by 0.4 $\mu g\ m^{-3}$. The underprediction of NH_3 may be attributable to the location of the Beaufort monitor in close proximity to a fertilized corn field. Total column

concentrations of NH_3 predicted by the model for North Carolina were in good agreement with daytime IASI satellite retrievals.

The model underpredicted wet deposition of NH_4^+ and dry deposition of NH_3. The concentration of NH_4^+ in rainfall was underpredicted by 22% at Clinton and up to 45% at Finley Farm in Central North Carolina. The model underpredicted monthly wet deposition NH_4^+ by 17% at Clinton, and by up to 61% at the Piedmont Research Station in Central North Carolina. The predicted daytime dry NH_3 deposition velocity was 57% less than that measured by Phillips *et al* in 2002, and the overall dry NH_3 deposition velocity was 56% less than that measured by Phillips *et al* (2004). The overestimation of NH_3 may be partially attributable to and underestimation of wet and dry deposition in North Carolina.

Chapter 4

Discussion of Satellite Retrievals and NH_3 Emissions

4.1. Satellite Retrievals

One goal of this research was to assess the feasibility of using satellite measurements to improve the emissions inventory for agricultural sources of NH_3. In the current research, measurements of atmospheric NH_3 have been used from three satellite-based instruments: the Tropospheric Emission Sounder (TES) on the Aura satellite, the Atmospheric Infrared Sounder (AIRS) on the Aqua satellite, and the Infrared Atmospheric Sounding Interferometer (IASI) on the MetOp satellite (Shephard *et al*, 2012; Warner *et al*, 2016; and Whitburn *et al*, 2015). The features of these instruments are discussed in Section 1.3.4, and compared in Table 1-2. A fourth system, the Cross-track Infrared Sounder (CrIS) on the Suomi NPP satellite and the Joint Polar Satellite System-1 (JPSS-1), was launched more recently, and is also being used to measure atmospheric NH_3 (Shephard and Cady-Pereira, 2015).

Because of their broad coverage, the AIRS, IASI, and CrIS satellite systems offer the prospect of measurement data that can be used to fill in the gaps between ground-based monitors. In addition, satellite retrievals can be used to identify regions where it might be beneficial to site new monitors. TES provides more detailed information on the vertical profile of NH_3, but gives much less spatial resolution than AIRS, IASI, or CrIS, and has a longer interval between measurements. All satellite retrievals of NH_3 are subject to considerable variability and uncertainty. As with ground-based systems, the uncertainty of satellite retrievals can be improved by combining multiple measurements. This aggregation can be achieved by spatial and temporal averaging. However, NH_3 concentrations are also subject to considerable spatial and temporal variability.

4.1.1. Spatial and Temporal Aggregation

The North Carolina case study (Chapter 3) showed that information such as permit data can be used to make improvements at the scale of the modeling grid. Aircraft measurements in the Northeast Colorado case study (Chapter 2) showed the atmospheric NH_3 is subject to significant variations at the scale of the model grid and below. The spatial resolution of satellite measurements is the same as or coarser than the model grid resolution – 12 km in the case of IASI and 45 km in the case of AIRS. Therefore, it is desirable to retain as much spatial resolution as possible comparisons between satellite measurements and the model.

Each of the satellite instruments makes both daytime and nighttime measurements. For a given region, these measurements are separated by about 12 hours. The frequency of coverage for a given region is daily for IASI, and every other day for AIRS. However, local cloudiness and other weather conditions may prevent measurements on any particular day. Because the flux of infrared radiation from the Earth is higher during the daytime than at night, the daytime measurements generally have a lower uncertainty than the nighttime measurements. The ground-based continuous monitor used in the North Carolina case study (Chapter 3), shows a consistent diurnal pattern, with the NH_3 concentration peaking between 10 a.m. and 3 p.m. local standard time (Figures 3-4 and 3-6). The daytime passages of AIRS and IASI both fall within this time period. Because of the diurnal pattern in NH_3 concentration, and the difference in the level of uncertainty between daytime and nighttime satellite measurements, the daytime and nighttime retrievals should be aggregated separately.

The temporal resolution of the CMAQ model is nominally one hour. In practice, however, the emissions inventory does not provide this level of resolution. Although the inventory gives hourly estimates of NH_3 emissions, these must be viewed as best estimates of the

expected emission rate at a given hour of the day, over the course of the month or season. Information is not available on the timing of operations such as waste handling or waste distribution, which can produce short-term increases in emissions on an hourly or daily scale. However, monthly and seasonal changes in NH_3 emissions are incorporated into the emissions inventory using tools such as the Environmental Policy Integrated Climate (EPIC) model (Cooter *et al*, 2012). Thus, satellite measurements of NH_3 can be aggregated for periods of up to about a month for the purposes of evaluating emissions estimates within the current emissions inventory framework.

Weather conditions may limit the number of satellite measurements available over the course of a month for a given location. Therefore, it may be beneficial to aggregate measurements for a given month over multiple years. Although long term interannual trends have been measured (Warner *et al*, 2017), interannual differences in the U.S. are smaller than seasonal differences. This is illustrated by results at the Beaufort, North Carolina monitor, shown in Figure 3-7. Nevertheless, it must be noted that aggregation over multiple years will mask the effects of long term trends, as well as shorter term interannual factors such as crop rotation.

AIRS for NH_3 have been published in an aggregated format, with daytime retrievals averaged for each month at a spatial resolution of 1 degree latitude by 1 degree longitude (Warner *et al*, 2017). Figure 4-1 shows an example of AIRS results available for July 2011. The figure is a combination of NH_3 concentration retrievals at 918 hPa for and at 840 hPa for higher elevation regions. No retrievals are generated for elevations greater than about 1500 m. in

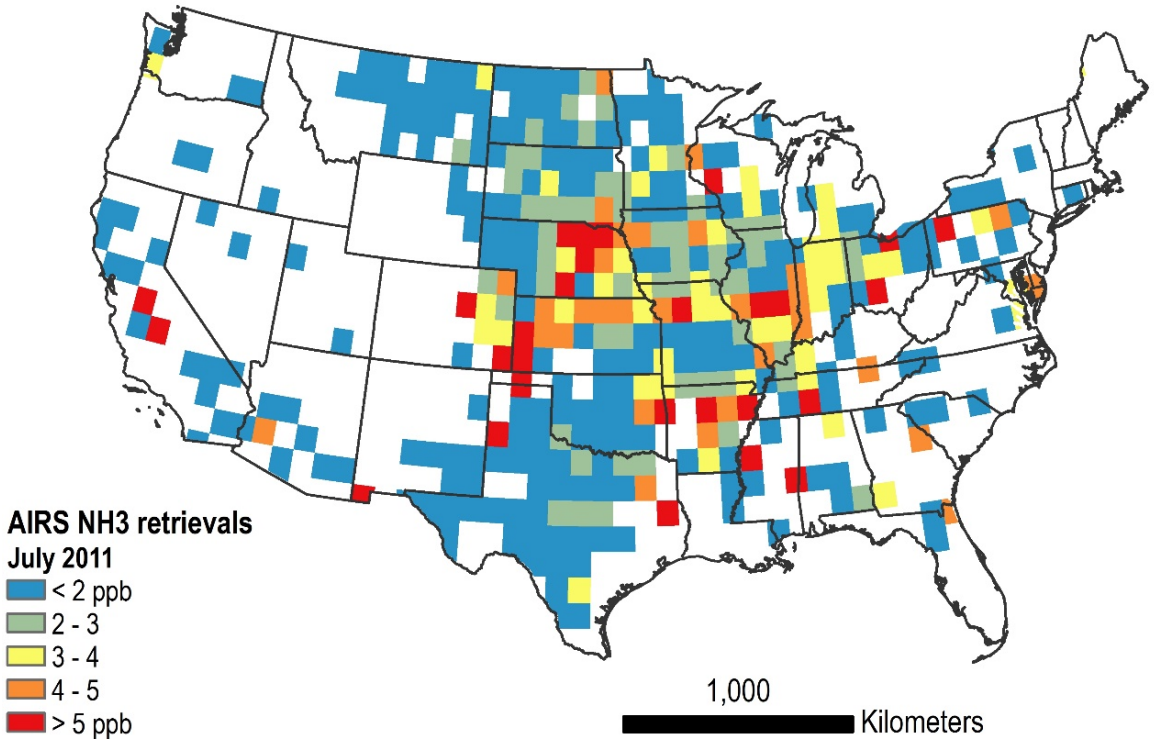

Figure 4-1. AIRS NH_3 retrievals for July 2011.
Source: http://atmos.umd.edu/~juying/projects.html

addition, weather conditions prevented the calculation of atmospheric NH_3 in many locations for July 2011. For comparison, Figure 4-2 shows the spatial pattern of NH_3 emissions for the month of July in the 2011 NEI.

Figure 4-3 gives an aggregation of daytime IASI retrievals for July 2011 at a spatial resolution of 1 degree by 1 degree. An average of 102 observations was available per latitude-longitude grid cell. For comparison, Figure 4-4 shows IASI retrievals aggregated for the month of July over multiple years with a finer spatial resolution of 12 km grids. In order to achieve this finer spatial resolution, July data are combined from 2008 through 2015. The figure shows only those grid cells with five or more observations. An average of 14 observations was available per 12 km grid cell.

4.1.2. Evaluation of Satellite Data

Satellite retrieval algorithms for NH_3 have been validated using *in situ* data from intensive aircraft measurement campaigns (Sun *et al*, 2015; Warner *et al*, 2016), but aircraft studies are necessarily restricted in their geographic coverage and duration. Broader scale and independent validations of satellite measurements are desirable. The Colorado case study (Chapter 2) provided an opportunity to evaluate TES retrievals, since the study area was targeted for intensive satellite measurements to correspond with a broad program of aircraft measurements during the DISCOVER-AQ campaign. TES retrievals also give vertically resolved information on atmospheric NH_3, allowing a direct comparison with aircraft measurements at a given altitude. The TES results were compared with overlapping aircraft measurements in Chapter 2 (Table 2-4 and Figure 2-7). The two datasets showed reasonable agreement, with a correlation coefficient of 0.78, or r^2 of 0.61.

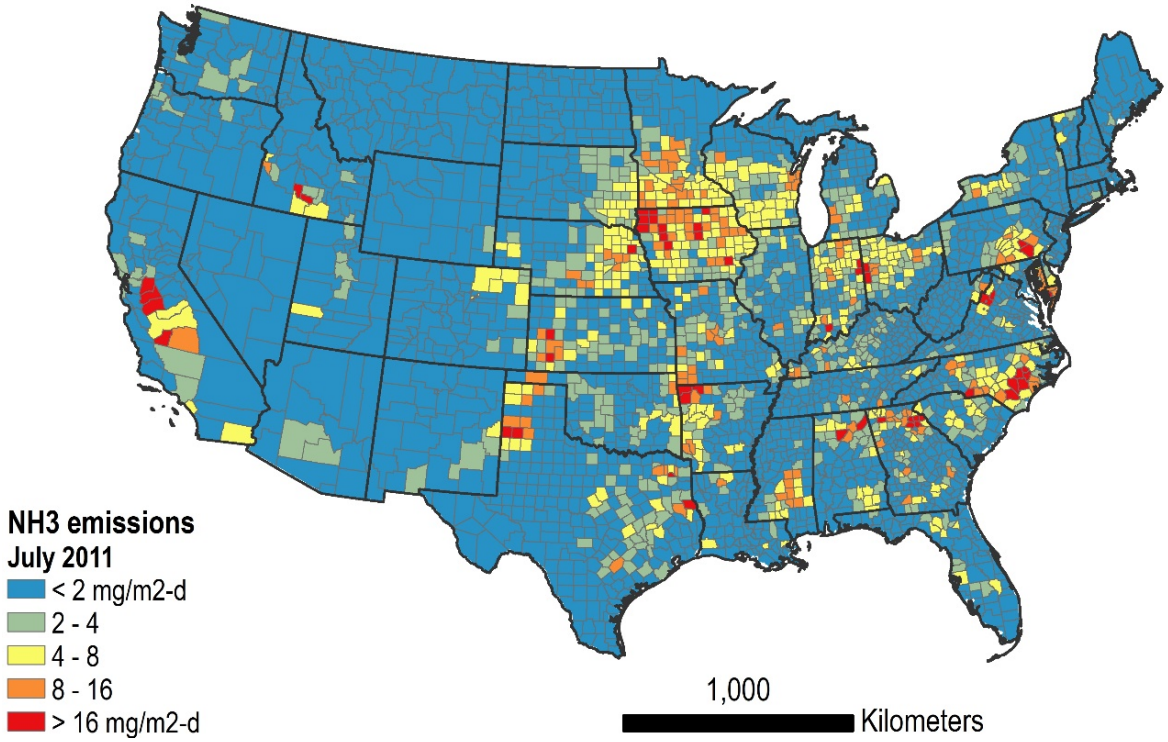

Figure 4-2. Spatial density of NH_3 emissions for July in the 2011 NEI.

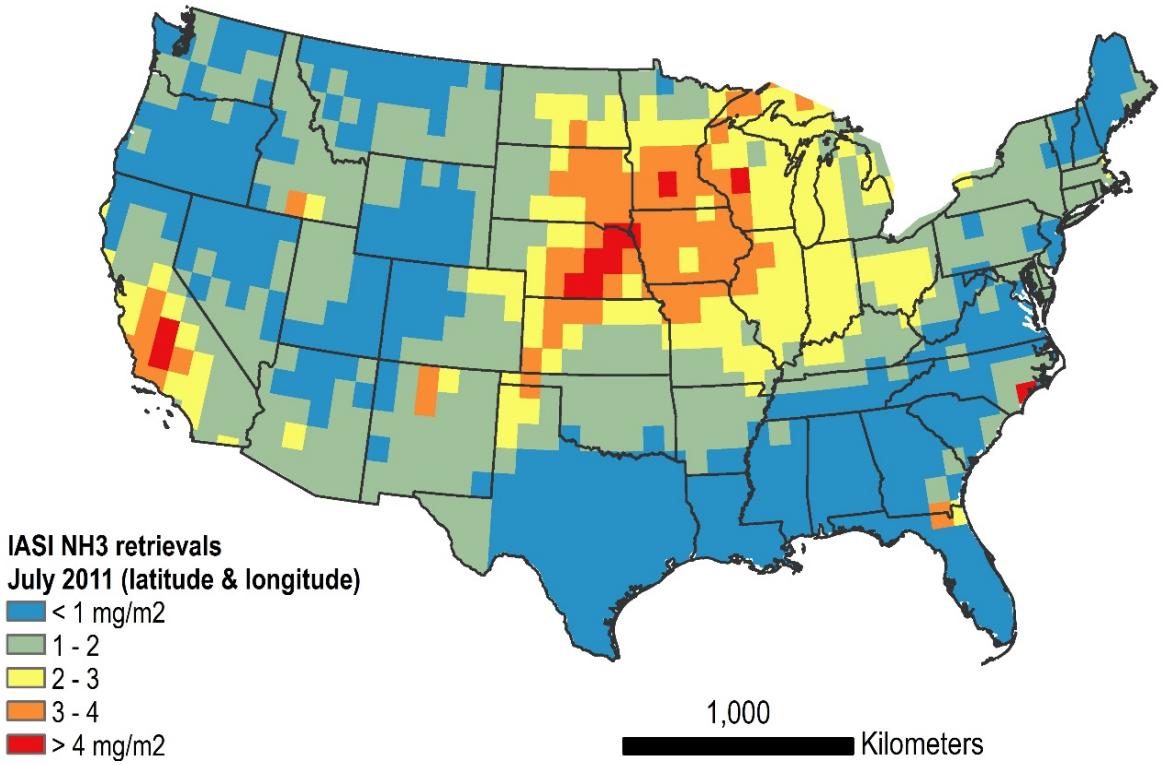

Figure 4-3. IASI NH_3 retrievals for July 2011 aggregated to 1 degree latitude by 1 degree longitude.

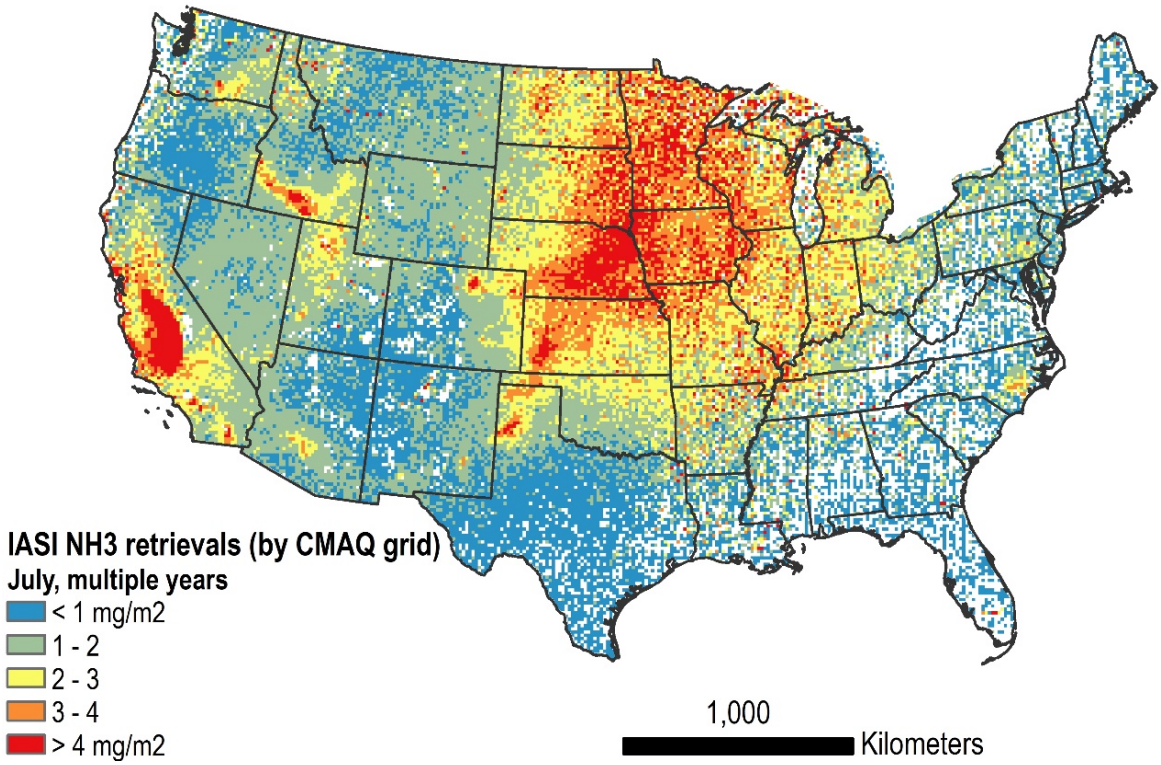

Figure 4-4. IASI NH_3 retrievals for July aggregated across multiple years (2008-2015) at a spatial resolution of 12 km.

In principle, the continuous NH_3 monitoring data used in the North Carolina case study (Chapter 3) appears to be another possible source of data for evaluating satellite measurements. The continuous monitor in Clinton, North Carolina measured hourly concentrations of NH_3 over an 8-year period from 2008 to 2015. Unfortunately, large spatial variations in the vicinity of the Clinton monitor complicated efforts to analyze the relation between measurements at the monitor and retrievals from the satellite. However, model biases computed using IASI satellite retrievals were consistent with model bias values computed based on the Clinton monitor.

4.2. Agricultural NH_3 Emissions Inventory

The U.S. National Emissions Inventory (NEI) for the agricultural sector is continuously evolving. The U.S. EPA compiles the NEI every three years. At this writing the 2014 emissions inventory has been developed in draft form (version 2), and the latest final inventory is the 2011 NEI. NAQFC modeling for the Colorado case study in Chapter 2 was based on the 2008 NEI. The North Carolina case study in Chapter 3 used the 2011 NEI, and a modified version of the 2011 NEI.

Methodologies for calculating agricultural NH_3 emissions are changing for the 2014 NEI, as the U.S. EPA is moving to more refined emissions models for both animal wastes and nitrogen fertilizers (McQuilling and Adams, 2015; Cooter *et al*, 2012). Therefore, the evaluation and validation of the emissions inventory must be an ongoing process. This process must also take into account the diversity of the inventory. In different regions of the country, the NH_3 inventory is dominated by different sources, as shown in Figure 4-5. The figure identifies the types of domestic livestock which account for the largest share of emissions in different regions of the continental U.S., based on the 2011 NEI. It must also be noted that the NEI does not provide separate estimates for all categories of livestock included in the Census of Agriculture.

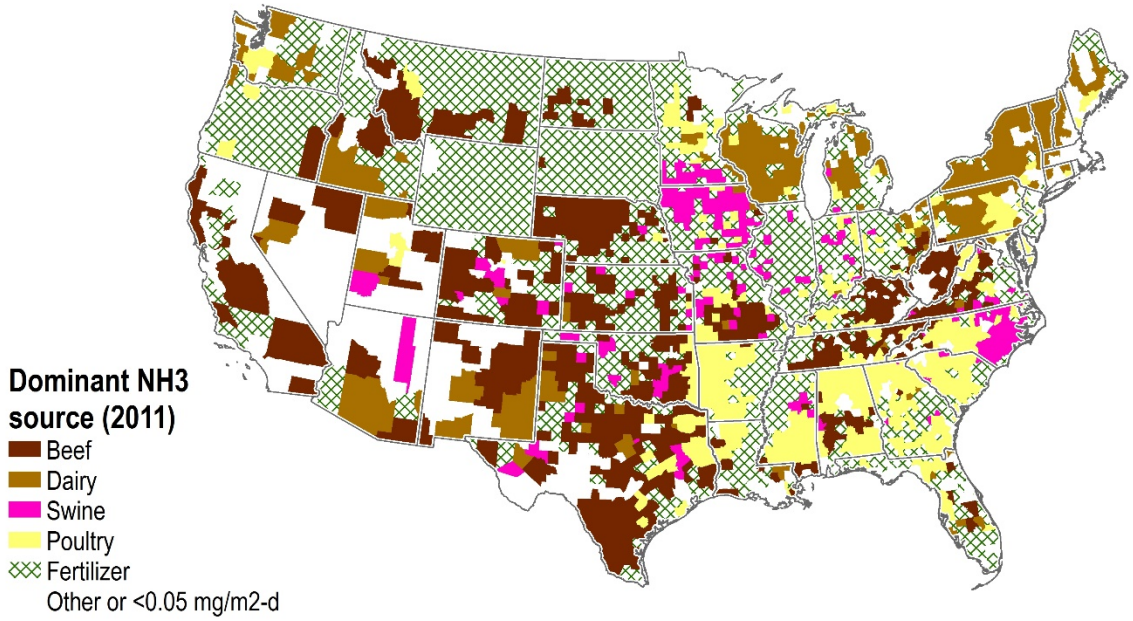

Figure 4-5. Dominant sources of NH_3 emissions by region, as estimated in the 2011 NEI.

For instance, the inventory does not currently differentiate between cattle in feedlots and cattle in pasture. Nor does the inventory provide separate calculations for turkey production, which represents a growing industry in some regions.

Appendix A gives results of a screening comparison of NAQFC model results with AMoN measurements and satellite-based measurements for the continental U.S. in July 2011. Because of the long averaging time of AMoN measurements and the variability of satellite-based measurements, the one-month model run was not sufficient to provide a definitive evaluation of model results or emissions inputs. In the absence of focused short-term measurements, such as those used in the Colorado and North Carolina case studies, a longer simulation period or multiple simulation periods would be required.

4.3. Spatial and Temporal Variations

Both the Colorado and North Carolina case studies showed large variations in the concentration of atmospheric NH_3 at scales smaller than the 12-km modeling grid size. Both of the case studies regions include large concentrations of CAFOs which may account for these spatial and temporal variations. For instance, in North Carolina, animal wastes are periodically distributed to fields using high pressure sprays which can produce localized emissions of NH_3.

Figure 4-6 shows the variation in NH_3 column loading over North Carolina for a single day in 2015. The North Carolina monitors in Clinton and Kinston showed changes exceeding 75 ppbv of NH_3 in the span of an hour. In Colorado, aircraft measurements show variations of up to 75 ppbv of NH_3 within a distance of 6 km. The large spatial variations in NH_3, coupled with the treatment of NH_3 emissions as an area source, complicate our ability to validate the model for NH_3. This is because any flaw in the spatial allocation process will cause a bias at any fixed monitoring location.

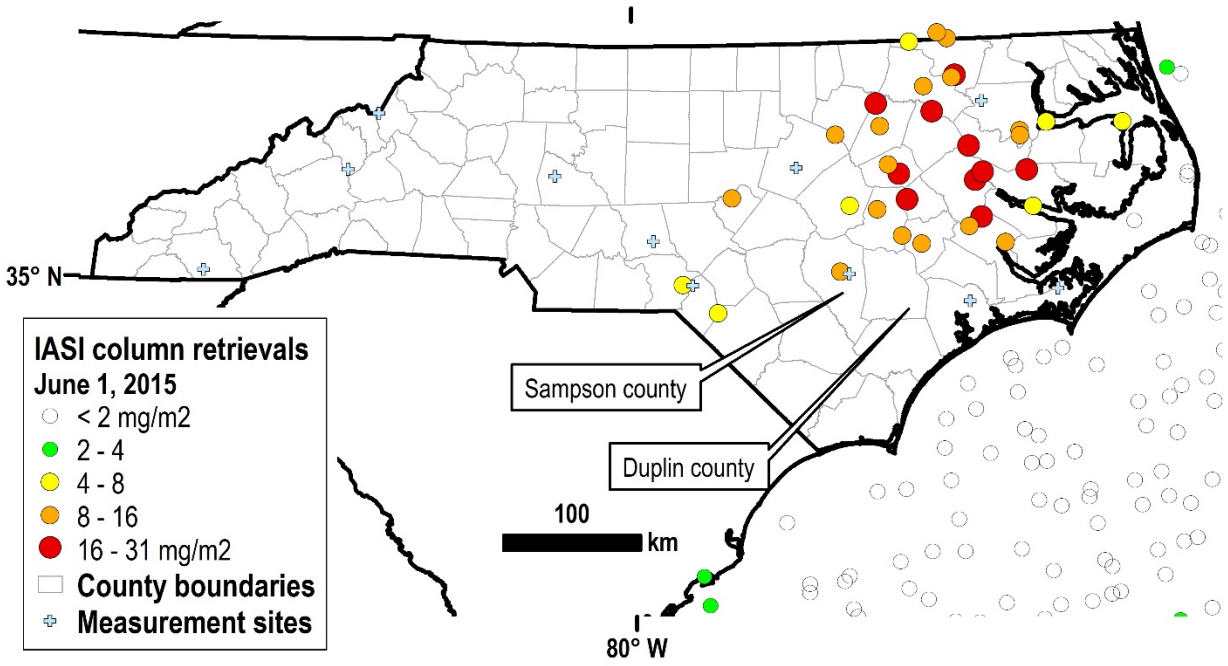

Figure 4-6. Spatial variations in total column NH_3 measured by IASI on a single day.

NH_3 is not the final endpoint of a typical CMAQ simulation; rather, it is an intermediate parameter in the calculation of $PM_{2.5}$ concentrations and deposition rates for reactive nitrogen and acid gases. Therefore, the accuracy of atmospheric NH_3 predictions may be viewed as less important than the accuracy of these other endpoints. However, variations in NH_3 on a scale smaller than the model grid size (generally 12 km) or the model time resolution (hourly for emissions) may adversely affect the accuracy of the model for simulating reactions where rates are nonlinear with respect to the NH_3 concentration.

Chapter 5

Summary and Conclusions

5.1. Impacts on the Nitrogen Cycle

Despite large uncertainties of the natural N fluxes at the global scale, the rapid growth of anthropogenic production now makes it unquestionably dominant relative to the total of natural sources. Most of the growth in anthropogenic nitrogen emission has occurred in the last 50 years. This is a significant perturbation of a global geochemical cycle in a relatively short period of time. Regulatory and voluntary measures have been adopted to address some components of the nitrogen stream. Nitrogen-use efficiency has increased in the U.S. and Europe in recent years. This suggests that increases in nitrogen-use efficiency can abate or perhaps reverse the worldwide increase in nitrogen fertilizer use. Unfortunately, there is no integrated regulatory approach for control of reactive nitrogen compounds. In particular, agricultural emissions of reactive nitrogen compounds to the atmosphere are not regulated in the U.S.

Human-induced changes to the global nitrogen cycle bear a number of similarities to our changes in the global carbon cycle. Fixed N and fossil C have provided great benefits to the human standard of living. The increased use of nitrogen has been critical for increased crop yields and protein production to keep pace with the growing world population. Like the burning of fossil carbon, increased fixation of nitrogen can have adverse environmental consequences at local, regional, and global scales. In addition, our use of fossil carbon and synthetically reactive nitrogen have both grown exponentially in the past 150 years. Anthropogenic production of reactive nitrogen has grown in relation to natural sources, so that the anthropogenic increment is nearly as great as the best estimate of the total natural nitrogen fixation in terrestrial and marine

environments. Demands for increased nitrogen usage will continue as world population and agricultural production continue to rise. Thus, reducing the demands for reactive nitrogen may prove to be more difficult than reducing emissions of CO_2.

The impacts of anthropogenic perturbations on the reactive nitrogen cycle are still mainly local, regional and global. Current estimates indicate that global nitrogen fixation is balanced by denitrification, although these budget calculations are subject to large uncertainties. Thus, the large increase in anthropogenic production may be balanced by increased denitrification. Nevertheless, if anthropogenic production continues to increase, denitrification processes may not continue to offset the increased production. Continued increases in reactive nitrogen production could accelerate species diversity impacts and N_2O production. As with carbon, public awareness of the impact of reactive nitrogen is also increasing. In the case of reactive nitrogen, anthropogenic contributions continue to grow in relation to the natural budget, with uncertain consequences. Mitigating both carbon and nitrogen is a grand challenge.

5.2. NH_3 Modeling

Emissions of NH_3 represent a large source of reactive nitrogen which is essentially unregulated in the U.S. There is currently no broad air pollution control program for NH_3 emissions in the U.S. comparable to the program for NO_X. The lack of regulatory attention for NH_3 emissions is understandable. The bulk of NH_3 emissions to the atmosphere in the U.S. emanate from agricultural operations, primarily animal waste management and synthetic nitrogen fertilizer application. Although the adverse impacts of NH_3 emissions are significant, they are also subtle, so that the effect of any given source can be difficult to ascertain. NH_3 can contribute to elevated levels of $PM_{2.5}$ even though the level of NH_3 is well below the perceptible

odor threshold. Similarly, the impacts of NH_3 deposition on eutrophication or species diversity are also difficult to separate from the impacts of other factors.

Atmospheric chemistry models such as the Community Multiscale Air Quality (CMAQ) model are used to simulate the reactions of NH_3 and other precursors to form $PM_{2.5}$, and to simulate the deposition of NH_3 and NH_4^+ to terrestrial and aquatic ecosystems. This type of modeling analysis is essential in evaluating the impacts of NH_3 emissions and the potential benefits of NH_3 controls. The U.S. National Oceanic and Atmospheric Administration (NOAA) uses the CMAQ model to forecast elevated levels of air pollution within the National Air Quality Forecast Capability (NAQFC). Methods are needed to evaluate the capability of NAQFC model to predict NH_3 within the NAQFC, and to identify potential improvements to NH_3 emissions estimates and prediction methods. The current research uses ground based measurements, *in situ* aircraft measurements, and satellite based measurements of NH_3 to evaluate and improve the handling of atmospheric models. Two detailed case study analyses were performed in collaboration with NOAA, drawing on detailed measurements for Northeast Colorado and North Carolina.

The Colorado case study used measurements gathered in the DISCOVER-AQ Colorado field campaign and the concurrent Front Range Air Pollution and Photochemistry Experiment (FRAPPE) in July and August 2014. *In situ* aircraft measurements of atmospheric NH_3 suggest that the NAQFC CMAQ model underestimated the NH_3 concentration in Northeastern Colorado by 63%. Comparisons with ground-level measurements and satellite based measurements give similar results. Measurements at two Ammonia Monitoring Network (AMoN) sites in the region indicate that the NAQFC model underestimated atmospheric NH_3 by 67%. Concentration

retrievals from the Tropospheric Emissions Spectrometer (TES) on the Aura satellite indicate that the model underestimated atmospheric NH_3 by 33% to 76%.

The underestimation of NH_3 was not accompanied by an underestimation of particulate NH_4^+, which is affected by other factors including acid availability, removal rate, and gas-particle partition. The average modeled concentration of NH_4^+ was 18% higher than the average measured concentration. The underestimation of NH_3 varied across the study domain, with the highest errors occurring in a region of intensive agriculture near Greeley, and in the vicinity of Denver. Seasonal patterns measured at an Ammonia Monitoring Network (AMoN) site in the region suggest that the underestimation of NH_3 is not due to the seasonal allocation of emissions, but to the overall annual emissions estimate.

In the North Carolina case study, a state-maintained permit database for Confined Animal Feeding Operations (CAFOs) in North Carolina was used to improve the spatial allocation of NH_3 emissions. In addition, based on initial model testing, a lower-end estimate was developed for NH_3 emissions from emissions from swine operations, resulting in the lowering of statewide NH_3 emissions by an average of 42%. Even with the downward adjustment of CAFO NH_3 emissions, the NAQFC model overpredicted atmospheric NH_3 by an average of 60% when compared with hourly measurements in Clinton, NC. The average concentration measured by the monitor was 6.6 ppbv for July 2011, while the average predicted by the model was 10.5 ppbv. The monitoring site is located in Sampson County, in a region of dense NH_3 emissions from swine operations. The other available ground level measurements are more distant from the region of dense CAFO emissions. Atmospheric NH_3 concentrations at the three North Carolina AMoN sites were 1.3 ppbv or less; and concentrations of particulate NH_4^+ were 1.3 $\mu g\ m^{-3}$ or less. Model errors with respect to these measurements were small in absolute magnitude. Model

predictions were in good agreement with daytime retrievals of the total atmospheric column NH_3 concentration from the Infrared Atmospheric Sounding Interferometer (IASI) on the MetOp satellite.

The model bias at the Clinton site was reduced by the use of CAFO permit information to improve the spatial allocation of NH_3 emissions. This spatial allocation modification reduced emissions by 41% in the model grid containing the Clinton monitor. Therefore, model bias without the spatial adjustment could be expected to be up to 41% higher than the current overprediction (60%).

This North Carolina case study is the first to use hourly NH_3 concentrations from the Clinton monitor to evaluate predictions by the NAQFC model, providing new information on the performance of the model for reproducing the diurnal pattern of NH_3 concentration. The diurnal pattern of predicted by the model was similar to the diurnal pattern measured by the continuous monitor, with both showing elevated concentrations in the mid-afternoon and lower concentrations at night.

The model underpredicted wet deposition of NH_4^+ by 17-22% based on rainfall concentration measurements at the Clinton National Trends Network (NTN) site. Wet deposition was also underpredicted at most other NTN sites across the state. In addition, the model predictions of dry NH_3 deposition were lower than literature reports. The combination of an overestimation of NH_3 and underestimation of wet and dry deposition suggests that the overstatement in NH_3 may result from a failure of the model to properly simulate NH_3 removal processes in North Carolina.

Results for both Colorado and North Carolina indicate that further improvement of the emission inventories and modeling approaches are required to reduce the bias in NAQFC NH_3

modeling predictions. Methodologies for calculating agricultural NH_3 emissions are changing for the 2014 NEI, as the U.S. EPA is moving to more refined emissions models for both animal wastes and nitrogen fertilizers. Therefore, the evaluation and validation of the emissions inventory must be an ongoing process. This process must also take into account the diversity of the inventory in different regions of the country. It must also be noted that the NEI does not provide separate estimates for all categories of livestock included in the Census of Agriculture. For instance, the inventory does not currently differentiate between cattle in feedlots and cattle in pasture.

Results for both case studies also show considerable variability of NH_3 concentrations at scales smaller than a 12-km modeling grid. This may adversely affect the accuracy of the model for simulating reactions where rates are nonlinear with respect to the NH_3 concentration. The spatial variability also makes it difficult to relate measurements from any particular fixed monitor to NH_3 concentrations on broader scales. Satellite measurements provide a valuable tool for evaluating the broad spatial patterns of NH_3 emissions and transport.

REFERENCES

AMEC. 2013. Clean Air Status and Trends Network (CASTNET) 2011 Annual Report. U.S. Environmental Protection Agency. www3.epa.gov/castnet/docs/

Aneja, V.P., W.H. Schlesinger, and J.W. Erisman. 2008. Farming pollution, *Nature Geoscience*, vol. 1, pp. 409-411.

Aneja, V.P., W.H. Schlesinger, and J.W. Erisman. 2009. Effects of Agriculture upon the Air Quality and Climate: Research, Policy and Regulations. *Environmental Science and Technology.* 43(12): 4234-4240.

Altieri, K.E., S.E. Fawcett, A.J. Peters, D.M. Sigman, and M.G. Hastings. 2016. Marine biogenic source of atmospheric organic nitrogen in the subtropical North Atlantic. *Proceedings of the National Academy of Sciences*, 113 (4) 925-930. doi: 10.1073/pnas.1516847113.

Appel, K.W., Napelenok, S.L., Foley, K.M., Pye, H.O., Hogrefe, C., Luecken, D.J., Bash, J.O., Roselle, S.J., Pleim, J.E., Foroutan, H. and Hutzell, W.T., 2017. Description and evaluation of the Community Multiscale Air Quality (CMAQ) modeling system version 5.1. *Geoscientific Model Development*, 10(4), p.1703.

Arya, S.P. 1999. Air pollution meteorology and dispersion. Oxford University Press, New York, NY.

Bash, J.O, E.J. Cooter, R.L. Dennis, J.T. Walker, and J.E. Pleim. 2013. Evaluation of a regional air-quality model with bidirectional NH_3 exchange coupled to an agroecosystem model. *Biogeosciences*. 10: 1635-1645.

Battye, W., V.P. Aneja, P.A. Roelle. 2003. Evaluation and improvement of ammonia emissions inventories. *Atmospheric Environment.* 37(27): 3873-3883.

Battye, W.H., C.D. Bray, V.P. Aneja, D. Tong, P. Lee, Y. Tang. 2016. Evaluating ammonia (NH_3) predictions in the NOAA National Air Quality Forecast Capability (NAQFC) using in situ aircraft, ground-level, and satellite measurements from the DISCOVER-AQ Colorado campaign. *Atmospheric Environment*, 140: 342-351.

Battye, W., V.P. Aneja, and W.H. Schlesinger. 2017. Is nitrogen the next carbon? *Earth's Future*, 5. doi 10.1002/2017EF000592.

Binkowski, F.S., and U. Shankar. 1995. The regional particulate model 1. Model description and preliminary results. Journal of Geophysical Research. 100 (D12): 26,191-26,209. doi:10.1029/95JD02093.

Boden, T.A., G. Marland, and R.J. Andres. 2013. Global, Regional, and National Fossil-Fuel CO_2 Emissions. Carbon Dioxide Information Analysis Center, Oak Ridge National Laboratory, U.S. Department of Energy, Oak Ridge, TN. doi: 10.3334/CDIAC/00001_V2013.

Boschetti, L., D. Roy, and A.A. Hoffmann. 2009. MODIS Collection 5 Burned Area Product-MCD45. User's Guide, Version 2. National Aeronautics and Space Administration (NASA), Goddard Space Flight Center.

Boussingault, J.B. 1856. Recherches sur la vegetation. Troisieme memoire. De l'action du salpetre sur le developpement des plants. *Ann. Chim. Phys. Ser*. 3 (45), 5–41.

Bouwman, L., K.K. Goldewijk, K.W. Van Der Hoek, A.H.W. Beusen, D.P. Van Vuuren, J. Willems, M.C. Rufino, and E. Stehfest. 2013a. Exploring global changes in nitrogen and phosphorus cycles in agriculture induced by livestock production over the 1900–2050 period. *Proceedings of the National Academy of Sciences*. 110(52): 20882–20887. doi/10.1073/pnas.1012878108.

Bouwman, A.F., A.H W. Beusen, J. Griffioen, J.W. Van Groenigen, M.M. Hefting, O. Oenema, P.J.T.M. Van Puijenbroek, S. Seitzinger, C.P. Slomp and E. Stehfest. 2013b. Global trends and uncertainties in terrestrial denitrification and N_2O emissions. Philosophical Transactions of the Royal Society B, 368: 20130112.

Bray, C.D, W. Battye, V.P. Aneja, D. Tong, P. Lee, Y. Tang, and J. B. Nowak. 2017. Evaluating ammonia (NH3) predictions in the NOAA National Air Quality Forecast Capability (NAQFC) using in-situ aircraft and satellite measurements from the CalNex2010 campaign
Atmospheric Environment, 163: 65-76.

Bullister, J.L. 2015. Atmospheric Histories (1765-2015) for CFC-11, CFC-12, CFC-113, CCl4, SF_6 and N_2O. NDP-095(2015). Carbon Dioxide Information Analysis Center, Oak Ridge National Laboratory, US Department of Energy, Oak Ridge, Tennessee. doi: 10.3334/CDIAC/otg.CFC_ATM_Hist_2015. http://cdiac.ornl.gov/ftp/oceans/CFC_ATM_Hist/CFC_ATM_Hist_2015.

Burns, D.A., Lynch, J.A., Cosby, B.J., Fenn, M.E., Baron, J.S. 2011, National Acid Precipitation Assessment Program Report to Congress 2011: An Integrated Assessment, National Science and Technology Council, Washington, DC. 114 p.

Burris, R.H. 1980. The global nitrogen budget – science or séance? In: Newton WE, Orme-Johnson W.H. (eds.), Nitrogen fixation, volume I. University Park Press, Baltimore, MD. pp 7-16.

Butler, T., R. Marino, D. Schwede, R. Howarth, J. Sparks, and K. Sparks. 2014. Atmospheric ammonia measurements at low concentration sites in the northeastern USA: implications for total nitrogen deposition and comparison with CMAQ estimates. *Biogeochemistry*. doi: 10.1007/s10533-014-0036-5.

Butterbach-Bahl, K., E. Nemitz, and S. Zachle, et al. 2011. "Nitrogen as a threat to the European greenhouse balance," in The European nitrogen assessment (Sutton, M.A. *et al*, eds.). Cambridge University Press.

Byun, D., and K.L. Schere. 2006. Review of the governing equations, computational algorithms, and other components of the models-3 Community Multiscale Air Quality (CMAQ) modeling system. *Applied Mechanics Review*. 59 (1-6), 51-77.

Cleveland, C.C., B.Z. Houlton, W.K. Smith, A.R. Marklein, S.C. Reed, W. Parton, S.J. Del Grosso, and S.W. Running. 2013. Patterns of new versus recycled primary production in the terrestrial biosphere. *Proceedings of the National Academy of Sciences*. 110(31): 12733–12737. doi/10.1073/pnas.1302768110.

Columella, Lucius Junius Moderatus. 70. On Agriculture. Harvard University Press.

Conant, R.T., A.B. Berdanier, and P.R. Grace. 2013. Patterns and trends in nitrogen use and nitrogen recovery efficiency in world agriculture. Global Biogeochemical Cycles, 27: 558-566. doi: 10.1002/gbe.20053.

Cooter, E.J., J.O. Bash, V. Benson, and L. Ran. 2012. Linking agricultural crop management and air quality models for regional to national-scale nitrogen assessments. *Biogeosciences*. 9: 4023-4035.

CMAS. 2016. Community Modeling and Analysis System. https://www.cmascenter.org/download.cfm

CSU. 2016. Agriculture – Weld County. Colorado State University, Cooperative Extension, Fort Collins, CO. http://coopext.colostate.edu/WELD/agriculture.htm

Cushman, G.T. 2013. Guano and the Opening of the Pacific World – a Global Ecological History. Cambridge University Press. pg. 47. doi: CBO9781139047470.

Day, E.E. X. Chen, K.A. Gebhart, C.M. Carrico, F.M. Schwandner, K.B. Benedict, B.A. Schichtel, J.L. Collett Jr.. 2012. Spatial and temporal variability of ammonia and other inorganic aerosol species. *Atmospheric Environment*, 61: 490-498, doi.org/10.1016/j.atmosenv.2012.06.045.

Delwiche, C.C. 1970. The Nitrogen Cycle. *Scientific American*.223: 137.

DeVries, T., C. Deutsch, P.A. Rafter, and F. Primeau. 2013a. Marine denitrification rates determined from a global 3-D inverse model. *Biogeosciences*, 10, 2481–2496. doi: 10.5194/bg-10-2481-2013.

DeVries, W., J. Kros, C. Krow, and S.P. Seitzinger. 2013b. Assessing planetary and regional nitrogen boundaries related to food security and adverse environmental impacts. *Current Opinion in Environmental Sustainability*, 5: 392-402. doi: 10.1016/j.cosust.2013.11.001.

Dombek, T. 2012. Quality Assurance Report National Atmospheric Deposition Program 2011. National Atmospheric Deposition Program, Illinois State Water Survey, University of Illinois at Urbana-Champaign.

Duce, R.A., J. LaRoche, K. Altieri, K.R. Arrigo, A.R. Baker, D.G. Capone, S. Cornell, F. Dentener, J. Galloway, R.S. Ganeshram, R.J. Geider, T. Jickells, M.M. Kuypers, R. Langlois, P.S. Liss, S. M. Liu, J.J. Middelburg, C.M. Moore, S. Nickovic, A. Oschlies, T. Pedersen, J. Prospero, R. Schlitzer, S. Seitzinger, L.L. Sorensen, M. Uematsu, O. Ulloa, M. Voss, B. Ward, and L. Zamora. 2008. Impacts of atmospheric anthropogenic nitrogen on the open ocean. *Science*, 320, 893-897.

Elser, J. J., M. E. S. Bracken, E. E. Cleland, D. S. Gruner, W. S. Harpole, H. Hillebrand, J. T. Ngai, E. W. Seabloom, J. B. Shurin, and J. E. Smith. 2007. Global analysis of nitrogen and phosphorus limitation of primary producers in freshwater, marine and terrestrial ecosystems. *Ecology Letters* 10:1135–1142.

Erisman, J.W., A. Bleeker, A. Hensen, and A. Vermeulen. 2008. Agricultural air quality in Europe and the future perspectives. *Atmospheric Environment*, 42: 3209-3217.

Erisman, J.W., J.N. Galloway, N.B. Dise, M.A. Sutton, A. Bleeker, B. Grizzetti, A.M. Leach, and W. DeVries. 2015. Nitrogen: too much of a vital resource. World Wildlife Fund Netherlands.

Erisman, J.W., M. Sutton, J. Galloway, Z. Klimont, W. Winiwarter. 2008. How a century of ammonia synthesis changed the world. *Nature Geoscience*, 1: 636 – 639.

Etheridge, D.M., L.P. Steele, R.L. Langenfelds and R.J. France. 1996. Natural and anthropogenic changes in atmospheric CO_2 over the last 1000 years from air in Antarctic ice and firn. *Journal of Geophysical Research*, 101(D2), 4115-4128.

Eugster, O. and N. Gruber. 2012. A probabilistic estimate of global marine N-fixation and denitrification. *Global Biogeochemical Cycles*, 26, GB4013. doi: 10.1029/2012GB004300.

FAO. 2015. FAOSTAT, production of crops by year. Food and Agriculture Organization of the United Nations, Statistics Division. http://faostat3.fao.org/download/Q/QD/E

Felix, J.D., and E.M. Elliott. 2013. The agricultural history of human-nitrogen interactions as recorded in ice core delta N^{15}-NO_3, *Geophysical Research Letters* 40: 1642-1646.

Fowler, D., M. Coyle, U. Skiba, M.A. Sutton, J.N. Cape, S. Reis, L.J. Sheppard, A. Jenkins, B. Grizzetti, J.N. Galloway, P. Vitousek, A. Leach, A.F. Bouwman, K. Butterbach-Bahl, F. Dentener, D. Stevenson, M. Amann, and M. Voss. 2013. The global nitrogen cycle in the twenty-first century. *Philosophical Transactions of the Royal Society B*, 368: 20130164.

Fowler, D. C.E. Steadman, D. Stevenson, M. Coyle, R.M. Rees, U.M. Skiba, M.A. Sutton, J.N. Cape, A.J. Dore, M. Vieno, D. Simpson, S. Zaehle, B.D. Stocker, M. Rinaldi, M.C. Facchini, C.R. Flechard, E. Nemitz, M. Twigg, J.W. Erisman, K. Butterbach-Bahl, and J.N. Galloway. 2015. Effects of global change during the 21st century on the nitrogen cycle, *Atmospheric Chemistry and Physics* 15, 13849-13893. Doi: 10.5194/acp-15-13849-2015

Galloway, J.N. and Cowling, E.B. 2002. Reactive nitrogen and the world: 200 years of change. *AMBIO: A Journal of the Human Environment* 31(2):64-71.

Galloway J.N., F.J. Dentener, D.G. Capone, E.W. Boyer, R.W. Howarth, S.P. Seitzinger, G.P. Asner, C.C. Cleveland, P.A. Green, E.A. Holland, D.M. Karl, A.F. Michaels, J.H. Porter, A.R. Townsend and C.J. Vorosmarty. 2004. Nitrogen cycles: past, present and future. *Biogeochemistry*, 70:153–226.

Galloway, J.N., A.R. Townsend, J.W. Erisman, M. Bekunda, Z. Cai, J.R. Freney, L.A. Martinelli, S.P. Seitzinger, M.A. Sutton. 2008. Transformation of the nitrogen cycle: recent trends, questions, and potential solutions. *Science* 320 (5878), 889-892. doi: 10.1126/science.1136674.

Gilliland, A.B., K.W. Appel, R.W. Pinder, and R.L. Dennis. 2006. Seasonal NH_3 emissions for the continental united states: Inverse model estimation and evaluation. *Atmospheric Environment*. 40: 4986–4998.

Groβkopf, T., W. Mohr, T. Baustian, H. Schunck, D. Gill, M.M.M. Kuypers, G. Lavik, R.A. Schmitz, D.W.R. Wallace, and J. LaRoche. 2012. Doubling of marine dinitrogen-fixation rates based on direct measurements. Nature, 488: 361. doi:10.1038/nature11338.

Gruber, N., and J.N. Galloway. 2008. An Earth-system perspective of the global nitrogen cycle. *Nature* 451 (17), 293-296. doi: 10.1038/nature06592.

Hastings, M.G., J.C. Jarvis, and E.J. Steig. 2009. Anthropogenic impacts on nitrogen isotopes of ice-core nitrate. Science, 324 (5932): 1288. doi: 10.1126/science. 1170510.

Herb, J., A.B. Nadykto, and F. Yu. 2011. Large ternary hydrogen-bonded pre-nucleation clusters in the Earth's atmosphere. *Chemical Physics Letters*. 518: 7–14.

Herridge, D.F., M.B. Peoples, and R.M. Boddey. 2008. Global inputs of biological nitrogen fixation in agricultural systems. *Plant Soil*, 311: 1-18. doi: 10.1007/sl 1104-008-9668-3.

Hofstra, N. and A.F. Bouwman. 2005. Denitrification in agricultural soils: summarizing published data and estimating global annual rates. *Nutrient Cycling in Agroecosystems*, 72: 267–278. doi: 10.1007/s10705-005-3109-y

Holmes, N.S. 2007. A review of particle formation events and growth in the atmosphere in the various environments and discussion of mechanistic implications. Atmospheric Environment. 41: 2183–2201.

Houlton, B.Z. and E. Bai. 2009. Imprint of denitrifying bacteria on the global terrestrial biosphere. *Proceedings of the National Academy of Sciences*, 106 (51): 21,713-21,716.

Houlton, B.Z., S.L. Morford, and R.A. Dahlren. 2018. Convergent evidence for widespread rock nitrogen sources in Earth's surface environment. *Science*, 360: 58-62.

Hurley, Ray, et al. 1959. U.S. Census of Agriculture. 1959. General Report – Volume II – Statistics by Subjects. U.S. Bureau of the Census, Washington, DC. www.agcensus.usda.gov/Publications/Historical_Publications/. pg 325.

International Energy Agency (IEA). 2017. IEA finds CO2 emissions flat for third straight year even as global economy grew in 2016. IEA News. March 17.

IFA. 2016. Nitrogen fertilizer consumption data. International Fertilizer Industry Association, Paris, France. http://ifadata.fertilizer.org/ucSearch.aspx. Retrieved March 12.

India Planning Commission (IPC). 2008. Eleventh Five Year Plan 2007-12, Volume III agrIculture, rural development, industry, services, and physical infrastructure. Oxford University Press.

IPCC. 2014. Climate Change 2013: The Physical Science Basis. Contribution of Working Group I to the Fifth Assessment Report of the Intergovernmental Panel on Climate Change, Stocker, T.F., D. Qin, G.-K. Plattner, M. Tignor, S.K. Allen, J. Boschung, A. Nauels, Y. Xia, V. Bex and P.M. Midgley (eds.). Cambridge University Press, Cambridge, United Kingdom and New York, NY. 1535 pp.

Jickells, T.D., E. Buitenhuis, K. Altieri, A.R. Baker , D. Capone, R.A. Duce, F. Dentener, K. Fennel, M. Kanakidou, J. LaRoche, K. Lee, P. Liss, J.J. Middelburg, J.K. Moore, G. Okin, A. Oschlies, M. Sarin, S. Seitzinger, J. Sharples, A. Singh, P. Suntharalingam, M. Uematsu, and L.M. Zamorau. 2017. A reevaluation of the magnitude and impacts of anthropogenic atmospheric nitrogen inputs on the ocean. Global Biogeochemical Cycles. 31. doi:10.1002/2016GB005586.

Jones, L., M.S. Nizam, B. Reynolds, S. Bareham, and E.R.B. Oxley. 2013. Upwind impacts of ammonia from an intensive poultry unit. *Environmental Pollution*. 180: 221-228.

Kelly, J.T., K.R. Baker, J.B. Nowak, J.G. Murphy, M.Z. Markovic, T.C. VandenBoer, R.A. Ellis, J.A. Neuman, R.J. Weber, J.M. Roberts, P.R. Veres, J.A. de Gouw, M.R. Beaver, S. Newman, and C. Misenis. 2014. Fine-scale simulation of ammonium and nitrate over the South Coast Air Basin and San Joaquin Valley of California during CalNex-2010. *Journal of Geophysical Research Atmospheres*. 119: 3600–3614. doi:10.1002/2013JD021290.

Kim, T-W, K. Lee, R.G. Najjar, H-D. Jeong, H.J. Jeong. 2011. Increasing N abundance in the northwestern Pacific Ocean due to atmospheric nitrogen deposition. *Science*, 334 (6055), 505-509. doi: 10.1126/science.1206583.

Kim. I-N., K. Lee, N. Gruber, D.M. Karl, J.L. Bullister, S. Yang and T-W. Kim. 2014. Increasing anthropogenic nitrogen in the North Pacific Ocean. *Science*, 346 (6213), 1102-1106. doi: 10.1126/science.1258396.

Kwok, R.H.F., Napelenok, S.L., and Baker, K.R. 2013. Implementation and evaluation of $PM_{2.5}$ source contribution analysis in a photochemical model. *Atmospheric Environment*. 80: 398–407.

Lelieveld, J., J.S. Evans, M. Fnais, D. Giannadaki, and A. Pozzer. 2017. The contribution of outdoor air pollution sources to premature mortality on a global scale. *Nature.* 525: 367-384. doi:10.1038/nature15371.

Li, Y., B.A. Schichtel, J.T. Walker, D.B. Schwede, X. Chen, C.M.B. Lehmann, M.A. Puchalski, D.A. Gay, and J.L. Collett. 2016. Increasing importance of deposition of reduced nitrogen in the United States. *Proceedings of the National Academy of Sciences,* doi: 10.1073/pnas.1525736113.

Lin, L.I-K. 1989. A concordance correlation coefficient to evaluate reproducibility. *Biometrics*. 45:255-268.

Lin, L.I-K. 1992. Assay validation using the concordance correlation coefficient. *Biometrics*. 48:599-604.

Lu, X., Q. Mao, F.S. Gilliam, Y. Luo, and J. Mo. 2014. Nitrogen deposition contributes to soil acidification in tropical ecosystems. *Global Change Biology*, 20: 3790–3801.

Mathur, R., J. Pleim, K. Schere, G. Pouliot, J. Young, and T. Otte. 2005. The community Multiscale Air Quality (CMAQ) model: Model configuration 475 and enhancements for 2006 air quality forecasting. Air Quality Forecaster Focus Group Meeting, September 16, 2005, Washington, DC.

McQuilling, A.M., and P.J. Adams. 2015. Semi-empirical process-based models for ammonia emissions from beef, swine, and poultry operations in the United States. *Atmospheric Environment*, 120: 127-136.

National Atmospheric Deposition Program (NADP). 2018. Ambient Ammonia Monitoring Network (AMoN). http://nadp.sws.uiuc.edu/AMoN/AMoNfactsheet.pdf

NCDEQ. 2016a. Air monitoring – ammonia. North Carolina Department of Environmental Quality, Raleigh, NC. https://xapps.ncdenr.org/aq/ambient/AmbtPollutant.jsp

Orsini, D.A., Y. Ma, A. Sullivan, B. Sierau, K. Baumann, R.J. Weber. 2003. Refinements to the particle-into-liquid sampler (PILS) for ground and airborne measurements of water soluble aerosol composition. *Atmospheric Environment* 37: 1243–1259.

Ortega, Luis. 1984. Nitrates, Chilean Entrepreneurs and the Origins of the War of the Pacific. *Journal of Latin American Studies.* 16: 339–46.Paerl, H.W. 1988. Nuisance Phytoplankton Blooms in Coastal, Estuarine, and Inland Waters, *Limnology and Oceanography.* 33: 823-847.

Paerl, H.W. 1988. Nuisance Phytoplankton Blooms in Coastal, Estuarine, and Inland Waters, *Limnology and Oceanography.* 33: 823-847.

Pan, Li, Daniel Tong, Pius Lee, H-C. Kim, and Tianfeng Chai. 2014. Assessment of NOx and O_3 forecasting performances in the US National Air Quality Forecasting Capability before and after the 2012 major emissions updates. *Atmospheric environment*, 95: 610-619.

Paulot, F., D.J. Jacob, M.T. Johnson, T.G. Bell, A.R. Baker, W.C. Keene, I.D. Lima, S.C. Doney and C.A. Stock. 2015. Global oceanic emission of ammonia: Constraints from seawater and atmospheric observations. *Global Biogeochemical Cycles,* 29: 1165–1178. doi:10.1002/2015GB005106.

Pay, M.T., P. Jiminez-Guerrero, and J.M. Baldasano. 2012. Assessing sensitivity regimes of secondary inorganic aerosol formation in Europe with the CALIOPE-EU modeling system. *Atmospheric Environment*. 51: 146-164.

Phillips, S.B., S.P. Arya, V.P. Aneja. 2004. Ammonia flux and dry deposition velocity from near-surface concentration gradient measurements over a grass surface in North Carolina. *Atmospheric Environment*, 38: 3469–3480.

Pinder, R.W., N.D. Bettez, G.R. Bonan, T.L. Greaver, W.R. Wieder, W.H. Schlesinger, and E.A. Davidson. 2013. Impacts of human alteration of the nitrogen cycle in the U.S. on radiative forcing. *Biogeochemistry*, 114: 25-40. doi: 10.1007s/10533-012-9787-z.

Pleim, J.E., J.O. Bash, J.T. Walker, and E.J. Cooter. 2013. Development and evaluation of an ammonia bidirectional flux parameterization for air quality models. *Journal of Geophysical Research: Atmospheres*, 118, 3794–3806, doi:10.1002/jgrd.50262.

Pope III, C., M. Ezzati, and D.W. Dockery. 2009. Fine-particulate air pollution and life expectancy in the United States. *New England Journal of Medicine.* 360 (4): 376–386.

Puchalski, M.A., M.E. Sather, J.T. Walker, C.M.B. Lehmann, D.A. Gay, J. Mathew and W.P. Robarge. 2011. Passive ammonia monitoring in the United States: Comparing three different sampling devices. *Journal of Environmental Monitoring*. 13: 3156-3167.

Puchalski, M.A., C.M. Rogers, R. Baumgardner, K.P. Mishoe, G. Price, M.J. Smith, N. Watkins, and C.M. Lehmann. 2015. A statistical comparison of active and passive ammonia measurements collected at Clean Air Status and Trends Network (CASTNET) sites. *Environmental Science Processes and Impacts*. 17: 358-369.

Ravishankara, A.R., J.S. Daniel and R.W. Portmann. 2009. Nitrous oxide (N_2O): The dominant ozone-depleting substance emitted in the 21st century. *Science* 326: 123-125.

Revell, L.E., F. Tummon, R.J. Salawitch, A. Stenke, and T. Peter. 2015. The changing ozone depletion potential of N_2O in a future climate, *Geophysical Research Letters*, 42, 10,047–10,055, doi:10.1002/2015GL065702.

Rockstrom J, W. Steffen, K. Noone, A. Persson, F.S. Chapin, E.F. Lambin, T,M. Lenton, M. Scheffer, C. Folke, H.J. Schellnhuber, *et al*. 2009. A safe operating space for humanity. *Nature*, 461: 472-475.

Rolph, G., Stein, A., and Stunder, B. 2017. Real-time Environmental Applications and Display sYstem: READY. *Environmental Modelling & Software*, 95, 210-228, https://doi.org/10.1016/j.envsoft.2017.06.025. (http://www.sciencedirect.com/science/article/pii/S1364815217302360).

Saylor, R.D., E.S. Edgerton, B.E. Hartsell, K. Baumann, D.A. Hansen. 2010. Continuous gaseous and total ammonia measurements from the southeastern aerosol research and characterization (SEARCH) study. *Atmospheric Environment*, 44: 4994-5004.

Schlesinger, W.H. 2009. On the fate of anthropogenic nitrogen. *Proceedings of the National Academy of Sciences*, 106 (1): 203-208.

Schlesinger, W.H. and E.S. Bernhardt. 2013. Biogeochemistry, an analysis of global change, third edition. Academic Press, Waltham, MA. pp. 447-460.

Seitzinger, S., J.A. Harrison, J.K. Bohlke, A.F. Bouwman, R. Lowrance, B. Peterson, C. Tobias, and G. Van Drecht. 2006. Denitrification across landscapes and waterscapes: a synthesis. *Ecological Applications*, 16(6), 2064–2090.

Sgouridis, F. and S. Ullah. 2015. Relative magnitude and controls of in situ N_2 and N_2O fluxes due to denitrification in natural and seminatural terrestrial ecosystems using ^{15}N tracers. *Environmental science and Technology.* 49: 14,110-14,119. doi: 10.1021/acs.est.5b03513.

Shephard, M.W., K. Cady-Pereira, M. Luo, D.K. Henze, R.W. Pinder, J.T. Walker, C.P. Rinsland, J.O. Bash, L. Zhu, V. H. Payne, and L. Clarisse. 2011. TES ammonia retrieval strategy and global observations of the spatial and seasonal variability of ammonia. *Atmospheric Chemistry and Physics*, 11(20), 10743.

Shendrikar, A.D., J. Steger, H. Kimball, W. Cornelius, M. Yirka, R. Bishop and N. Joyner. 2006. Atmospheric ammonia monitoring around hog farm industries in North Carolina. North Carolina Department of Environmental Quality. https://deq.nc.gov/about/divisions/air-quality/air-quality-data/special-studies

Shurtleff, William and Akiko Aoyagi. 2004. History of World Soybean Production and Trade. Soyfoods Center, Lafayette, CA. www.soyinfocenter.com/HSS/production_and_trade1.php

Smil, V. 2001. Enriching the Earth: Fritz Haber, Carl Bosch and the Transformation of World Food Production. MIT Press, ISBN 026219449X, 411 pp.

Steffen, W., K. Richardson, J. Rockstrom, S.E. Cornell, I. Fetzer, E.M. Bennett, R. Biggs, S.R. Carpenter, W. DeVries, C.A. de Wit, C. Folke, D. Gerten, J. Heinke, G.M. Mace, L.M. Persson, V. Ramanathan, B. Reyers, and S. Sorlin. 2015. Planetary boundaries: Guiding human development on a changing planet. *Science*, 347, 1259855. doi: 10.1126/science.1259855.

Stein, A.F., Draxler, R.R, Rolph, G.D., Stunder, B.J.B., Cohen, M.D., and Ngan, F. 2015. NOAA's HYSPLIT atmospheric transport and dispersion modeling system, *Bull. Amer. Meteor*. Soc., 96, 2059-2077, http://dx.doi.org/10.1175/BAMS-D-14-00110.1

Sun, K., K. Cady-Pereira, D.J. Miller, L. Tao, M.A. Zondlo, J.B. Nowak, J.A. Neuman, T. Mikoviny, M. Müller, A. Wisthaler, A.J. Scarino, and C.A. Hostetler. 2015. Validation of TES ammonia observations at the single pixel scale in the San Joaquin Valley during DISCOVER-AQ. *Journal of Geophysical Research: Atmospheres*. 120 (10): 5140-5154. doi:10.1002/2014JD022846.

Sutton, M.A., C.M. Howard, J.W. Erisman, G. Billen, A. Bleeker, P. Grennfelt, H. van Grinsven, and B. Grizzetti (eds.). 2011. The European nitrogen assessment. Cambridge University Press.

Tang, Y., T. Chai, L. Pan, P. Lee, D. Tong, H. Kim, and W. Chen. 2015. Using optimal interpolation to assimilate surface measurements and satellite AOD for ozone and $PM_{2.5}$: A case study for July 2011. *Journal of the Air & Waste Management Association.* 65 (10): 1206-1216. doi: 10.1080/10962247.2015.1062439.

Tang, Y., M. Pagowski, T. Chai, L. Pan, P. Lee, B. Baker, R. Kumar, L. Delle Monache, D. Tong, and H. Kim. 2017. A Case Study of Aerosol Data Assimilation with the Community Multi-Scale Air Quality Model over the Contiguous United States using 3D-Var and Optimal Interpolation Methods, *Geosci. Model Dev*., 10(12), 4743–4758. (https://doi.org/10.5194/gmd-10-4743-2017)

Tevlin, A.G., Y. Li, J.L. Collett, E.E. McDuffie, E.V. Fischer, and J.G. Murphy. 2017. Tall tower vertical profiles and diurnal trends of ammonia in the Colorado Front Range. *Journal of Geophysical Research: Atmospheres,* 122: 12,468-12,487.

Tomich, T.P., S.B. Brodt, R.A. Dahlgren, and K.M. Snow (eds.). 2016. The California Nitrogen Assessment: Challenges and Solutions for People, Agriculture, and the Environment. University of California Press.

Tong, Daniel Q., Lok Lamsal, Li Pan, Charles Ding, Hyuncheol Kim, Pius Lee, Tianfeng Chai, Kenneth E. Pickering, and Ivanka Stajner. 2015. Long-term NOx trends over large cities in the United States during the great recession: Comparison of satellite retrievals, ground observations, and emission inventories. *Atmospheric Environment*, 107: 70-84.

UN. 2010. Hemispheric Transport of Air Pollution 2010, Part A: Ozone and Particulate Matter, Air Pollution Studies No. 17, United Nations. 2010.

UNEP. 2007. Global Environmental Outlook 4 (GEO-4). United Nations Environment Program, Nairobi, Kenya.

USDA. 2014. 2012 Census of Agriculture. U.S. Department of Agriculture, National Agricultural Statistical Service, Washington, DC.

U.S. Environmental Protection Agency Science Advisory Board (U.S. EPA). 2007. Hypoxia in the Northern Gulf of Mexico: An Update by the EPA Science Advisory Board. EPA-SAB-08-003, U.S. Environmental Protection Agency Science Advisory Board, Washington, DC.

U.S. Environmental Protection Agency (U.S. EPA). 2009. 2005 National Emissions Inventory Data & Documentation. www.epa.gov/ttn/chief/net/2005inventory.html

U.S. Environmental Protection Agency Science Advisory Board (U.S. EPA). 2011. Reactive nitrogen in the United States: an analysis of inputs, flows, consequences, and management options, EPA-SAB-11-013. U.S. Environmental Protection Agency.

U.S. Environmental Protection Agency (U.S. EPA). 2015. 2011 National Emissions Inventory Data & Documentation. www.epa.gov/ttn/chief/net/2011inventory.html

U.S. EPA. 2016. Technical Support Document (TSD) – Preparation of Emissions Inventories for the Version 6.3, 2011 Emissions Modeling Platform. https://www.epa.gov/air-emissions-modeling/2011-version-63-technical-support-document

U.S. Environmental Protection Agency (U.S. EPA). 2017. Air Pollutant Emissions Trends Data. Research Triangle Park, NC. https://www.epa.gov/air-emissions-inventories/air-pollutant-emissions-trends-data

U.S. EPA. 2018a. Clean Air Status and Trends Network (CASTNET), raw measurement data, filter pack concentrations. Clean Air Markets Division. www.epa.gov/castnet. Accessed February 17, 2018.

U.S. EPA. 2018b. 2014 National Emissions Inventory Data & Documentation. https://www.epa.gov/air-emissions-inventories/2014-national-emissions-inventory-nei-data

Van Damme, M., Whitburn, S., Clarisse, L., Clerbaux, C., Hurtmans, D., & Coheur, P.-F. 2017. Version 2 of the IASI NH_3 neural network retrieval algorithm: near-realtime and reanalysed datasets. *Atmospheric Measurement Techniques*, 10(12), 4905-4914. doi:10.5194/amt-10-4905-2017.

Vitousek, P.M., D.N.L. Menge, S.C. Reed and C.C. Cleveland. 2013. Biological nitrogen fixation: rates, patterns and ecological controls in terrestrial ecosystems. *Philosophical Transactions of the Royal Society B.* 368: 20130119.

Vukovich, J., and T. Pierce. 2002. The Implementation of BEIS-3 within the SMOKE modeling framework. Presented at "Emissions Inventories—Partnering for the Future," the 11th Emissions Inventory Conference of the U.S. Environmental Protection Agency, Research Triangle Park, NC.

Walker, J.T., W.P. Robarge, Y. Wu, and T.P. Meyers. 2006. Measurement of bi-directional ammonia fluxes over soybean using the modified Bowen-ratio technique. *Agricultural and Forest Meteorology*. 138: 54-68.

Wang, X., W. Wang, L. Yang, X. Gao, W. Nie, Y. Yu, P. Xu, Y. Zhou, and Z. Wang. 2012. Secondary formation of inorganic aerosols in the droplet mode through heterogeneous aqueous reactions under haze conditions. *Atmospheric Environment.* 63: 68–76.

Warner, J.X., Z. Wei, L.L. Strow, R.R. Dickerson, and J.B. Nowak. 2016. The global tropospheric ammonia distribution as seen in the 13-year AIRS measurement record. *Atmospheric Chemistry and Physics*, 16: 5467-5479. doi:10.5194/acp-16-5467-2016.

Warner, J. X., R.R. Dickerson, Z. Wei, L.L. Strow, Y. Wang, and Q. Liang. 2017. Increased atmospheric ammonia over the world's major agricultural areas detected from space. *Geophysical Research Letters.* 44(6): 2875-2884. doi: 10.1002/2016GL072305.

Whitburn, S., M. VanDamme, L. Clarisse, S. Bauduin, C.L. Heald, J. Hadji-Lazaro, D. Hurtmans, M.A. Zondlo, C. Clerbaux, and P.F Coheur. 2016. A flexible and robust neural network IASI-NH_3 retrieval algorithm. *Journal of Geophysical Research: Atmospheres*, 121, 6581–6599, doi:10.1002/2016JD024828.

Winiwarter, W., J.W. Erisman, J.N. Galloway, Z. Klimont, and M.A. Sutton. 2013. Estimating environmentally relevant fixed nitrogen demand in the 21st century. Climatic Change, 120: 889-901. doi: 10.1007/s10584-013-0834-0.

WMO. 2016. Monthly global average CO_2 mole fractions. WMO Greenhouse Gas Bulletin No. 11, November 2015. World Data Centre for Greenhouse Gases, Japan Meteorological Agency. http://ds.data.jma.go.jp/gmd/wdcgg/pub/global/2015/co2_monthly_20151109.csv

Zhang, X., E.A. Davidson, D.L. Mauzerall, T.D. Searchinger, P. Dumas, and Y. Shen. 2015. Managing nitrogen for sustainable development. *Nature* 528: 51. doi:10.1038/nature15743.

Zaehle, S., P. Ciais, A.D. Friend, and V. Prieur. 2011. Carbon benefits of anthropogenic reactive nitrogen offset by nitrous oxide emissions. *Nature Geoscience*, 4: 601-605.

Zhu, L., D.K. Henze, K.E. Cady-Pereira, M.W. Shephard, M. Luo, R.W. Pinder, J.O. Bash, and G.-R. Jeong. 2013. Constraining U.S> ammonia emissions using TES remote sensing observations and the GEOS-Chem adjoint model. *Journal of Geophysical Research: Atmospheres*. 118 (8): 3355-3368. doi: 10.1002/jdrd.50166.

APPENDICES

APPENDIX A

Is Nitrogen the Next Carbon?

William Battye and Viney Aneja
Department of Marine, Earth, and Atmospheric Sciences North Carolina State University, Raleigh, NC

William Schlesinger
Duke University, Durham, NC

Abstract of California Air Resources Board Chair Lecture,
Given by Dr. Viney Aneja
Sacramento, California, February 28, 2018

Abstract

Just as carbon fueled the Industrial Revolution, nitrogen has fueled an Agricultural Revolution. The use of synthetic nitrogen fertilizers and the cultivation of nitrogen-fixing crops both expanded exponentially during the last century, with most of the increase occurring after 1960. As a result, the current flux of reactive, or fixed, nitrogen compounds to the biosphere due to human activities is roughly equivalent to the total flux of fixed nitrogen from all natural sources, both on land masses and in the world's oceans. Natural fluxes of fixed nitrogen are subject to very large uncertainties, but anthropogenic production of reactive nitrogen has increased almost five-fold in the last half-century, and this rapid increase in anthropogenic fixed nitrogen has removed any uncertainty on the relative importance of anthropogenic fluxes to the natural budget. The increased use of nitrogen has been critical for increased crop yields and protein production needed to keep pace with the growing world population. However, similar to carbon, the release of fixed nitrogen into the natural environment is linked to adverse consequences at local, regional, and global scales. Anthropogenic contributions of fixed nitrogen continue to grow relative to the natural budget, with uncertain consequences.

APPENDIX B

Evaluating Ammonia (NH_3) Predictions in the NOAA National Air Quality Forecast Capability (NAQFC) using Ground-Based and Satellite-Based Measurements on a National Scale

William Battye, Casey Bray, and Viney Aneja
Department of Marine, Earth, and Atmospheric Sciences North Carolina State University, Raleigh, NC

Daniel Tong, Pius Lee, and Youhua Tang
NOAA Air Resources Laboratory, College Park, Maryland, MD

Extended abstract of poster presented at the 15th Annual CMAS Conference, Chapel Hill, NC, October 24-26, 2016

B.1. Introduction

Ammonia (NH_3) gas in the atmosphere contributes to the formation of airborne fine particulate matter ($PM_{2.5}$), which is associated with adverse health effects. Atmospheric NH_3 also deposits into terrestrial and aquatic ecosystems, potentially contributing to eutrophication and impacts on species diversity. The U.S. National Oceanic and Atmospheric Administration (NOAA) is responsible for forecasting elevated levels of $PM_{2.5}$ within the framework of National Air Quality Forecast Capability (NAQFC), and these forecasts require reliable estimates of precursor NH_3 concentrations. The Community Multiscale Air Quality (CMAQ) model is used to simulate emissions of NH_3, atmospheric transport, and conversion of NH_3 to $PM_{2.5}$. CMAQ is also used to calculate the deposition of NH_3 and other nitrogen compounds to sensitive ecosystems. However, emission, transport, and deposition processes for NH_3 are subject to considerable uncertainty.

The objective of the current research is to design a framework for using satellite-based measurements improve CMAQ predictions of NH_3. We also use ground-based measurements to

test the validity of satellite observations and to evaluate model performance. Ultimately, we expect refined predictions of NH_3 to result in improved predictions of $PM_{2.5}$ and nitrogen deposition.

B.2. Background

Agricultural sources account for about 90% of atmospheric NH_3 emissions in the U.S. Emissions emanate primarily from animal waste management and synthetic nitrogen fertilizer application. Other sources include chemical and petroleum processes, wastewater treatment, forest fires, and the use of NH_3 in control systems for reducing NO_X emissions such as selective catalytic reduction (SCR). Emissions estimates for NH_3 are subject to considerable uncertainty, and prior model-to-monitor comparisons suggest emissions may be underestimated in some regions of the U.S.

B.3. Methods and Data

B.3.1. Modeling

CMAQ version 5.0.2 was used for air quality modeling. Meteorological inputs are derived from the Nonhydrostatic Multiscale Model on B-grid (NMMB). The modeling domain is the continental U.S. and the time period simulated was July 2011. Model grid horizontal resolution is 12 km, and 42 vertical layers are used, starting with a lowest layer 8 m above ground level. The vertical domain top is 50 hPa. The AERO5 model is used for aerosol chemistry, and deposition is based on the M3Dry module.

NH_3 emissions are derived from the U.S. Environmental Protection Agency (EPA) 2011 National Emissions Inventory (NEI). The NEI estimates emissions at the county level based on daily meteorological conditions. County-level emissions are allocated to the CMAQ grid using the Sparse Matrix Kernel Emissions (SMOKE). SMOKE diurnal allocation factors were also

used to generate hourly emissions estimates. The NAQFC CMAQ modeling framework does not yet incorporate bi-directional flux of NH_3 from crops treated with chemical fertilizer.

B.3.2. Ground-level Measurements

The Ammonia Monitoring Network (AMoN) measures concentrations of atmospheric NH_3 on a 2-week average basis using passive diffusion samplers. We obtained data from 48 AMoN sampling locations active in July 2011. We also obtained data on the mass of ammonium ions (NH_4^+) in the particle phase chemically-speciated $PM_{2.5}$ monitors located near the AMoN sites. The Clean Air Status and Trends Network (CASTNet) includes 27 sites located within 12 km of AMoN sites active in 2012. The Interagency Monitoring network for Protected Visual Environments (IMPROVE) includes another 20 monitors within 12 km of AMoN sites.

B.3.3. Satellite-Derived NH_3 Measurements

We obtained daytime measurements of atmospheric NH_3 during July 2011 from two satellite platforms. The Tropospheric Emission Spectrometer (TES) on the Aura satellite makes measurements over the continental U.S. between 1:00 and 3:00 pm local time. The Atmospheric Science Data Center at the NASA Langley Research Center publishes TES retrievals of the total atmospheric column loading of NH_3 and the vertical profile of atmospheric NH_3 concentrations (Shepherd *et al*, 2011). These retrievals also include estimates of the degrees of freedom for signal (DOFS). We use TES retrievals with DOFS greater than or equal to 0.5, or a thermal contrast of greater than or equal to 7 K.

The Infrared Atmospheric Sounding Interferometer (IASI) on the MetOp satellite makes measurements over the continental U.S. between 9:40 and 10:20 am local time. The Atmospheric Spectroscopy group of the Université Libre de Bruxelles, Belgium has retrieved total atmospheric column loadings of NH_3 from IASI measurements (Whitburn *et al*, 2015). These

retrievals also include estimates of the measurement error. We use IASI retrievals where the relative error is less than 100% or the absolute error is less than 1.4 mg/m^2 (5×10^{-15} molecules/cm^2)

The IASI instrument scans a broader angle than the TES instrument, and takes more measurements in a given satellite pass. For the month of July 2011, 209 TES retrievals were available meeting the screening criteria, while 58,341 IASI retrievals were available.

For each satellite retrieval, we compute a corresponding model value for NH_3 by interpolating from the four surrounding model grids and the two nearest time steps.

B.3.4. Model-to-Monitor Comparisons

Normalized mean bias (NMB) of model predictions is computed as follows:

$$NMB = \frac{1}{N}\frac{\sum_{i=1}^{N}[C_{mod}(i) - C_{obs}(i)]}{\sum_{i=1}^{N}C_{obs}(i)}$$

where $C_{mod}(i)$ and $C_{obs}(i)$ are, respectively, the model prediction and the observed concentration at a given location and time, and N is the number of observations.

B.4. Results and Discussion

Figure B-1 plots ground level measurements of NH_3 from the AMoN network against model predictions. Figure B-2 plots ground level measurements of particulate NH_4+ from the CASTNet and IMPROVE networks against model predictions. Figures B-3 and B-4, respectively, plot TES and IASI retrievals of total column NH_3 against model predictions.

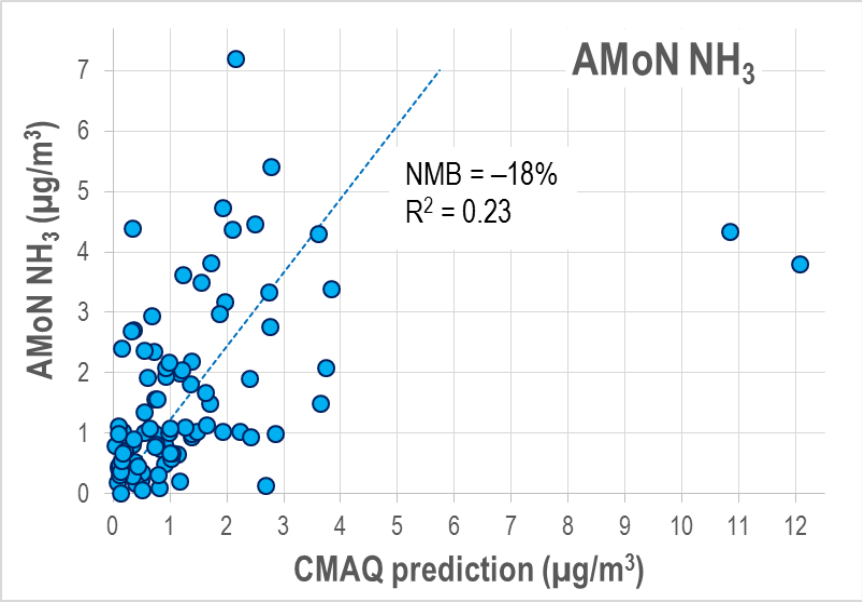

Figure B-1. Ground level NH_3 measurements (AMON) compared with model predictions.

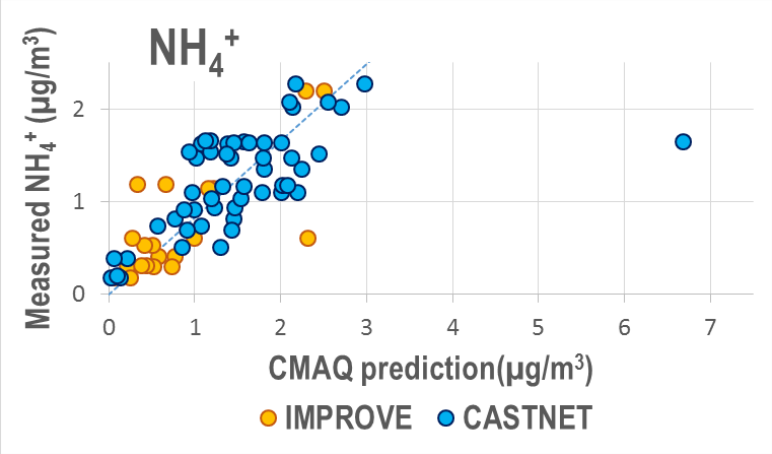

Figure B-2. NH_4^+ measurements (IMPROVE and CASTNET) vs. model predictions.

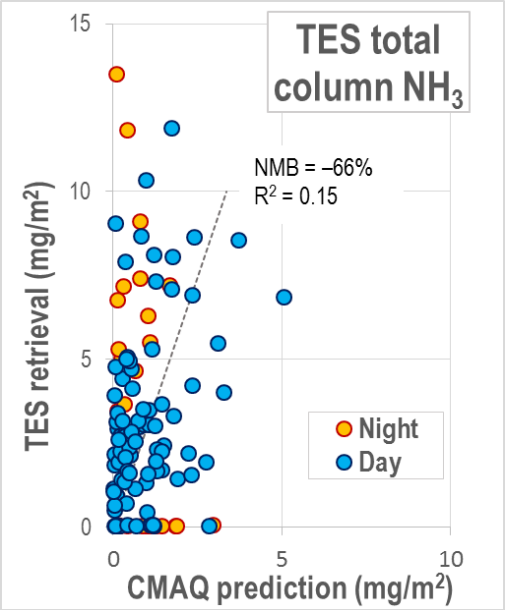

Figure B-3. TES satellite retrievals of total column NH_3 plotted against model predictions.

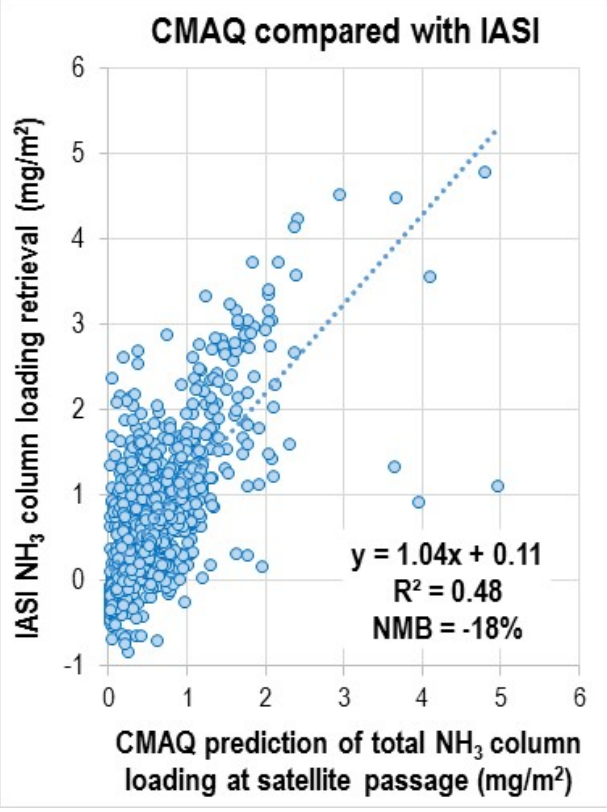

Figure B-4. IASI retrievals of total column NH_3 plotted against model predictions.

Each point represents an average over a 120 km x 120 km region.)All of the measurement data sets are subject to significant variability, and there is low correlation between model predictions and particular corresponding measurements. Model evaluation results also differ somewhat for the measurement data sets. Comparisons with AMoN and IASI show an average negative bias of about 18% (underprediction). Comparisons with TES indicate a larger negative average bias. Some of this bias may stem from errors in predicting short-term concentrations at the time of satellite passage.

Model prediction bias is subject to spatial variation at large and small scales. Figure B-5 plots spatial variations in model bias as indicated by AMoN and TES comparisons. The figure maps the average difference between measured and modeled concentrations at the surface for all observations in July 2011. (As noted above, TES retrievals estimate the vertical profile of NH_3, including the concentration at the surface). The model-measurement differences are superimposed against a background layer showing the modeled concentration.

Figure B-6 maps spatial variations in the average difference between measured and modeled total column concentrations of NH_3. In order to analyze regional patterns, IASI observations were averaged to a spatial resolution of 120 km x 120 km (10 x 10 CMAQ modeling grids). Figure 6 plots the spatially averaged model-measurement differences, superimposed against a background layer showing the modeled column loading.

As Figures B-5 and B-6 show, results of the regional comparisons vary among the three measurement datasets. However, all three datasets suggest that the model may be underpredicting atmospheric NH_3 in the Midwest and in the Central Valley of California, and overpredicting NH_3 in parts of the Southeast U.S.

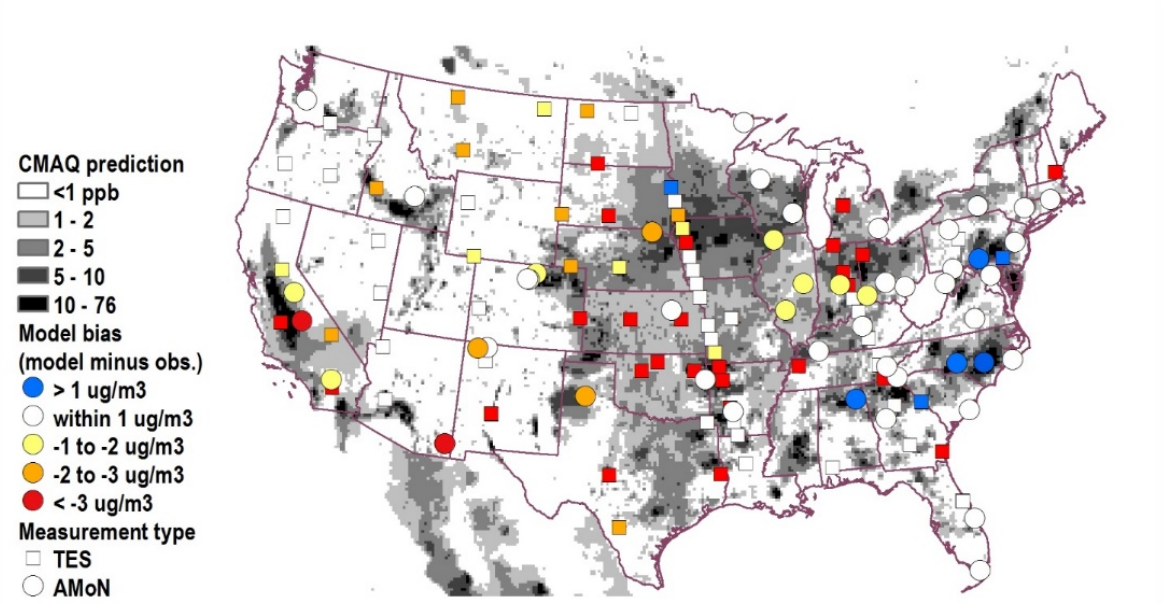

Figure B-5. Spatial variation in model prediction error based on AMON measurements and TES retrievals of surface concentrations over a background of model predictions.

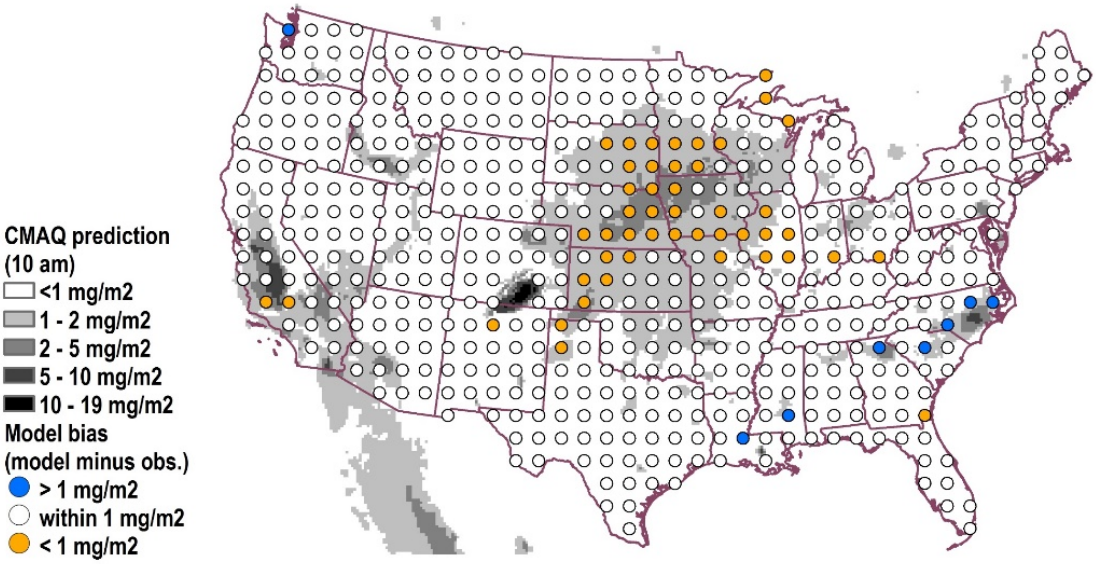

Figure B-6. Spatial variation in model prediction error based on IASI retrievals of total column concentration over a background of model predictions.

Note: Each icon represents at least 31 observations, and an average of 108 observations.

Differences between modeled and measured concentrations may stem from uncertainties in the NH_3 emissions inventory, spatial and temporal allocation methods used in the inventory, model deposition processes, or other model processes. A recently developed bidirectional flux algorithm for NH_3 could be expected to raise NH_3 concentrations in the summer months, thereby ameliorating some underprediction. However, it must also be noted that model bias estimates are subject to considerable uncertainty because of large variabilities associated with all of the measurement data sets.

Acknowledgements

This research has been carried out under the NASA Earth and Space Science Fellowship (NESSF) program, grant No. NNX15AN15H. TES retrieval data were obtained from the NASA Langley Research Center Atmospheric Science Data Center. We acknowledge the Atmospheric Spectroscopy group of the Université Libre de Bruxelles, Belgium, for providing access to IASI retrievals, and advice on filtering and analyzing IASI data. We also acknowledge the NOAA National Air Quality Forecast Program, and the North Carolina State University Air Quality Research Group.

References for Appendix B

Shephard, M.W., K. Cady-Pereira, M. Luo, D.K. Henze, R.W. Pinder, J.T. Walker, C.P. Rinsland, J.O. Bash, L. Zhu, V. H. Payne, and L. Clarisse. 2011. TES ammonia retrieval strategy and global observations of the spatial and seasonal variability of ammonia. *Atmospheric Chemistry and Physics*, 11 (20), 10743.

Whitburn, S., M. VanDamme, L. Clarisse, S. Bauduin, C.L. Heald, J. Hadji-Lazaro, D. Hurtmans, M.A. Zondlo, C. Clerbaux, and P.F Coheur. 2016. A flexible and robust neural network IASI-NH3 retrieval algorithm. *Journal of Geophysical Research: Atmospheres*, 121, 6581–6599, doi:10.1002/2016JD024828.

APPENDIX C

Evaluating ammonia (NH_3) predictions in the NOAA National Air Quality Forecast Capability (NAQFC) using ground-based and satellite-based measurements on a national scale

William Battye, Casey Bray, and Viney Aneja
Department of Marine, Earth, and Atmospheric Sciences North Carolina State University, Raleigh, NC

Daniel Tong, Pius Lee, and Youhua Tang
NOAA Air Resources Laboratory, College Park, Maryland, MD

Abstract of poster presented at the NASA Air Quality Applied Sciences Team (AQAST) 10th Semiannual Meeting
EPA, Research Triangle Park, January 5-7, 2016

Abstract

Ammonia (NH_3) gas in the atmosphere contributes to the formation of airborne fine particulate matter ($PM_{2.5}$), which is linked to adverse health effects. Atmospheric NH_3 also deposits into terrestrial and aquatic ecosystems, potentially contributing to eutrophication and impacts on species diversity. The U.S. National Oceanic and Atmospheric Administration (NOAA) is responsible for forecasting elevated levels of $PM_{2.5}$ within the framework of National Air Quality Forecast Capability (NAQFC), and these forecasts require reliable estimates of precursor NH_3 concentrations. The Community Multiscale Air Quality (CMAQ) model is used to simulate atmospheric emissions and transport and conversion of NH_3 to $PM_{2.5}$; however, emissions and transport processes for NH_3 are subject to considerable uncertainty. The objective of the current research is to design a framework for using satellite-based measurements improve CMAQ predictions of NH_3.

Measurements of NH_3 by the Tropospheric Emission Spectrometer (TES) on the Aura satellite were compiled for the continental U.S. over the entire operational period of the instrument (2004 through the present). These were compared with available ground-based measurements from the Ammonia Monitoring Network (AMoN) and other sources. Both of these data sets were to evaluate CMAQ NH_3 predictions for a one-month case study period – July 2011. For the TES comparisons, model predictions were compared with satellite retrievals of ground level concentrations, total column concentrations, and concentrations at the altitude of maximum satellite sensitivity. Model biases were computed, and regional patterns in bias were evaluated using cluster analysis.

Correlation between model predictions and measurements is poor, indicating that there is a need to improve CMAQ predictions. Model biases are subject to considerable spatial variation, with notable underprediction in parts of the West and Midwest and overprediction in the Southeast. Additional longer-term analysis is needed to determine if these patterns of bias are persistent, and to develop corrective mechanisms.

APPENDIX D

Evaluation of ammonia predictions within the NOAA National Air Quality Forecast Capability (NAQFC) using aircraft in situ ammonia measurements

William Battye, Casey Bray, and Viney Aneja
Department of Marine, Earth, and Atmospheric Sciences North Carolina State University, Raleigh, NC

Daniel Tong, Pius Lee, and Youhua Tang
NOAA Air Resources Laboratory, College Park, Maryland, MD

Abstract of poster presented at the Joint FRAPPÉ / DISCOVER-AQ Science Team Meeting
4-8 May 2015
UCAR Center Green, Boulder, Colorado

Abstract

Ammonia (NH_3) gas in the atmosphere contributes to the formation of airborne fine particulate matter ($PM_{2.5}$). Atmospheric NH_3 also deposits into terrestrial and aquatic ecosystems, leading to an increase in the level of biologically available nitrogen in those reservoirs. The U.S. National Oceanic and Atmospheric Administration (NOAA) is responsible for forecasting elevated levels of air pollution within the National Air Quality Forecast Capability (NAQFC). NOAA uses the Community Multiscale Air Quality (CMAQ) model version 5.0.2 to simulate atmospheric emissions and transport and conversion of NH_3 to $PM_{2.5}$.

The current research uses measurements gathered in the DISCOVER-AQ Colorado field campaign and the concurrent Front Range Air Pollution and Photochemistry Experiment (FRAPPE) to test performance of the NAQFC CMAQ modeling framework for predicting NH_3. The DISCOVER-AQ and FRAPPE field campaigns were carried out in July and August 2014 in Northeast Colorado. Model predictions are compared with measurements of NH_3 gas

concentrations and the NH_4^+ component of fine particulate matter concentrations measured directly by the aircraft in flight. We also compare CMAQ predictions with NH_3 measurements from ground-based monitors within the DISCOVER-AQ Colorado geographic domain, and from the Tropospheric Emission Spectrometer (TES) on the Aura satellite.

In situ aircraft measurements carried out in July and August of 2014 suggest that the NAQFC CMAQ model underestimated the NH_3 concentration in Northeastern Colorado by a factor of 2.7 (NMB = –63%). Ground-level monitors also produced a similar result. Average satellite-retrieved NH_3 levels also exceeded model predictions by a factor of 1.5 to 4.2 (NMB = -33 to -76%). The underestimation of NH_3 vapor did not, however, cause an underestimation of particulate NH_4^+, which is further controlled by factors including acid availability, removal rate, and gas-particle partition. The average measured concentration of NH_4^+ was close to the average predication (NMB = +18%).

Seasonal patterns measured at an AMoN site in the region suggest that the underestimation of NH_3 is not due to the seasonal allocation of emissions, but to the overall annual emissions estimate. The underestimation of NH_3 varied across the study domain, with the highest errors occurring in a region of intensive agriculture near Greeley, Colorado, and in the vicinity of Denver. The CMAQ framework did not include a recently developed bidirectional flux algorithm for NH_3, which has shown to considerably improve NH_3 modeling in agricultural regions. The bidirectional flux algorithm, however, is not expected to obtain the magnitude of this increase sufficient to overcome the underestimation of NH_3 found in this study. Our results suggest that further improvement of the emission inventories and modeling approaches are required to reduce the bias in NAQFC NH_3 modeling predictions.